DISSERTATION

THE FABRICATION OF GOLD NANOTUBULAR MEMBRANES AND THEIR APPLICATIONS IN SEPARATIONS

Submitted by

Kshama B. Jirage

Department of Chemistry

In partial fulfillment of the requirements

for the Degree of Doctor of Philosophy

Colorado State University

Fort Collins, CO

Fall 1999

COLORADO STATE UNIVERSITY

March 29, 1999

WE HEREBY RECOMMEND THAT THE DISSERTATION PREPARED UNDER OUR SUPERVISION BY KSHAMA B. JIRAGE ENTITLED "THE FABRICATION OF GOLD NANOTUBULAR MEMBRANES AND THEIR APPLICATIONS IN SEPARATIONS" BE ACCEPTED AS FULFILLING IN PART REQUIREMENTS FOR THE DEGREE OF DOCTOR OF PHILOSOPHY.

Committee on Graduate Work

Adviser

Department Head

ABSTRACT OF DISSERTATION

THE FABRICATION OF GOLD NANOTUBULAR MEMBRANES AND THEIR APPLICATIONS IN SEPARATIONS

Membrane based template synthesis and an electroless deposition method was used to fabricate Au nanotubular membranes. The inside diameter of the nanotubules was controlled by varying the time of deposition. The final diameters of the nanotubules were on the order of few angstroms, comparable to the size of molecules. It was demonstrated that these membranes show, "molecular sieving" and can completely separate molecules differing in size. Furthermore, the chemical environment of the nanotubules can be controlled by chemisorbing thiols with different terminal groups. Membranes modified with hydrophobic thiols, are selective to hydrophobic molecules and when modified with hydrophilic thiols, the membranes are selective to hydrophilic molecules. In addition, these membranes can separate molecules when present in a mixture.

Au nanotubular membranes can be modified by thiols with charged terminal groups. For e.g., membranes modified with $-COO^-$ terminated thiol, were cation-permselective. When modified with $-NH_3^+$ terminated thiol, the membranes were anion-permselective. Membranes were permselective in a larger range of electrolyte concentrations for large anions. Finally, Au-Polyacrylic acid (PAA) composite was synthesized in a polyester template membrane by the consecutive deposition of Au and PAA. Au was deposited by electroless deposition and PAA wad deposited by vacuum assisted deposition method. This

composite can function as a chemical valve, upon change with pH in the presence of buffer. Furthermore, the composite also functions as an electrochemically controlled valve by the generation of H^+ and OH^- ions at the Au surface.

Kshama B. Jirage
Chemistry Department
Colorado State University
Fort Collins, CO 80523
Fall 1999

DEDICATED TO MY PARENTS

ACKNOWLEDGEMENTS

I would like to acknowledge my parents, without whose love and encouragement I would not have set out to pursue this degree. I would also like to thank my sister, Daya and brother, Suraj for their constant support.

I would like to thank Chuck for his support during the last four years of my graduate career. I consider myself fortunate to have had the opportunity to work on several interesting and challenging projects. I am appreciative of the independence that Chuck always fostered, both in the way the experiments were designed as well as setting my own pace.

During the course of my graduate work, I had to use several instruments from other labs to obtain crucial data. I would like to acknowledge the Electron Microscopy Center in the Anatomy Department and the help of the staff- Dr. John Chandler, Dr. John Rash Dr. Tom Yasumura and Dr. Bob Lee- with the use of the electron microscopes and the equipment in the digital imaging center. I am thankful to Dr. Tom Solie for allowing me to use the fluorometer. I am also grateful to Dr. Steve Strauss for granting me permission to do elemental analysis using ICP. I would like to express my gratitude to several members of the Strauss group as well for their help.

At CSU, I enjoyed being a part of the Martin group - a group of enthusiastic, extremely helpful and fun-loving people. I would like to thank a few of them who influenced my life during my stay in Fort Collins. First, I would like to thank Dr. Veronica Cepak, for her extreme patience in proof reading my dissertation, for the helpful discussions with regard to experiments and for being an awesome roommate. I am extremely fortunate to have met and worked with David Mitchell, Charles Patrissi, Pucci Arman and Michelle Steen, from all of whom I have learnt a lot and without whom the lab would have been a dull and boring place to be.

I must mention several wonderful roommates that I lived with who made life at home fun and interesting: Sumana Srinath, Srivani Jade, Laura Sharp, Veronica Cepak and Jill Glover.

Last but not the least, I would like to thank my husband, Maithreyan for his constant support and encouragement throughout my graduate career.

Kshama B. Jirage
March 29, 1999

TABLE OF CONTENTS

CHAPTER 2. Gold Nanotubular Membranes For "Molecular Filtration"

LIST OF TABLES

LIST OF FIGURES

CHAPTER 1

SYNTHESIS AND APPLICATIONS OF NANOMATERIALS AND MEMBRANE-BASED SEPARATIONS

INTRODUCTION

A nanoparticle is a particle with at least one dimension less than or equal to 100 nm(1). Recently, there has been a surge of interest in the development of nanomaterials and their applications(2, 3). Nanomaterials have several applications in analytical chemistry(1), drug delivery(4), bioencapsulation(5); and electronic, optical and mechanical devices(3, 6-8).

In addition to applications, there is also fundamental interest in these materials as electronic, magnetic and optical properties of a nanoscopic particle differ from the bulk material. For example, there are several applications that have been developed based on the optical properties of colloidal gold particles.

This chapter deals with one of methods to fabricate nanomaterials called "template synthesis". This involves the use of a natural or synthetic materials as templates to synthesize materials of nanoscopic dimension. Some of the applications of nanomaterials in analytical chemistry will also be discussed. Lastly, a brief summary of membrane based separations will be presented.

BACKGROUND

Template Synthesis Of Nanomaterials

As mentioned, template synthesis involves synthesis of a desired material in a host with naturally occurring or artificially induced voids. A variety of host materials are available with wide range of void sizes, ranging from a few nanometers to microns(9, 10). Almost any synthetic process can be adapted such that it occurs in the voids, thus nearly any material can be deposited including metals, semiconductors, conducting and insulating polymers(11).

Synthesis of nanostructured materials using a template mimics naturally occurring processes. For example, voids in ferritin protein are used as a template to accumulate iron oxide particles as part of an iron storage system(12, 13). Magnetotectic bacteria use cellular vesicles as template to synthesize nanoscopic ferrite particles which they use to navigate(14, 15). In another example microscopic aquatic animals fabricate SiO_2 and $CaCO_3$ shells in the same manner by constructing each individual piece using vesicles as template(14, 15). Other biologically produced templates include phospholipid tubules(16), rhapidosomes(17), and cytoskeletons of eukaryotic cells(18).

Zeolites were first to be used in artificial template synthesis. Zeolites are molecular sieves which have pores with dimensions in subnanometer to nanometer regime. Deposition of materials in zeolites has been accomplished using chemical vapor deposition or ion-exchange. Various materials deposited, include conducting polymers such as polypyrrole and polyaniline(9, 19), semiconductors (CdS and CdTe)(20, 21), nanoparticles of Pt(22).

Porous glasses have been used as template for the deposition of semiconductors(23-25). Justus and coworkers demonstrated that GaAs nanocrystals can be deposited by a metal organic chemical vapor deposition (MOCVD) method(23). Other semiconductors such as CdS, CdSe, PbS, PbSe and MoS_2 have also been deposited in porous glass by the gas phase reaction of hydrogen chalcogenide and the metal ion impregnated in the glass(26). The semiconductors, Se and Te have been deposited by pressure forcing the melt through porous glass(24).

Another template that has been used to fabricate nanomaterials is "inverse micelles". Nanowires of $BaCO_3$ were synthesized by the reaction of Ba^{2+} and CO_3^{2-} ions in the core of inverse micelles(27). Nanowires with lengths up to 100 μm and diameters as small as 10-30 nm were obtained by this method. Other materials such as ferrite particles, semiconductors (CdS, CdSe, ZnS, TiO_2) and metals (Ag, Au, Pt, Ru) have all been synthesized in reverse micelles(28).

Magnetic and nonmagnetic nanoscale iron oxides have been synthesized using self-assembled lipid tubules as template. Mann et al. demonstrated that the morphology of the materials formed could be manipulated by varying the reaction conditions(29). Conducting polymers such as polypyrrole have also been deposited in lipid tubules(30). Highly uniform nanofibers of polypyrrole with diameter between 10 and 50 nm were obtained by this method. The lengths of the resulting nanofibers can be as long as hundreds of microns as it is not confined in a channel or pore(30).

It has been demonstrated that, two-dimensionally ordered arrays can be used a template to fabricate nanoscale architecture(31). For example, silica particles have been used to form an ordered array as a replica template. TiO_2 was formed on the ordered array by the pyrolysis of titanyl acetylacetonate. This composite was placed on a Ni substrate with the SiO_2 particles facing upwards. The SiO_2 particles were dissolved in HF to yield nanostructured TiO_2.

Recently, C nanotubes prepared by various methods have been used as a template to deposit materials in them. Nanorods of GaN by the vapor phase reaction of Ga_2O and NH_3 in a C nanotube confined reaction(32). Hollow nanotubes of zirconia and titania have also been obtained by deposition in C nanotubes and then removing the template C nanotube by oxidation(33). Materials such as V_2O_5, have also been deposited within C nanotubes by partial oxidation in air or nitric acid which aids in the opening the tips of the nanotubes(34).

Membrane Based Template Synthesis Of Nanomaterials

Two types of synthetic membranes that are commonly used as templates to fabricate micro- and nanomaterials are "track-etched" membranes and anodically grown aluminum oxide (AAO) membranes(10). The "track-etched" polymeric or mica membranes are obtained by producing damage tracks with high energy charged particles, that are subsequently etched in base or HF to obtain pores of desired diameters(35). AAO membranes are formed when polished aluminum metal is anodized in acidic electrolytes(36).

Figure 1.1 shows typical SEMs of the two types of membranes. The

membranes are commercially available from suppliers such as Poretics, Whatman and Corning. The polymeric membranes are available in a variety of pore sizes (30 nm to 10 μm), pore densities ($6x10^8$ to $1x10^4$ pores cm^{-2}) and thicknesses (6 μm to 20 μm). Figure 1.1a shows the surface of a polyester membrane with 1 μm diameter pores and Figure 1.1b, the surface of an AAO membrane. The AAO membranes are 60 μm thick while the pore density is on the order of $1x10^9$ pores cm^{-2} and the porosity is approximately 60%. Membranes with different thicknesses and diameters can be fabricated by controlling the anodization conditions.

In 1970, Possin discovered that track-etched mica membranes can be used to electrodeposit metals to prepare wires as small as 40 nm(37). The process was refined by Williams and Giordano to obtain wires as small as 8 nm(38). Since then, track-etched membranes have been used to deposit a large variety of materials ranging from metals, semiconductors, conducting and insulating polymers, concentric tubular composites to layered composites. Several reviews of membrane based nanomaterials can be found in literature(10, 11, 39, 40).

Properties And Applications Of Nanomaterials

Metal nanoparticles such Au and Ag colloids show a characteristic visible absorption band called surface plasmon resonance (SPR) absorption(41). The color depends among other things on the size of the particle, the metal and the distance between the particles. There are several applications that have been developed exploiting this optical property of the colloidal particles.

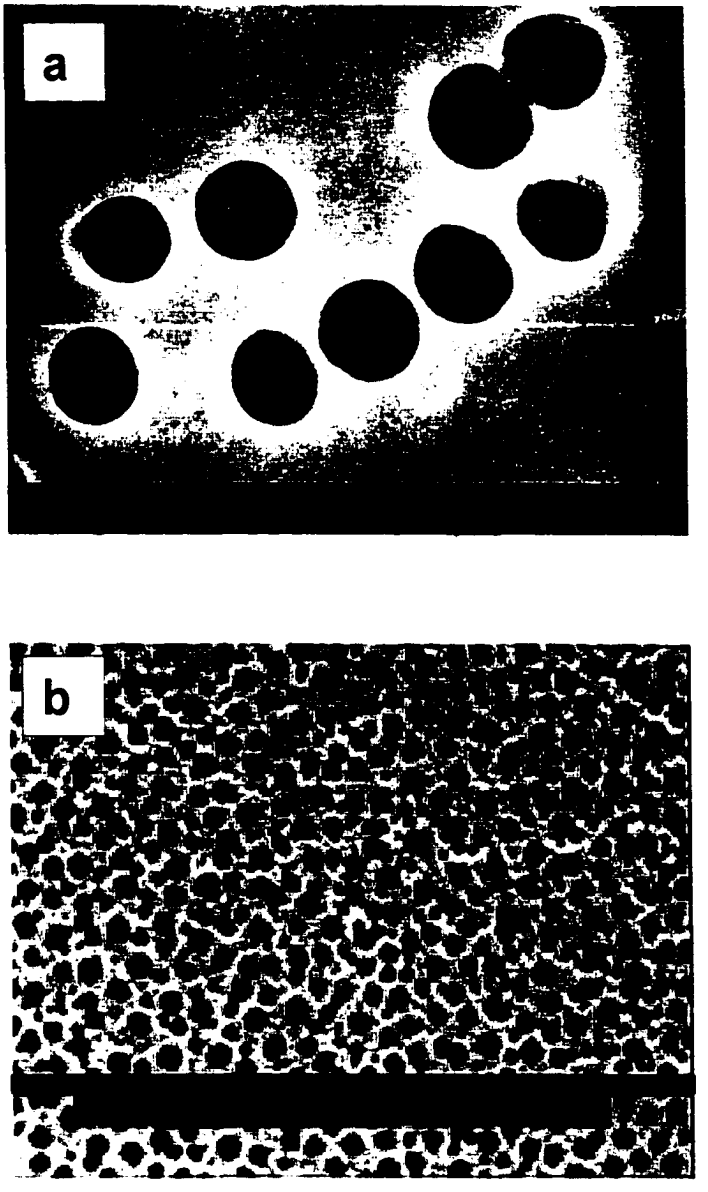

Figure 1.1 Scanning electron micrograph of
a) Track etched polycarbonate membranes with 1μm diameter pores
b) AAO membrane with 0.2 μm diameter pore

One example is the Carter Wallace home pregnancy test 'First Response'(42). This test uses latex particles and gold nanoparticles (less than 50 nm) which are pink. These particles are derivatized with antibodies to human chroionic gonadotrophin, a hormone released by pregnant women. When a urine sample containing the hormone is mixed with these particles, the two particle coagglutinate and the resulting clumps are pink.

Mirkin and coworkers have exploited the SPR absorption of gold to develop a proposed DNA detection method(43). A single stranded thiol terminated oligonucleotide was immobilized on a 13 nm gold colloidal particle. The particles have a strong absorption at 520 nm. When the linking oligonucleotide was added, the gold nanoparticles agglutinated and the color changed to purple. This is because of a shift in the SPR with a change in the distance between the particles. A detection limit as low as 10 fmol was achieved for the target oligonucleotide.

Gold nanoparticles have been used as specific staining agents in electron microscopy(44). Since gold nanoparticles have a high back scatter coefficient, they appear bright in a scanning electron microscope image while appearing dark in a transmission electron microscope image. Hence, they are routinely used for site specific staining, by labeling the particles with antibodies that would react with the antigen of interest.

It has been observed that direct adsorption of proteins on bulk metal surfaces causes them to denature and there is loss of activity. However, when proteins are adsorbed on colloidal gold particles they do not, thus retaining their

activity. For example, Natan et al. demonstrated that reversible cyclic voltammetry was obtained when cytochrome c was adsorbed on gold nanoparticle(45). When the protein was adsorbed on a bulk gold substrate a quasi-reversible or irreversible cyclic voltammetry was observed indicating denaturation. This further illustrates the unique properties of nanoparticles.

Nanomaterials fabricated using membrane based template synthesis have interesting properties and a large number of applications are being developed(10, 39, 40). For example, it has been observed that polypyrrole fibrils have orders of magnitude higher conductivity than bulk polypyrrole(46). Because the polymer chains on the outer surfaces of the nanofibrils are aligned the conductivity is enhanced.

It has been demonstrated that enzymes can be immobilized in the pores of a template polycarbonate membrane and plugging the ends of the pore with polypyrrole plugs(5). The enzyme was active and can function as a micro-reactor. Moreover, a membrane with the enzyme immobilized in the pores can perform as a facilitated transport membrane(47). The enzyme can act as a carrier and transport a species that it binds to from a mixture preferentially over another that it does not bind to. Molecules as similar as enantiomers have been separated using this method.

Gold deposited in template polycarbonate membranes also has several applications. An electroless gold deposition method was developed to fabricate gold fibrils(48). The procedure leads to the deposition on the surface and the pore walls. Removal of the surface layers exposed gold disks that are inlaid in

the membrane which were successfully used as a nanoelectrode ensemble. These template-prepared nanoelectrodes had several advantages over conventional electrodes. In fundamental electrochemistry, they offer the possibility to explore the kinetics of very fast electron transfer processes. In applied electrochemistry, ensembles of nanoelectrodes have achieved lower detection limits(48).

Applications of nanostructures developed using sol-gel chemistry have also been explored. Semiconductor materials such as TiO_2, V_2O_5, ZnO and WO_3 were synthesized using sol-gel chemistry(49). Larger surface areas were accessible for photocatalysis when TiO_2 was deposited in anodic AO membrane compared to a thin film(50). It has also been shown that V_2O_5 deposited in polycarbonate membrane can be used as Li-ion battery materials(51).

Chemical vapor deposition (CVD) has been used to deposit carbon in AAO membranes(52). Both carbon nanotubes and nanofibers can be obtained depending upon the time of deposition. Deposition of electrocatalytic nanoparticles in the carbon nanotubes was achieved by immersing the membrane in the metal ion solution followed by reduction with hydrogen. Such membranes electrocatalyzed O_2 reduction and methanol oxidation indicate that these membranes could be important in fuel-cell technology(53).

A combination of CVD and the template method was used to fabricate Au-TiS_2 composite(54). These electrodes showed higher capacities and lower resistance than thin film TiS_2 electrodes. This was due the same amount of material that is distributed on larger surface area created by the Au microtubules.

Fundamental studies of nanomaterials deposited in the template membranes have been explored. For example, Au nanoparticles can be deposited electrochemically in AAO membranes(55). It is well known that the colors of colloidal gold suspensions can range from red to purple to blue depending on the diameter of the particles. Similar colors have been observed with Au nanoparticles of different dimensions when deposited in AAO membrane(56, 57).

The deposition of semiconductors in the membranes has been explored for fundamental applications. Sailor et al. have shown that II-IV semiconductors such as CdS, CdSe can be deposited electrochemically in AAO membranes to obtain an array of semi-conductor fibrils(58). Other semi-conductors such as MoS_2 have also been deposited by a thermal decomposition procedure(59). Electrochemical deposition of several metals and detailed analysis of the morphology of the nanomaterials thus obtained, have been studied.

Membrane-Based Separations

Membrane-based separation is a rapidly growing field. There are several advantages of using membranes in separation compared to conventional method such as distillation, adsorption, absorption etc.(60). These advantages include energy efficiency, process flexibility and their use in the presence of impurities. Furthermore, membranes can be developed that discriminate between molecules based on several factors such as size, shape, polarity and chemical interaction. Due to these factors, membranes can be used to separate molecules where it would be difficult to use conventional techniques.

would be difficult to use conventional techniques.

Membranes for separations have been fabricated based on a variety of principles such as reverse osmosis, facilitated transport, molecular imprinting, ion-exchange, separation of gases based on Knudsen diffusion and sieving and so on(61). Some of the principles will now be discussed.

Industrially Important Separations

Chiral separations are important especially in the drug and pharmaceutical industry(62) and are generally achieved by electrophoretic and chromatographic techniques. There have been several attempts to develop membrane-based methods. Hinze and co-workers have reported chiral separation by using chiral surfactants as the carrier in a liquid membrane(63). They were able separate dansyl amino acids by using bile salts and quartenary ammonium salts as the carriers.

There have also been attempts to synthesis polymeric membranes with optically active pendant groups in order to achieve chiral separations. A novel norbornadiene polymeric membrane was used to separate of pharmaceutically important compounds(64, 65). Another example of chiral separations with membranes was demonstrated by using a combination of an enzyme reaction and membrane extraction for amino acids (66). The enzyme α-chymotrypsin to hydrolyze the enantiomers of the amino acid. This enzyme is known to selectively hydrolyze the L- amino acid ester in the presence of D-amino acid ester. The reaction mixture was placed in a hollow fiber membrane, the unreacted ester was removed by extraction with organic solvents and the

enriched L-amino acid was isolated. A method was also developed to recycle the enzyme by coating it with surfactant, so they are easy to recover and reuse.

Another major separation that costs millions of dollars every year is the separation of gases(67). An example is the separation of natural and petroleum gases into methane and the combined heavy hydrocarbon fraction.

The use of membranes in the commercial separation of petroleum and natural gases is hindered by a couple of factors. One factor is the well-balanced and successful distillation processes that are available. The other factor is the unavailability of long-term stability of membrane materials in contact with high pressure streams. Hence, several improvements in the current membrane technology have to be made before membranes will make inroads in this sector.

Another example is separation of permanent gases such as air, nitrogen, hydrogen etc. The separation of air to obtain oxygen and nitrogen is also an important industrial process. Membrane based methods have been developed to produce these gases in high purity, but only in a multi-stage process. However, there are several applications for enriched oxygen and nitrogen. Hence, the separations of these gases achieved using single stage of these gases can still be useful.

One of the major breakthroughs was made in the area of membrane technology was by Loeb and Sourirajan in 1960 by the development of the asymmetric membrane(68). These membranes are porous throughout, but have a dense film at one surface. This dense film causes the separation but higher fluxes can be achieved because the membrane is porous throughout the

thickness of the membrane. Such membranes have been successfully used in applications such as reverse osmosis, microfiltration and ultrafiltration, hyperfiltration and pervaporation(69).

To summarize, membrane based separation processes have several advantages over conventional methods and are being used in some commercial applications. However, if these types of separations have to make a larger impact there have to be improvements in the stability of the membranes and the selectivities that are achieved in the separation processes.

OBJECTIVES OF DISSERTATION

This dissertation focuses on the fabrication of nanotubular and microtubular membranes using an electroless gold deposition process and the template method. "Track-etched" polycarbonate and polyester membranes were used for all the studies undertaken.

Chapter 2 describes a method to develop gold nanotubular membranes with precisely controlled diameters. The diameter of the tubules is determined by the length of the deposition time. The template polycarbonate membrane has 30 nm diameter pores. These pores can be made as small as a few angstroms by the deposition of gold. It will be demonstrated that these membranes can show "molecular sieving". Furthermore, they can completely separate the smaller molecule when present in a mixture with a larger molecule, based only on the difference in size.

In chapter 3, a method is described to control the chemical environment within the gold nanotubules in order determine if molecules could be separated

based on their chemical nature. This was achieved by self-assembling a thiol with the requisite properties. For example, a long chain ($-C_{16}$) hydrocarbon thiol is expected to be hydrophobic and a short chain hydroxyl terminated thiol, hydrophilic. It will be demonstrated that the membrane is rendered hydrophobic when modified with a $-C_{16}$ thiol and is selective for hydrophobic molecule such as, toluene. Also, a membrane modified with a $-C_2H_4OH$ thiol is hydrophilic and is selective for hydrophilic molecule such as pyridine. Furthermore, when the two molecules were in a mixture, the $-C_{16}$ thiol modified membrane was selective to toluene.

Chapter 4 describes the modification of the Au nanotubular membranes with thiols with appropriate terminal groups in order to create a charged surface to utilize the membranes for charge based separations. Two thiols were used to either obtain a negatively charged (COO^-) or a positively charged membrane NH_3^+). It will be demonstrated that these membranes are permselective to the ion of opposite charge on the membrane, because they repel ions of like charge. It will also be demonstrated that nanotubular membranes with very small tubules are permselective in a larger concentration range than observed before because of "molecular sieving".

The fabrication of an Au-Polyacrylic acid composite by the sequential deposition of the two materials is discussed in chapter 5. It will be demonstrated that the composite can function as a chemical valve by changing the pH of the system. Moreover, this composite membrane can also function as a valve by changing the pH at the surface of the Au surface by electrochemical generation

of H^+ and OH^-.

CONCLUSIONS FOR CHAPTER 1

Nanomaterials have interesting properties compared to bulk material. There are several methods that can be adapted to prepare nanomaterials. One of the methods is "template synthesis". A variety of synthetic routes can be applied to a variety of templates to obtain the nanomaterial of choice.

Membranes such as "track-etched" polymeric materials and anodic alumina membranes have been used as templates. The pores in the template are uniform and run throughout the thickness of the membrane and this is reflected in the resulting nanomaterial. Also, the template membrane can be removed or kept intact depending on the application of the nanomaterial.

Several applications have been developed using nanomaterials such as gold nanoparticles. Nanomaterials synthesized using membrane based "template method" have interesting properties and several applications.

Membrane based separations are being developed as an alternative to conventional strategies in separation. Some of the template based nanomaterials are being explored for use in separations.

REFERENCES FOR CHAPTER 1

(1) Mitchell, D. T.; Martin, C. R., Anal. Chem. **1998,** *70*, 322A.

(2) Ozin, G. A., Adv. Mater. **1992,** *4*, 612.

(3) *"Engineering a Small World: From Atomic manipulation to Microfabrication"* Science **1991,** *254*, 1300.

(4) Gref, R., Science **1994,** *263*, 612.

(5) Parthasarthy, R.; Martin, C. R., Nature **1994,** *369*, 298.

(6) Bate, R. T., Sci. Am. **1988,** *258*, 96.

(7) Jewell, J. L.; Harbinson, J. P.; Scherer, A., Sci. Am. **1991,** *265*, 86.

(8) Devoret, M. H.; Esteve, D.; Urbina, C., Nature **1992,** *360*, 547.

(9) Bein, T.; Enzel, P., Angew. Chem. Int. Ed. Engl. **1989,** *28*, 1692.

(10) Martin, C. R., Science **1994,** *266*, 1961.

(11) Hulteen, J. C.; Martin, C. R., J. Mat. Chem **1997,** *7*, 1075.

(12) Harrison, P. M. *Biomineralization: Chemical and Biochemical Prespectives*; VCH: Weinheim, **1989**.

(13) Harrison, P. M. *Advances in Inorganic Chemistry*; Academic: San Diego, **1991**.

(14) Mann, S., Nature **1993,** *365*, 499.

(15) Calvert, P.; Rieke, P., Chem. Mater. **1996,** *8*, 1715.

(16) Schnur, J. M.; Price, R.; Schoen, P.; Yager, P.; Calvert, J. M.; Georger, J.; Singh, A., Thin Solid Films **1987,** *152*, 181.

(17) Pazirandeh, M.; Baral, S.; Campbell, J. R., Biomimetics **1992,** *1*, 41.

(18) Kirsch, R.; Mertig, M.; Pompe, W.; Wahl, R.; Sadowski, G.; Bohm, K. J.; Unger, E., Thin Solid Films **1997,** *305*, 248.

(19) Wu, C. G.; Bein, T., Science **1994,** *264*, 1757.

(20) Wang, Y.; Herron, N., J. Phys. Chem. **1988,** *92*, 4988.

(21) Brigham, E. S.; Wesbeker, C. S.; Rudzinski, W. E.; Mallouk, T. E., Chem. Mater. **1996,** *8*, 2121.

(22) Ryoo, R.; Ko, C. H.; Kim, J. M.; Howe, R., Chem. Lett. **1996,** *37*, 29.

(23) Justus, B. L.; Tonucci, R. J.; Berry, A. D., App. Phys. Lett. **1992,** *61*, 3151.

(24) Huber, C. A.; Huber, T. E., J. App. Phys. **1988,** *64*, 6588.

(25) Rajh, R.; Vucemilovic, M. I.; Dimitrijevic, N. M.; Micic, O. I.; Nozik, A. J., Chem. Phys. Lett. **1988,** *43*, 305.

(26) Borrelli, N. F.; Luong, J. C., SPIE **1987,** *466*, 104.

(27) Qi, L.; Ma, J.; Chemg, H.; Zhao, Z., J. Phys. Chem. B **1997,** *101*, 3460.

(28) Meldrum, F. C.; Kotov, N. A.; Fendler, J. H., J. Chem. Soc. Faraday Trans. **1994,** *90*, 673.

(29) Mann, S.; Burkett, S. L.; Davis, S. A.; Fowler, C. E.; Mandelson, N. H.; Sims, S. D.; Walsh, D.; Whilton, N. T., Chem. Mater. **1997,** *9*, 2300.

(30) Qi, Z.; Lennox, R. B., Electrochem. Soc. Proc. **1997,** *173*, 97.

(31) Matsushita, S.; Miwa, T.; Fujishima, A., Chem. Lett. **1997**, 925.

(32) Han, W.; Fan, S.; Li, Q.; Hu, Y., Science **1997,** *277*, 1287.

(33) Rao, C. N. R.; Satishkumar, B. C.; Govindraj, A., Chem. Comm. **1997**, 1581.

(34) Ajayan, P. M.; Stephan, O.; Redlich, P.; Colliex, C., Nature **1995,** *375*, 564.

(35) Fleischer, R. L.; Price, P. B.; Walker, R. M. *Nuclear Tracks in Solids*; University of CA Press: Berkeley, **1975**.

(36) Despic, A.; Parkhutik, V. P. *Modern Aspects of Electrochemistry*; Plenum: New York, **1989**.

(37) Possin, G. E., Rev. Sci. Instrum. **1970,** *41*, 772.

(38) Williams, W. D.; Giordano, N., Rev. Sci. Instrum. **1984,** *55*, 410.

(39) Martin, C. R., Chem. Mater. **1996,** *8*, 1739.

(40) Martin, C. R., Acc. Chem. Res. **1995,** *28*, 61.

(41) Hornyak, G. L.; Patrissi, C. J.; Martin, C. R., J. Phys. Chem. **1997,** *101*, 1548.

(42) Bangs, L. B., Pure Appl. Chem. **1996,** *68*, 1873.

(43) Elghanian, R.; Stirhoff, J. J.; Mucic, R. C.; Letsinger, R. L.; Mirkin, C. A., Science **1997,** *277*, 1078.

(44) Bendayan, M. *Practical Electron Microscopy*; Cambridge University Press: New York, **1993**.

(45) Brown, K. R.; Fox, A. P.; Natan, M. J., J. Am. Chem. Soc. **1996,** *118*, 1154.

(46) Cai, Z.; Lei, J.; Liang, W.; Menon, V. P.; Martin, C. R., Chem. Mater. **1991,** *3*, 960.

(47) Lakshmi, B. B.; Martin, C. R., Nature **1997,** *388*, 758.

(48) Menon, V. P.; Martin, C. R., Anal. Chem. **1995,** *67*, 1920.

(49) Lakshmi, B. B.; Patrissi, C. J.; Martin, C. R., Chem. Mater. **1998,** *9*, 2544.

(50) Lakshmi, B. B.; Dorhout, P. K.; Martin, C. R., Chem. Mater. **1997,** *9*, 857.

(51) Patrissi, C. J.; Martin, C. R., J. Electrochem. Soc. **1999,** *submitted.*

(52) Che, G.; Lakshmi, B. B.; Martin, C. R.; Fisher, E. R.; Ruoff, R. S., Chem. Mater. **1998,** *10*, 260.

(53) Che, G.; Lakshmi, B. B.; Fisher, E. R.; Martin, C. R., Nature **1998,** *393*, 346.

(54) Che, G.; Jirage, K. B.; Fisher, E. R.; Martin, C. R., J. Electrochem. Soc. **1997,** *144*, 4296.

(55) van de Hulst, H. C. *Light Scattering by Small Particles*; Dover: New York, **1981**.

(56) Foss, C. A.; Hornyak, G. L.; Stokert, J. A.; Martin, C. R., J. Phys. Chem. **1992,** *96*, 7497.

(57) Foss, C. A.; Hornyak, G. L.; Stokert, J. A.; Martin, C. R., J. Phys. Chem. **1994,** *98*, 2963.

(58) Kressin, A. M.; Doan, V. V.; Klein, J. D.; Sailor, M. J., Chem. Mater. **1991,** *3*, 1051.

(59) Zelenski, C. M.; Dorkout, P. K.; Martin, C. R., J. Am. Chem. Soc. **1998,** *120*, 734.

(60) Paul, D. R.; Yampol'skii, Y. P. *Polymeric Gas Separation Membranes*; CRC Press: Boca Raton, FA, **1994**.

(61) Mulder, M. *Basic Principles in Membrane Technology*; Kluwer Academic: Dordrecht, Netherlands, **1990**.

(62) Stinson, S. C., Chem. Eng. News **1995,** *73*, 44.

(63) Hinze, W. L., Colloids and Surfaces **1990,** *48*, 79.

(64) Aoki, T.; Shinohara, K.; Kaneko, T.; Oikawa, E., Macromolecules **1996,** *29*, 4192.

(65) Aoki, T., Polymer **1997,** *38*, 235.

(66) Abe, K.; Goto, M.; Nakashio, F., Sep. Sci. Tech. **1997,** *32*, 1921.

(67) Henis, J. M. S.; Tripodi, M. K., Science **1983,** *220*, 4592.

(68) Loeb, S.; Sourirajan, S. ; University of CA,: Los Angeles, 1960; Vol. Report 60-60.

(69) Ho, W. S. W.; Sirkar, K. K. *Membrane Handbook*; Van Nostrand Reinhold: New York, **1992**.

CHAPTER 2

GOLD NANOTUBULAR MEMBRANES FOR "MOLECULAR FILTRATION"

INTRODUCTION

Membrane based methods are currently used to perform separations for a wide variety of mixtures of increasing diversity and scale(1-3). Some examples include microfiltration(4) and ultrafiltration(5) (sieving mechanism), hyperfiltration and pervaporation(6) (solution-diffusion), gas separation(7) (solution/diffusion or Knudsen diffusion in gases), facilitated transport (in liquid membranes with carrier mediated transport) and membrane distillation (vapor-liquid equilibrium).

One of the principles of membrane based separation methods is 'molecular sieving'. As the name implies, it is the separation of molecules based on size. Sieving occurs when the size of the molecules is comparable to the size of the pores in the membrane used in the separation. Such separations have been commonly achieved using zeolites. Zeolites are aluminosilicates with porous structure whose structural cavities are comparable to the size of molecules(8). The most common separation has been performed on a mixture of gases or hydrocarbons(9-13). However, all these methods do not yield reproducible results due to defects(9, 14).

The development of a simple, inexpensive, highly reproducible method for the fabrication of gold nanotubular membranes is described in this chapter. These membranes exhibit 'molecular sieving' and can completely separate molecules of two different sizes. These membranes were also investigated to study "hindered diffusion", which is the diffusion of molecules in confined environments.

BACKGROUND

Membrane Based Separation Processes

A membrane can be considered as a permselective barrier between two phases. Transport processes occur through a membrane when a driving force is applied to the components in one of the phases. The driving force can be a pressure or concentration or a temperature difference. Table I outlines the classification of membrane processes according to the driving forces.

Thus, membranes are used in a large number of separations ranging from different types of filtration to gas separation and pervaporation. Membrane based separations are not as energy intensive and expensive as conventional techniques like distillation, crystallization, chromatography etc. However, improvements in membrane based separation need to be made to make them viable for large scale commercial use, in terms of both higher fluxes and selectivity(15-19).

Characterization Of Porous Membranes

Membranes can be classified into two main groups: porous and non-porous (Figure 2.1). Porous membranes have pores in the membrane through

Table 2.I Characterization of membrane processes based on the driving forces

Driving Force	Membrane process
Pressure Difference	Microfiltration, Ultrafiltration, Hyperfiltration, Piezodialysis
Concentration Difference	Pervaporation, Gas Separation, Dialysis, Liquid Membranes
Temperature Difference	Thermo-osmosis, Membrane Distillation

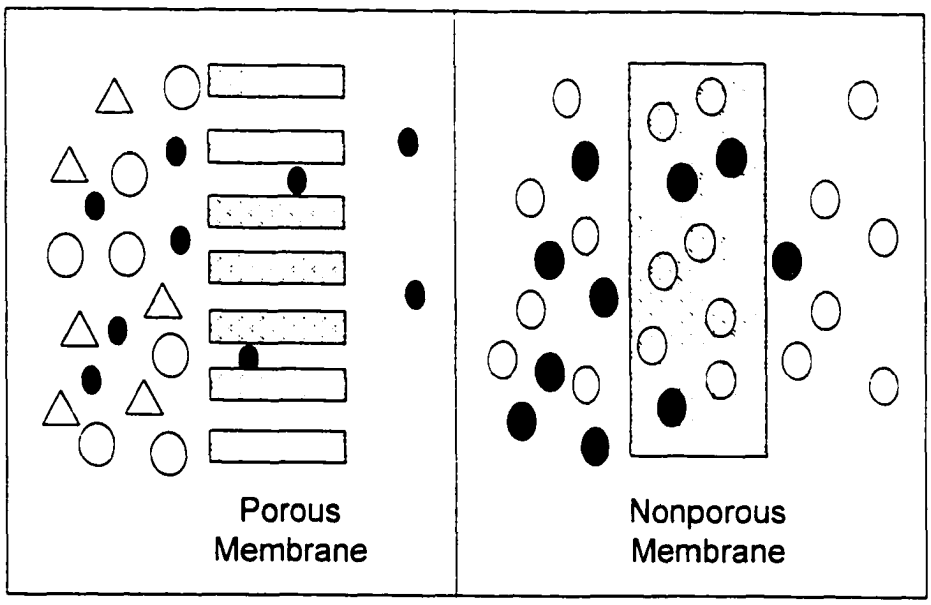

Figure 2.1 Schematic drawing of a porous and nonporous membrane

which the molecules pass. In contrast, non-porous membranes are membranes in which separation is based on the physical property of the membrane material.

In general, porous membranes can be classified into: macroporous (pore size greater than 50 nm), mesoporous (pore size between 2 and 50 nm) and microporous (pore size less than 2 nm). The type of material in a porous membrane is not important. The separation efficiency is determined by the size of the pores and the pore size distribution. For example, the pore size determines which molecules are retained and which can permeate through the membrane.

Non-porous membranes which are used in applications such as pervaporation/gas separation, do not have pores present. The material which composes the membranes determines the performance of separation. The morphology of the polymer material (crystalline, amorphous, glassy, rubbery) used to fabricate the membrane, directly affects the permeability. Factors that affect the performance include temperature, the interaction of the solvent and solute with the polymeric membrane. These factors affect the nature of the material and hence the performance characteristics.

Porous and non-porous membranes can be characterized by a variety of analytical techniques. For example, microfiltration and ultrafiltration membranes are characterized by scanning and transmission electron microscopy, bubble point measurements, mercury intrusion porometry, permeation measurements (gas or liquid), gas adsorption-desorption, thermoporometry, permporometry, rejection measurements to name a few. The various techniques are described in

detail elsewhere(20).

One of the techniques used in the characterization is gas permeation. The transport of a gas through a porous membrane can occur by three different mechanisms which are represented in Figure 2.2. The mechanism of the transport of the gas depends on the size of the pore, the mean free path and the size of the gas molecule. The first mechanism called 'viscous flow' occurs when the pore diameter is much greater than the mean free path of the gas. The mean free path of a gas is given by equation 2.1

$$\Lambda = \frac{kT}{\pi d^2 P\sqrt{2}} \qquad (2.1)$$

where, k is the Boltzmann constant, T is the temperature in K, d is the diameter of the gas molecule and P is the pressure.

The second mechanism known as 'Knudsen Diffusion' occurs when the mean free path of the gas is less than the pore diameter. For Knudsen diffusion, the flux of a gas through a porous membrane is given by equation 2.2.

$$Q = \frac{4}{3}\left[\frac{2\pi}{MR_oT}\right]^{1/2}\frac{n R^3 P}{l}$$

where, Q is the flux of the gas in moles cm^{-2} s^{-1}, n is the pore density in number of pores cm^{-2}, R is the pore radius in cm, ΔP is the differential pressure in dynes cm^{-2}, M is the molecular weight of the gas in g mol^{-1}, R_o is the gas constant in erg K^{-1} mol^{-1}, T is the temperature in Kelvin and L is the thickness of the membrane in cm. Thus, by measuring the flux of a gas at a known pressure, the radius of

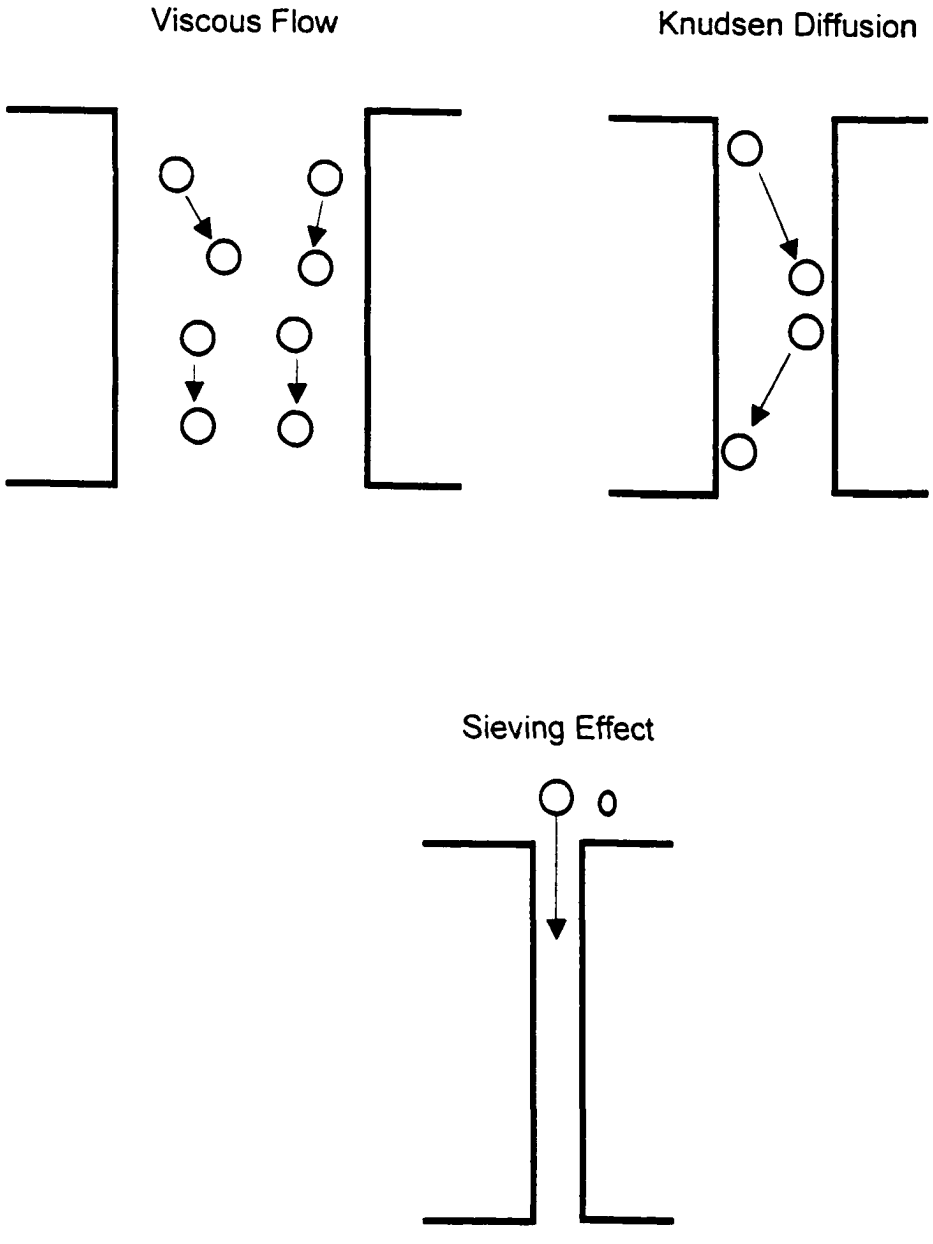

Figure 2.2 Mechanisms of flux of a gas through a pore

pores can be calculated because all the other factors are known.

The third mechanism is called 'molecular sieving' and occurs when the size of the gas molecule is comparable to the size of the pore(20). The mean free paths of He and CH_4 at 20 psig, are 50 and 25 nm respectively. The permeation of He will occur by Knudsen diffusion in a membrane with pores less than 50 nm and will change to 'molecular sieving when the size of the pores is comparable to the size of He molecule.

'Molecular Sieving' Or 'Separations Based On Size'

'Molecular sieving' is a popular method for separating molecules(20). Both natural and synthetic zeolites are well known 'molecular sieves'. They have cavities formed by the crystal structure(8). Zeolites have been used in large number of instances to achieve separation of various gases and hydrocarbons, based on the difference in size(10, 12, 13, 21). One common gas pair studied in separation science is the n-butane/i-butane. Yan et al. reported a selectivity value of approximately 10 using a MFI type zeolite membrane(11). A ratio of 50 at 20^0C for the gas pair has been reported, using a zeolite membrane(12). Large values like 90 have been reported by Vroon and coworkers using a MFI type zeolite membrane with alumina support(22). However, in all these cases and other such examples, the main drawback has been reproducibilty of the membrane fabrication process(9).

One of the methods developed to improve the selectivity or the separation factor has been to deposit materials within the pores of zeolite and zeolite like materials to make them smaller. Niwa and coworkers showed that the sorption

characteristics of zeolite A was reversed after deposition of silicon methoxide in the pores using chemical vapor deposition (CVD)(23). Zeolite A preferentially adsorbed N_2 relative to O_2. This was due to the chemical nature and not based on size (N_2 is larger than O_2). However, this trend is reversed with the zeolite modified with the silicon methoxide. The modified zeolite adsorbed O_2 and not N_2. This result was due to the smaller cavities obtained.

Ozin and Steele demonstrated that MOCVD (metal organic CVD) can be used to decrease the pore size of zeolite Y, in order to discriminate between H_2S and H_2Se(24)(differ in kinetic diameters by only 0.2 Å). Colloidal silica has also been used to plug large pores of Anodisc alumina membrane to decrease the defects in the membrane(25). Pd has been deposited using CVD to achieve larger selectivity values in H_2/N_2 separation. A selectivity as high as 1000 was achieved for H_2/N_2 separation by depositing Pd in an α-alumina support membrane(26).

There are a large number of instances where tetraexthoxysilane (TEOS) and methyltriethoxysilane (MTES) have been used to decrease the pore size in zeolites to achieve more effective separations. A CO_2/CH_4 selectivity of 71 was obtained after the deposition of TEOS compared to a value of 12 obtained before the deposition of TEOS(27). Nomura and coworkers achieved an n-butane/i-isooctane selectivity of 88 after deposition of TEOS in a zeolitic membrane(28).

As mentioned before, zeolite or zeolite-type materials have been used with and without modification to achieve different types of separations. However, a major drawback in these cases has been the reproducibility of the method.

Also, in most of these cases even though large values of selectivity have been reported, there are very few instances of complete separations that have achieved in the range <1 nm.

In a recent report, de Vos and Verweij, describe a method to fabricate silica membranes that show large fluxes and complete separation of gases(14). However, the method required stringent conditions of cleanliness and the fabrication process was complex.

This chapter describes unique membranes developed to separate molecules base on size. These membrane were fabricated using a template method and electroless gold deposition. Gold nanotubular membranes with precisely controlled diameters were obtained by this method. The fabrication process was simple, inexpensive and highly reproducible. It will be demonstrated that these membranes can discriminate molecules which differ in size by approximately 0.5 nm.

Hindered Diffusion

There is a great deal of interest in studying the diffusion properties of molecules in confined or restricted environments(29) and has generated numerous theories to understand hindered diffusion(30, 31). One of the earliest studies of hindrance factors from steric considerations was conducted by Ferry in 1936(32). One objective to study hindered diffusion was to better understand the permeability properties in biological structures such as blood capillaries(30, 31). More recently, the concept has been investigated to better understand transport in fine pores for use in separations and reaction engineering(33, 34).

One of the commonly accepted theories for "hindered diffusion" was put forth by Renkin in 1954(31). He proposed that the total restriction to diffusion was due to the combined effects of steric hindrance at the entrances to the pores and the frictional resistance within the pores. He studied the diffusion of several molecules including water, urea, glucose, and hemoglobin among others and compared these diffusions to theory. A good agreement between experiment and theory was observed. He also demonstrated that 'molecular sieving' during ultrafiltration was a function of the total pore area per unit length, pore radius, molecular radius, and filtration rates(31).

Most of experimental studies on hindered diffusion performed in the past were conducted with relatively large pores like microporous polycarbonate membranes, or porous glass and the molecules chosen were large macromolecules(35-38). This is because only membranes with such large pores were available at that time. The effect of molecular size and configuration on the diffusion in microporous polycarbonate membrane has been evaluated(39). Studies have also been conducted in glass capillaries, mica and similar materials(36). In all these cases, the experiments were conducted with polymers or large molecules and this was compared to the most commonly accepted theories.

This chapter reports the investigation of gold nanotubular membranes to study 'hindered diffusion'. The flux of ninhydrin was first determined in different membranes with different diameters. Then, using Fick's law the diffusion coefficient of ninhydrin was determined for nanotubules of different sizes.

EXPERIMENTAL

Materials

Polycarbonate "track-etched" membranes (6 μm thick, 30 nm diameter and $6x10^8$ pore cm^{-2}) were obtained from Poretics. Anhydrous $SnCl_2$, $AgNO_3$, $NaHCO_3$ (Aldrich), trifluoroacetic acid, Na_2SO_3, NH_4OH, H_2SO_4, formaldehyde, anhydrous methanol (Mallinckrodt) were used as received. Methylviologen, pyridine, quinine, ninhydrin (Aldrich), Ruthenium tris(2, 2' -bipyridine) (GFS) were used as received. Commercial Au plating solution (Oromerse SO Part B) was obtained from Technic Inc. Milli-Q 18Ω water was used to prepare all solutions and to rinse the membranes.

Electroless Gold Deposition

An electroless deposition procedure developed previously in the group was adapted to obtain more uniform deposition of Au(40). The template membrane was rinsed in methanol for 5 minutes and then immersed in a solution that was 0.025 M in $SnCl_2$/0.07 M in trifluoroacetic acid for 45 minutes. The membrane was rinsed in methanol two consecutive times for 2.5 minute each. The membrane with the sensitizer, Sn^{2+} anchored to the membrane was immersed in an aqueous solution of ammoniacal $AgNO_3$ for 5 minutes. The membrane was rinsed with methanol for 5 minutes to remove excess Ag solution. Finally the membrane was placed in the Au plating bath which consisted of 0.5 ml of the commercial Au plating solution, 0.127 M Na_2SO_3, 0.625 M formaldehyde and 0.025 M $NaHCO_3$. The pH of this solution was 12; it was adjusted to 10 by dropwise addition of 0.5 M H_2SO_4, with constant stirring. The

temperature of this plating bath was maintained at 5°C. Membranes were placed in the gold plating bath for different periods of time to obtain nanotubules of different diameters.

Gas Flux Measurements And Nanotubule Diameter Determination

The inside nanotubule diameter was determined by measuring the gas flux (He and H_2) across the membrane. The gas transport cell described previously was used(18). The gas permeation samples were placed in a vacuum oven for at least 12 hours prior to making the flux measurement. This was done to remove traces of water or any volatile species absorbed by the membrane. Reproducible values of fluxes were obtained after treating the samples in this manner. The membrane was placed in a cell and the upper and lower portions of the cell were evacuated. The upper half was pressurized at 20 psig. The pressure versus time transient at steady state was measured. This was converted to flux (moles cm^{-2} s^{-1}), from which the nanotubule diameter values were obtained.

Permeation Experiments

Permeation experiments were carried out in U-tube set up in Figure 2.3. The sample was placed between two O-rings joints of the U-tube and then secured by a clamp. The samples were prepared by sandwiching the membrane between two pieces of tape (3M Scotch brand # 375). The tape was punched with a hole to expose the membrane to the solution. The membrane was placed in a U-tube setup for at least 12 hours with water in the U-tube, to ensure that the membrane was wetted. The solutions in both halves of the U-tube were stirred

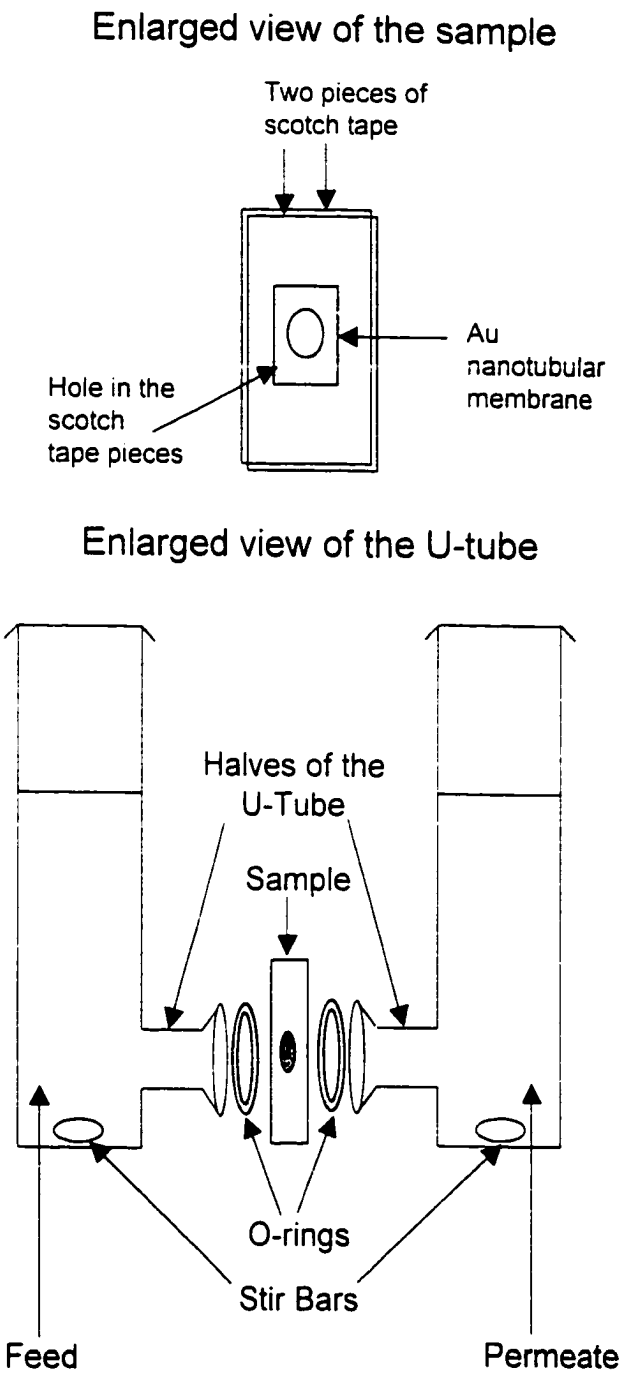

Figure 2.3 Experimental setup used in a permeation experiment

continuously during the permeation experiment.

The permeation experiments were conducted with 50 mM MV^{2+} (methylviologen), 25 mM $Ru(bpy)_3^{2+}$ Ruthenium tris(2, 2' -bipyridine), 0.5 mM pyridine, 0.5 mM quinine, 10 mM ninhydrin (feed concentrations). While comparing the flux of two molecules the flux was normalized for the feed concentration. The flux was obtained either by monitoring the UV-absorbance with a Hitachi U-3502 UV-Vis-NIR spectrophotometer at regular intervals or by continuously monitoring the absorbance of the permeate with a Waters 482 detector. The wavelengths at which each molecule was monitored was as follows: MV^{2+} (258 nm), RB^{2+} (286 nm), pyridine (252 nm), quinine (340 nm), ninhydrin (232 nm). For more sensitive detection of quinine, fluorescence was determined ($\lambda_{ex.}$ = 308 nm, λ_{em} = 403 nm) with a HP Fluorometer.

RESULTS AND DISCUSSION

Fabrication Of Gold Nanotubular Membranes

An electroless deposition procedure was used to fabricate gold nanotubular membranes with polycarbonate "track-etched" membranes as a template(40). Figure 2.4 shows the three steps in the deposition procedure(40). The first step was activation of the surface of the membrane by immersing the membrane in an acidic Sn^{2+} solution. The surface of the membrane is negatively charged due to surface species like OH^- formed during the etching step in the membrane fabrication process. The Sn^{2+} ions were anchored to the membrane surface and its pore walls. The second step involved immersing the membrane in an ammoniacal $AgNO_3$ solution. This caused the displacement of the Sn^{2+}

Step 1. Activation of the pore walls

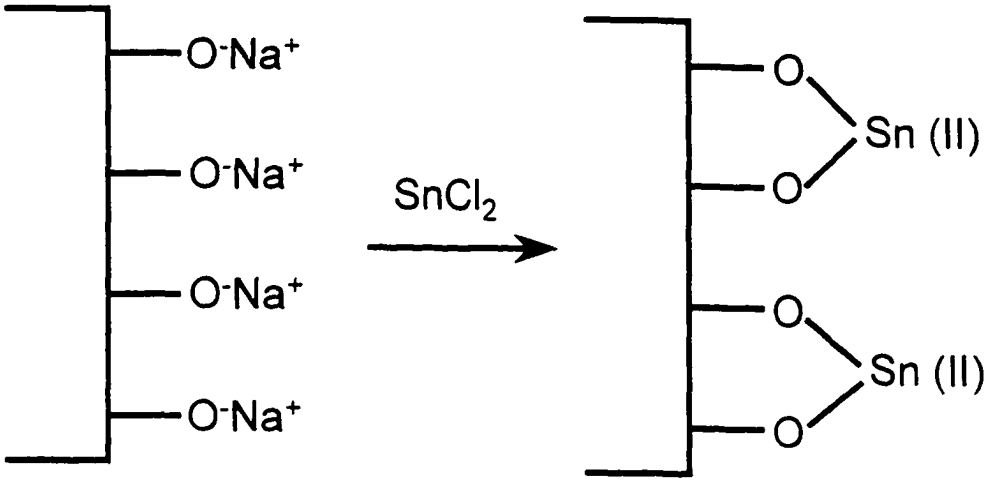

Step 2. Electroless deposition of Ag

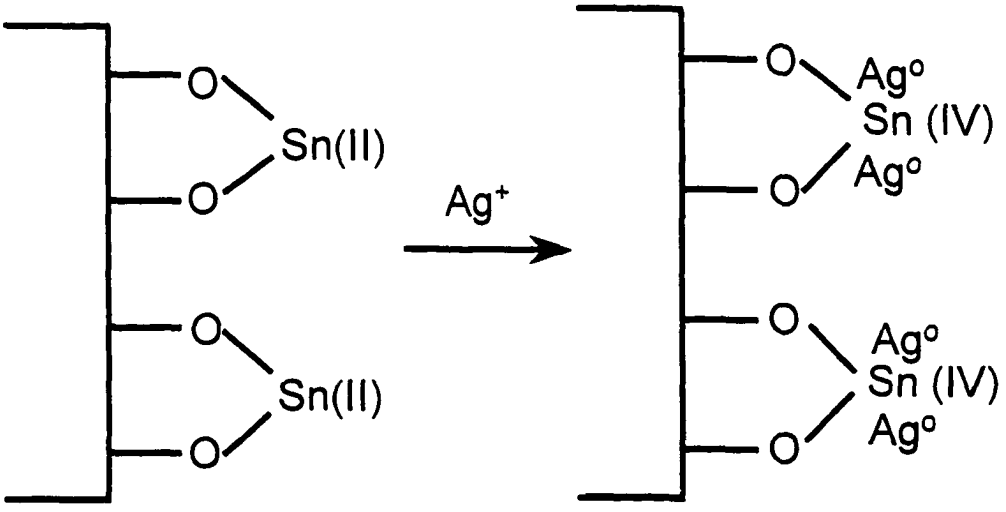

Step 3. Redox displacement of Ag by Au, to create an Au activated surface

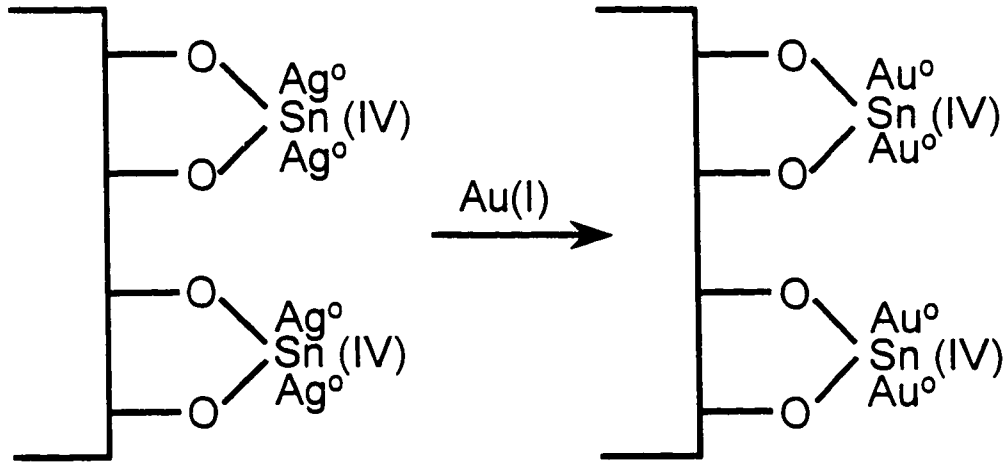

$$2Au(I) + HCHO + 3OH^- \longrightarrow HCOO^- + 2H_2O + 2Au(0)$$

Figure 2.4 Electroless deposition of gold in a polycarbonate template membrane

cations by metallic Ag to result in a monolayer of Ag. The third step was to place the membrane in the gold plating solution which contained the gold complex, $Na_2[Au(SO_3)]$ and a reducing agent, formaldehyde. The pH of the solution was lowered from 12 to 10 to decrease the rate of deposition.

This method was used to deposit gold in the pores of the membrane. If the time of deposition was very long, the pores were completely filled and fibers were obtained. It has been demonstrated that with the membrane intact, the surface layer can be removed to access the end of these Au fibers which appeared as an ensemble of nanoelectrodes(40). If necessary, the template membrane can be removed to access the micro- or nanostructures. In contrast, if the time of deposition is short, gold nanotubules were obtained as shown in Figure 2.5(2, 41). Au nanotubules of different diameters were obtained by placing the membrane in the Au plating solution for varying lengths of time(41).

Characterization Of Gold Nanotubular Membranes

The diameter of the pores in the template membrane was 30 nm. The Au nanotubules formed by consequent deposition of Au made the tubules smaller than 30 nm. Gold nanotubular membranes samples were microtomed to image using a transmission electron microscope (TEM). Figure 2.6a shows the TEM of a plain polycarbonate membrane, 2.6b shows a membrane plated with Au for an hour. Further Au plating resulted in fibers and is shown in Figure 2.6c. The Au tubules as can be seen in the micrographs were smeared by the microtome process; therefore this technique could not be used for determination of the tubule diameter. However, gas flux through porous membranes has been

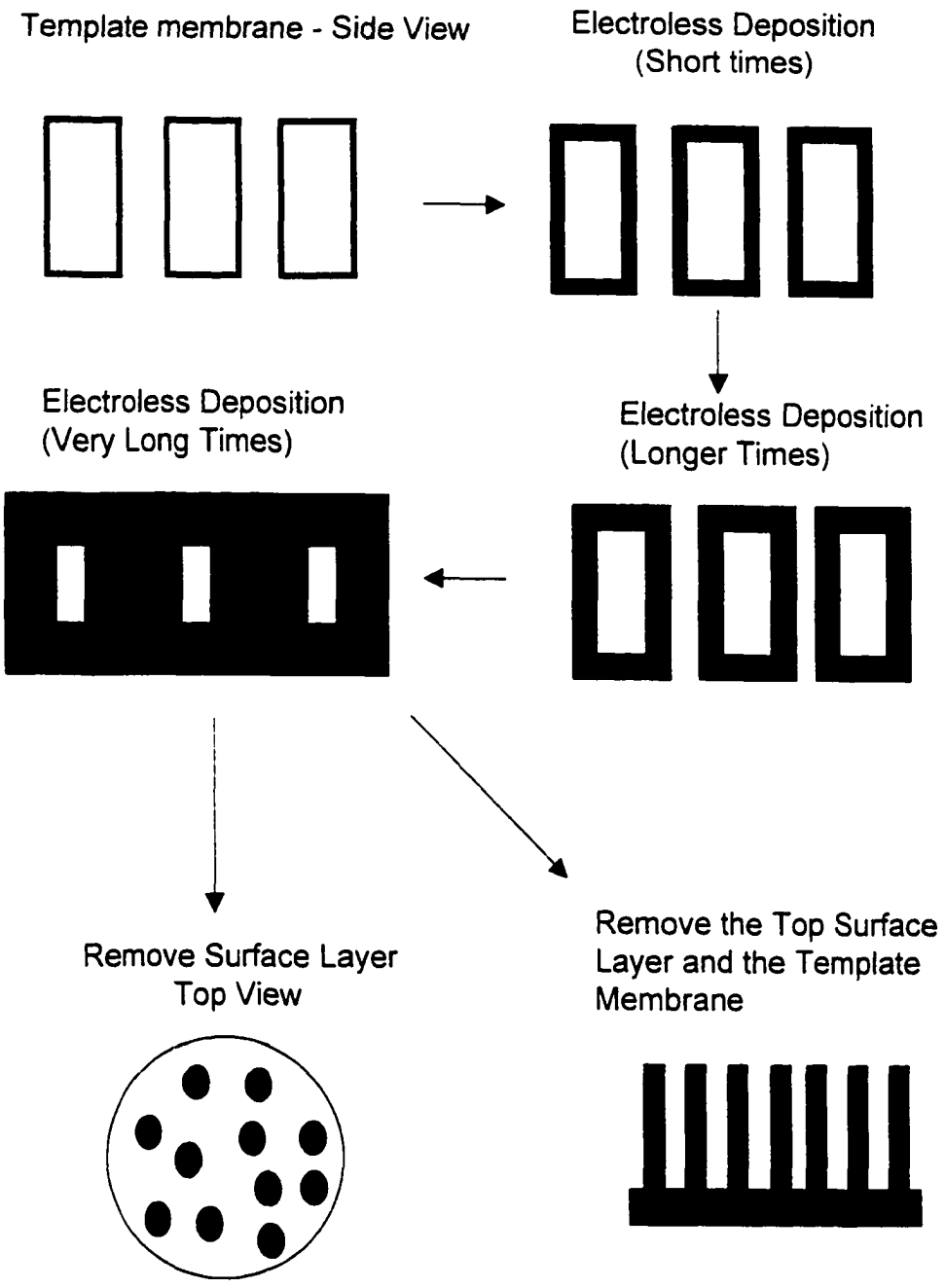

Figure 2.5 Fabrication of Gold Nanotubules, Nanoelectrode ensemble and Nanofiber array

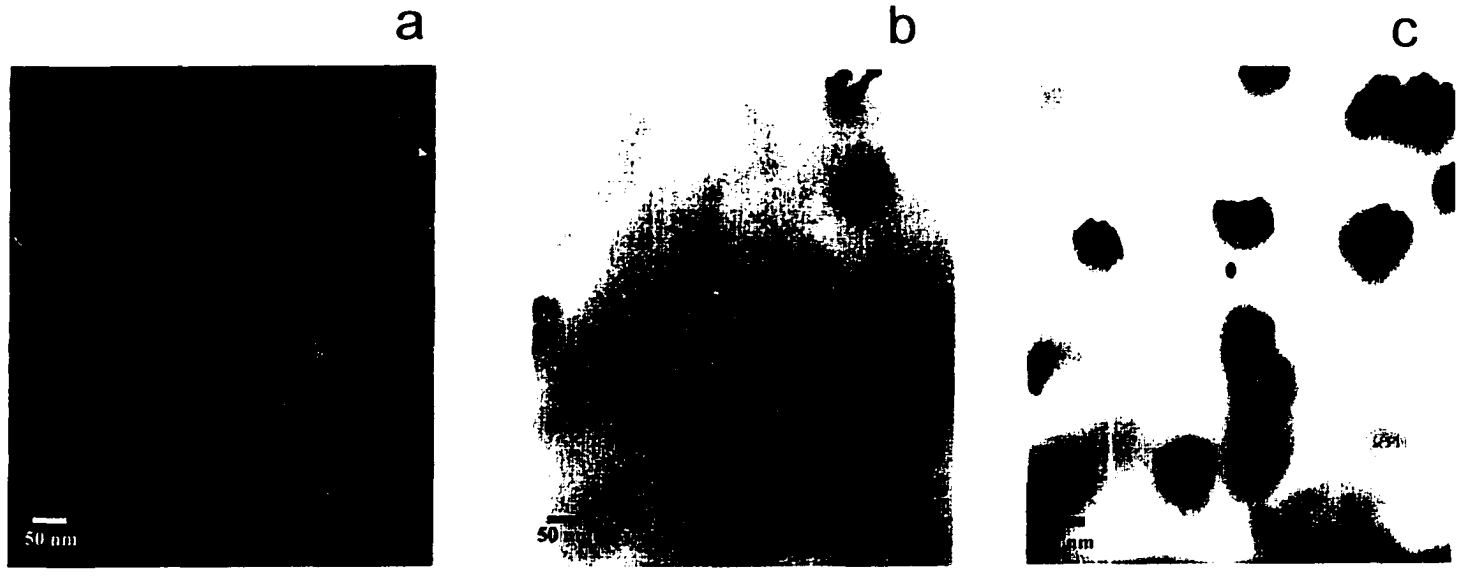

Figure 2.6 Transmission electron micrographs of a) plain polycarbonate membrane b) gold nanotubules and c) gold nanofibres

previously used to determine the size of the pores(42). This method was adapted to characterize the gold nanotubular membranes.

Gas Permeation Experiments

Gold nanotubular membranes of different diameters were fabricated by varying the plating time. Fluxes of N_2, O_2, H_2 and He were determined. Figure 2.7 shows a graph of selectivities for the gas pairs (O_2/N_2 and H_2/He) with plating time. If the mechanism of diffusion were Knudsen diffusion, the flux of a gas would be inversely proportional to the molecular weight of the gas. The calculated ratios of the flux of two gases would be the inverse of the ratio of their molecular weights. Thus, in the case of Q_{O2}/Q_{N2} would be 0.93 and in the case of Q_{H2}/Q_{He} the ratio would be 1.41. As can be seen in Figure 2.7, Q_{H2}/Q_{He} ratio of 1.38 was obtained at all plating times, but for Q_{N2}/Q_{O2}, the ratio was 1.06 at short plating times and increased to 2.85 at the longest plating time.

It was concluded that H_2 and He gases had small enough diameters that the mechanism of transport was by Knudsen diffusion. However, for N_2 and O_2, the mechanism was Knudsen diffusion in large nanotubules and changed over to 'molecular sieving' in small nanotubules. To reiterate, molecular sieving is observed when the flux is determined by the kinetic diameter of the gas.

Therefore, the flux of H_2 and He gases and equation (2.2) were used to determine the Au nanotubule diameters at different plating times. Figure 2.8 shows the data obtained from these calculations. The pore diameter of the plain polycarbonate membrane is 30.0 nm, after plating Au for 4 hours the diameter was 3.0 nm. The rate of deposition at the initial stages is much faster than in the

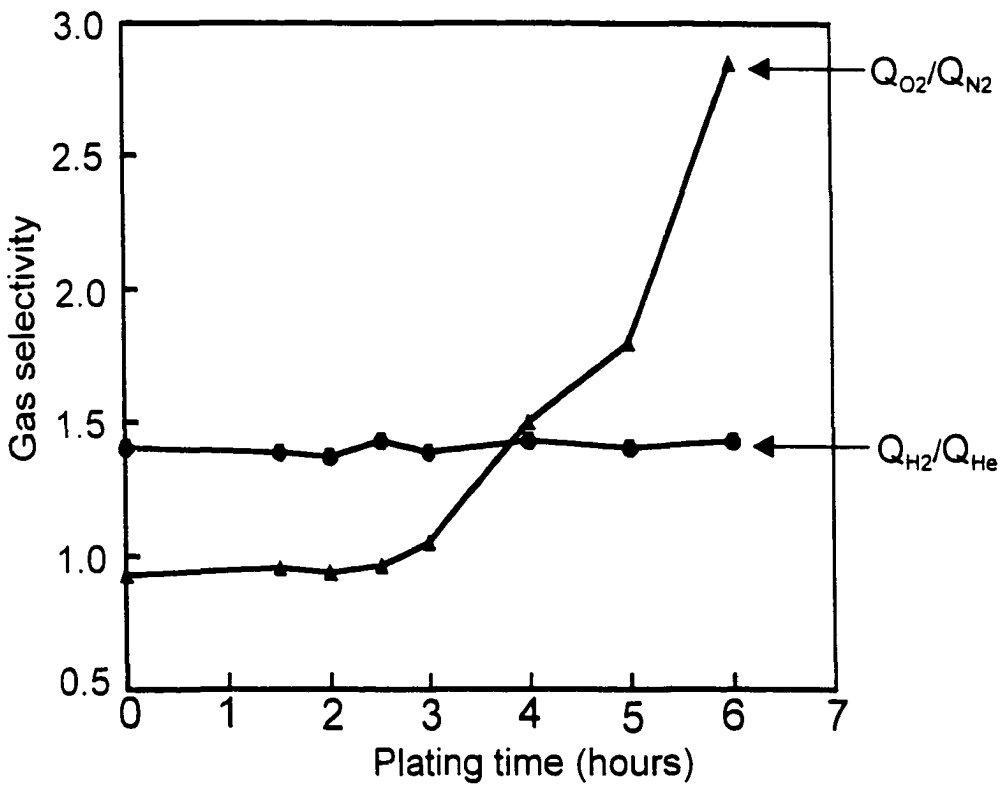

Figure 2.7 Variation of selectivity (Q_{O2}/Q_{N2} and Q_{H2}/Q_{He}) with plating time

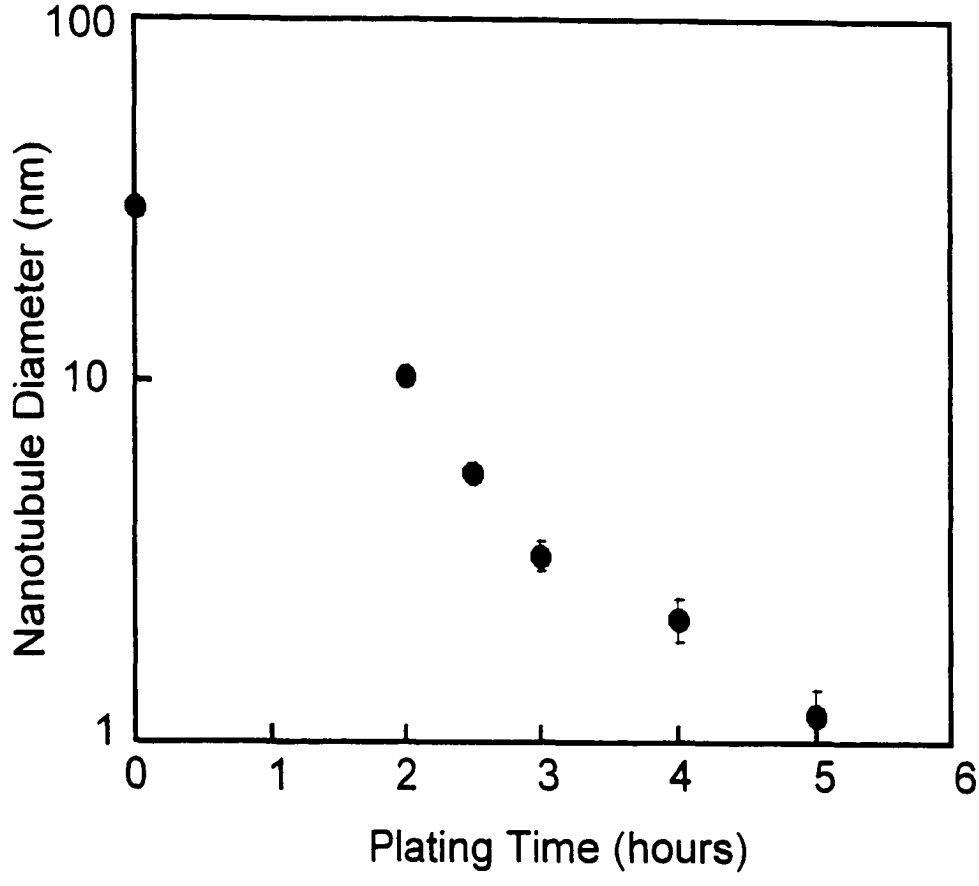

Figure 2.8 Variation of gold nanotubule diameter with plating time

later stages. Nanotubules as small as 0.6 nm were obtained by this method.

Permeation Experiments

Gold nanotubules with very small diameters approaching the size of molecules were fabricated. Since the diameters of these tubules were comparable to the size of molecules, experiments were designed to test these membranes for "molecular filtration".

Single Molecule Permeation Experiments

The objective of these experiments was to determine if these membranes were selective for the smaller molecule in a given "small molecule/large molecule" pair. The flux of the small molecule was first determined. The membranes were rinsed with water, placed in a U-tube with water overnight, then the flux of the "large molecule" was determined. The flux of both the molecules was compared after normalizing for the feed concentration.

The "small molecule/large molecule" pair chosen for this experiment was "methylviologen/ruthenium- trisbipyridine" (MV^{2+}/ RB^{2+}). The chemical structure of the two molecules is shown in Figure 2.9. These molecules were chosen because they are soluble in water, absorb UV light and have the same charge(+2). Furthermore, these molecules have similarities in their chemical structures.

First, a control experiment was conducted with as received polycarbonate membrane with 30 nm diameter pores. Figure 2.10 shows the flux of these two molecules in the plain membrane. The ratio of the fluxes was 3 and was within experimental error of the ratio of the diffusion coefficients of these molecules (D

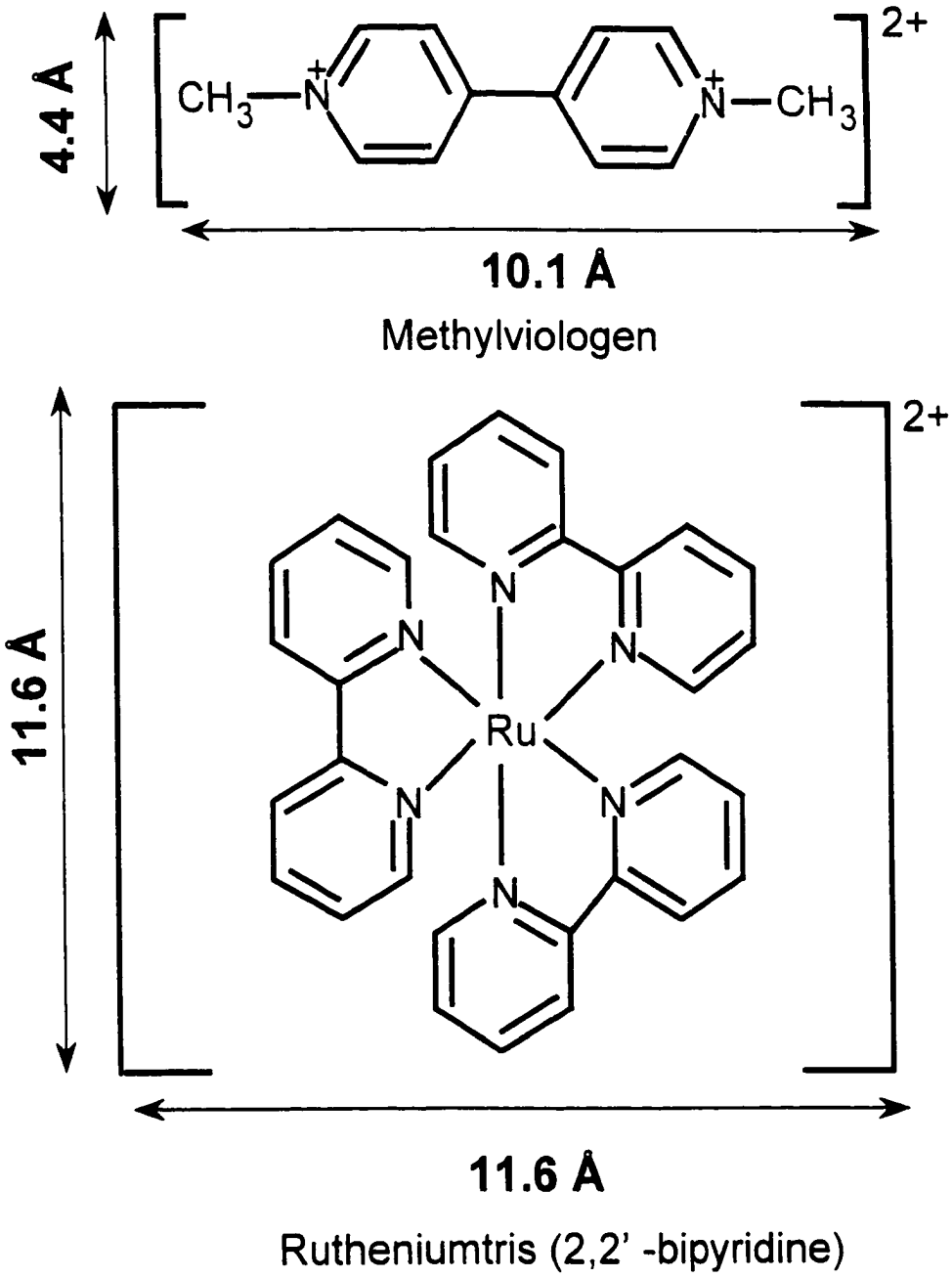

Figure 2.9 Structures of methylviologen and rutheniumtris (2, 2' -bipyridine)

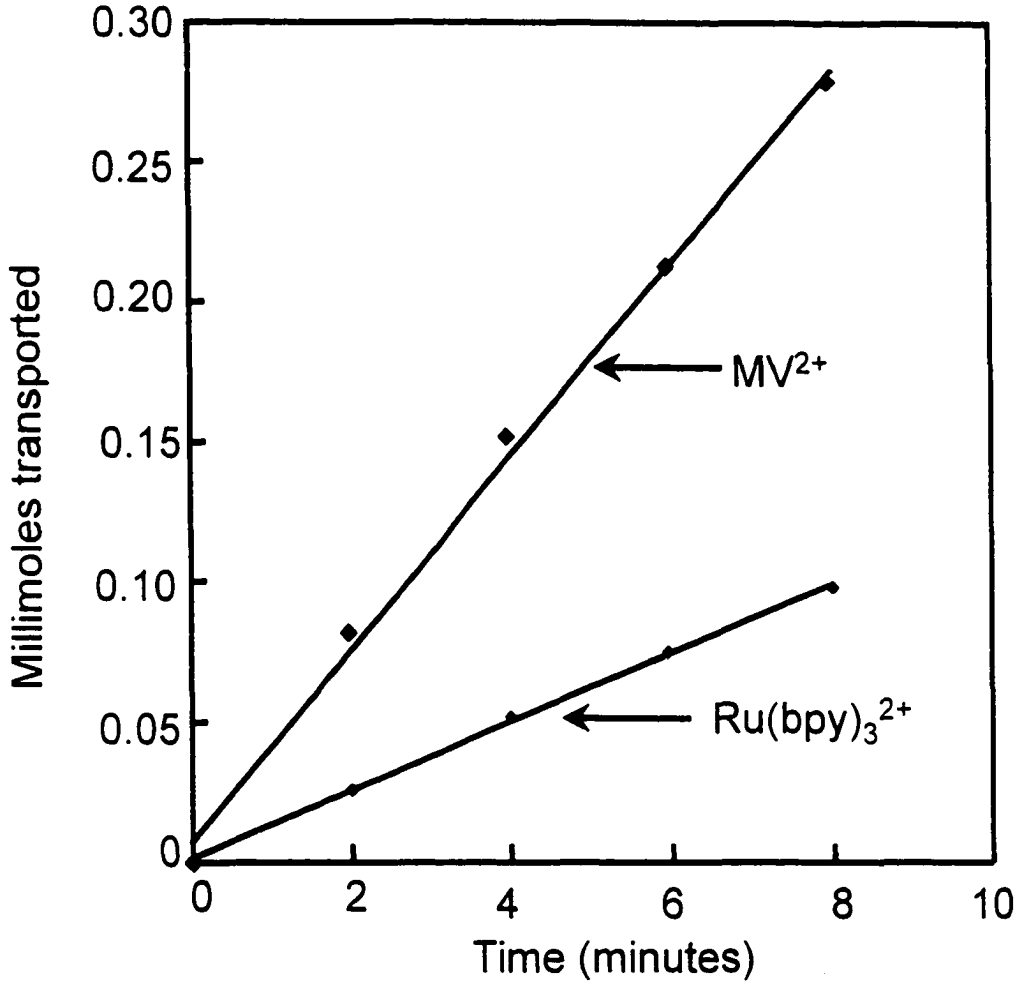

Figure 2.10 Moles of MV^{2+} and $Ru(bpy)_3^{2+}$ transported versus time in a plain 30 nm diameter plain polycarbonate membrane

of MV^{2+} = $9.3x10^{-6}$ cm^2 s^{-1}, RB^{2+} = $6.2x10^{-6}$ cm^2 s^{-1}). Thus, the plain polycarbonate membrane exhibited little sieving.

The flux of both MV^{2+} and RB^{2+} was determined in Au nanotubular membranes with a series of diameters. Figure 2.11 shows the variation of the flux of both the molecules in Au nanotubular membranes with plating time. Figure 2.12 shows the variation of the selectivity with plating time. The flux of both the molecules decreased with decrease in nanotubule diameter, while the selectivity for the smaller increased with decrease in nanotubule diameter. The selectivities observed for MV^{2+} with respect to RB^{2+} were 50 for 10 nm tubules, 90 for 3 nm tubules, 200 for 2 nm tubules and infinity for less than 0.6 nm respectively. This trend is expected for molecular sieving. However, an interesting anomaly was observed (Appendix I). The membrane with the smallest nanotubule (less than 0.6 nm) showed infinite selectivity because no flux of RB^{2+} was observed. "Molecular sieving" was demonstrated using single molecule permeation experiments. In addition, membranes smallest tubules (less than 0.6 nm) completely eliminated the flux of the "large molecule", RB^{2+}, yet showed a measurable flux for the "small molecule", MV^{2+}.

Nanotubule Structure

Initially, it was believed that the electroless gold deposition rate was identical on the surface and the pore walls of the membrane. However, it was concluded from the experiments described below that the deposition was faster on the surface than in the pores. That is, "bottle-neck" tubules were obtained by this deposition procedure.

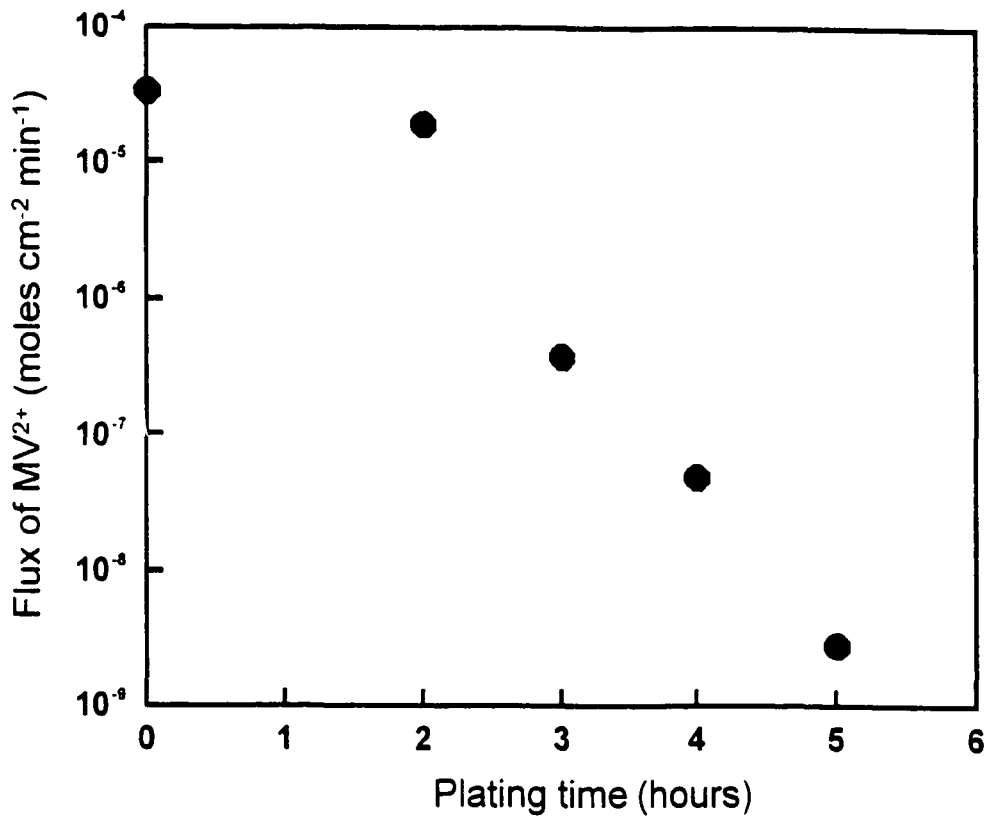

Figure 2.11 a Variation of flux of MV^{2+} with plating time

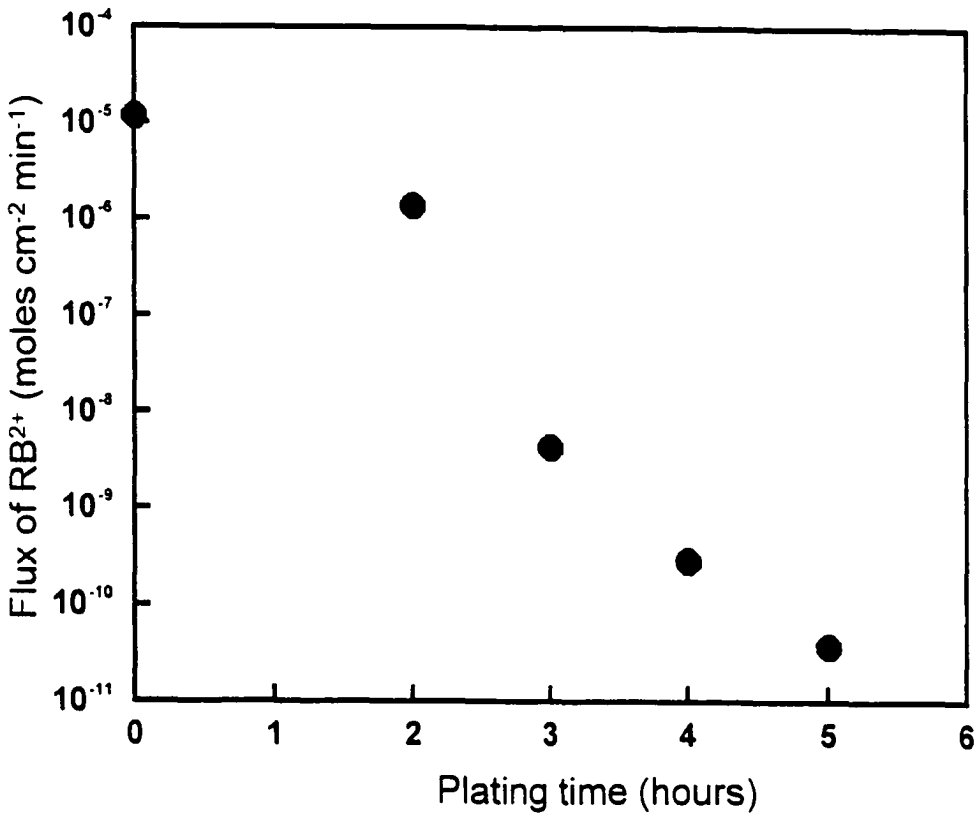

Figure 2.11 b Variation of flux of $Ru(bpy)_3^{2+}$ with plating time

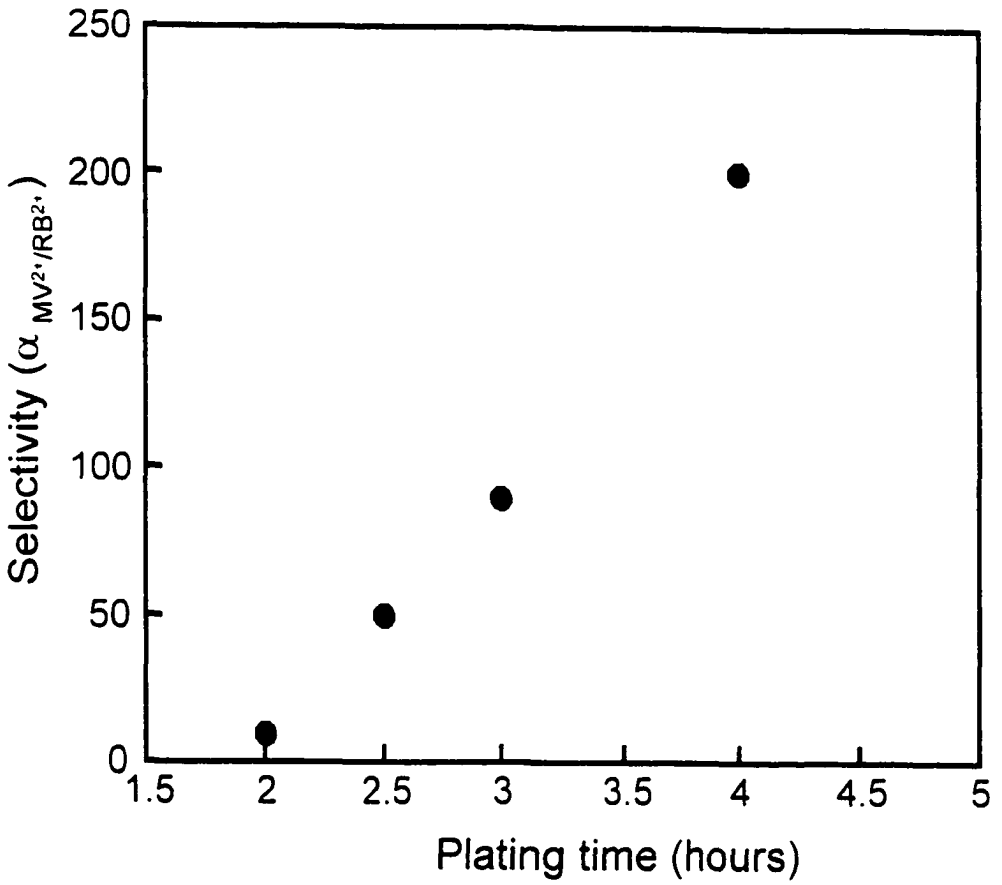

Figure 2.12 Variation of selectivity, $\alpha_{MV^{2+}/RB^{2+}}$ with plating time

The gas flux through a membrane plated for 4 hours with the surface layers present was 2.8×10^{-7} moles cm^{-2} s^{-1}. This flux increased to 2.3×10^{-6} moles cm^{-2} s^{-1} after the removal of the surface layers. Permeation experiments were also conducted with ninhydrin and the same trend was observed. The flux with both the surface layers present 1.4×10^{-11} and both the surface layers removed was 1.8×10^{-10} moles cm^{-2} s^{-1}.

Furthermore, when Au plating was conducted at pH 12, the constriction at the surface was larger. A membrane plated for 8 hours was able to separate MV^{2+} from RB^{2+} as opposed to a membrane plate for 24 hours at pH 10. It is advantageous to fabricate nanotubules with bigger constriction because a higher flux can be achieved without compromising the selectivity of the separation.

Mixed-Molecule Experiments

Experiments conducted with a single molecule indicate that membranes can be fabricated to allow the passage of only the "small molecule" in a "small molecule/large molecule". However, the practical experiment would be to demonstrate if sieving takes place when the two molecules are present in a mixture. Two sets of "small molecule/large molecule" pairs were tested to determine if the "large molecule" did not permeate through the membrane due to size exclusion. They were MV^{2+}/RB^{2+} and pyridine/quinine. These experiments were conducted with membranes that showed no flux for RB^{2+} and quinine in the single molecule experiment. The UV spectrum of the permeate was taken after 72 hours.

A large absorbance corresponding to the "small molecule" in both the

cases was observed and no absorbance due the "large molecule" was observed. The absence of the "large molecules" RB^{2+} and quinine was further confirmed by a more sensitive tool, fluorescence. No fluorescence signal corresponding to RB^{2+} and quinine was observed.

Figure 2.13a shows the UV spectrum of MV^{2+} and RB^{2+} of equal concentration. Figure 2.13b shows the permeate after 72 hours of filtration. As demonstrated by this figure, the permeate contains only MV^{2+}. The absence of RB^{2+} was also confirmed by using a more sensitive technique, fluorescence.

Figure 2.14a shows the UV spectrum of pyridine and quinine of equal concentration. Figure 2.14b shows the permeate after 72 hours of filtration. The permeate contains pyridine. The absence of quinine was also confirmed by fluorescence.

Calculations were done to determine the minimum selectivity observed in these two cases. This was carried out as follows. At first, the concentration of pyridine and MV^{2+} was determined from the UV spectrum. Then, the detection limit for each molecule by fluorescence was determined. Since, no fluorescence signal was observed in each case, the permeate contains, if any, an amount less than the detection limit for the two molecules. The minimum selectivity was calculated by taking the ratio of the concentration of pyridine or MV^{2+} to that of the detection limit of quinine or RB^{2+} respectively. These values are reported in Table 2.

Hindered Diffusion And Diffusion Coefficients In Nanotubules

There is great interest in determining the diffusion coefficients of

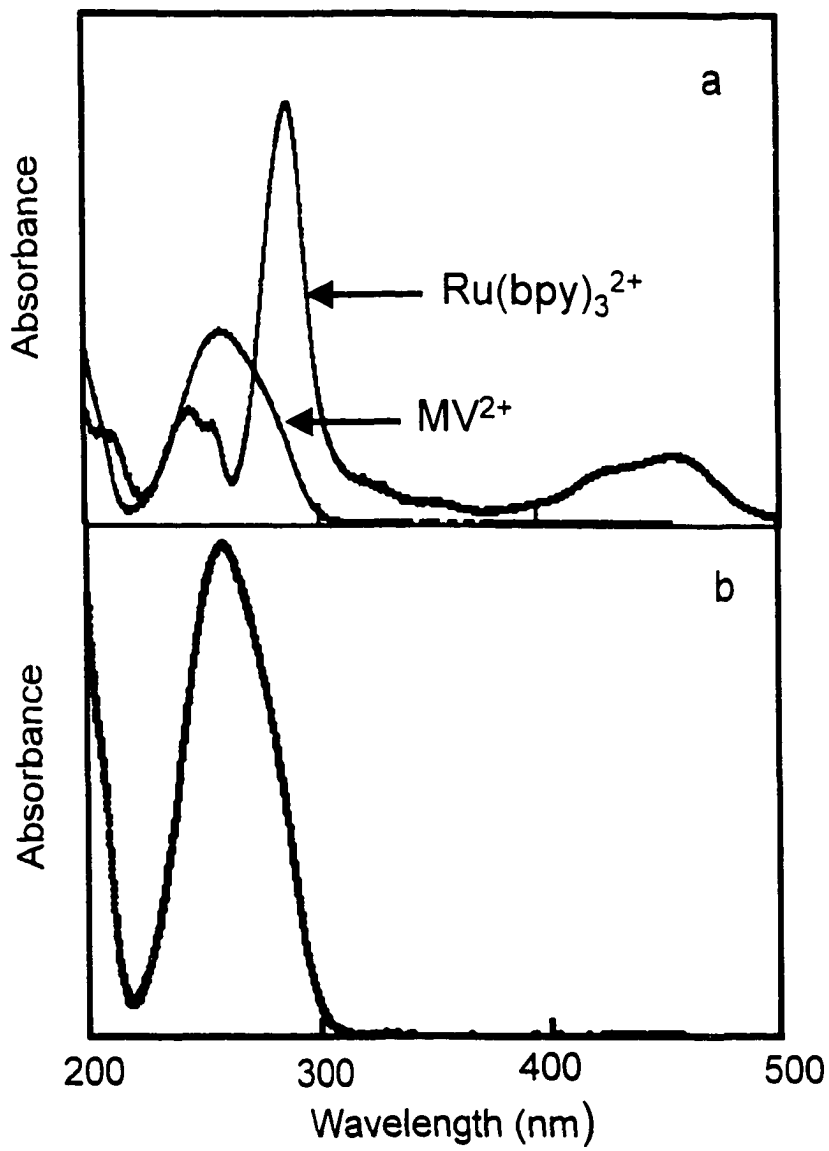

Figure 2.13 a) UV spectrum of equal concentrations of MV^{2+} and RB^{2+}
b) UV spectrum of the permeate after 72 hours

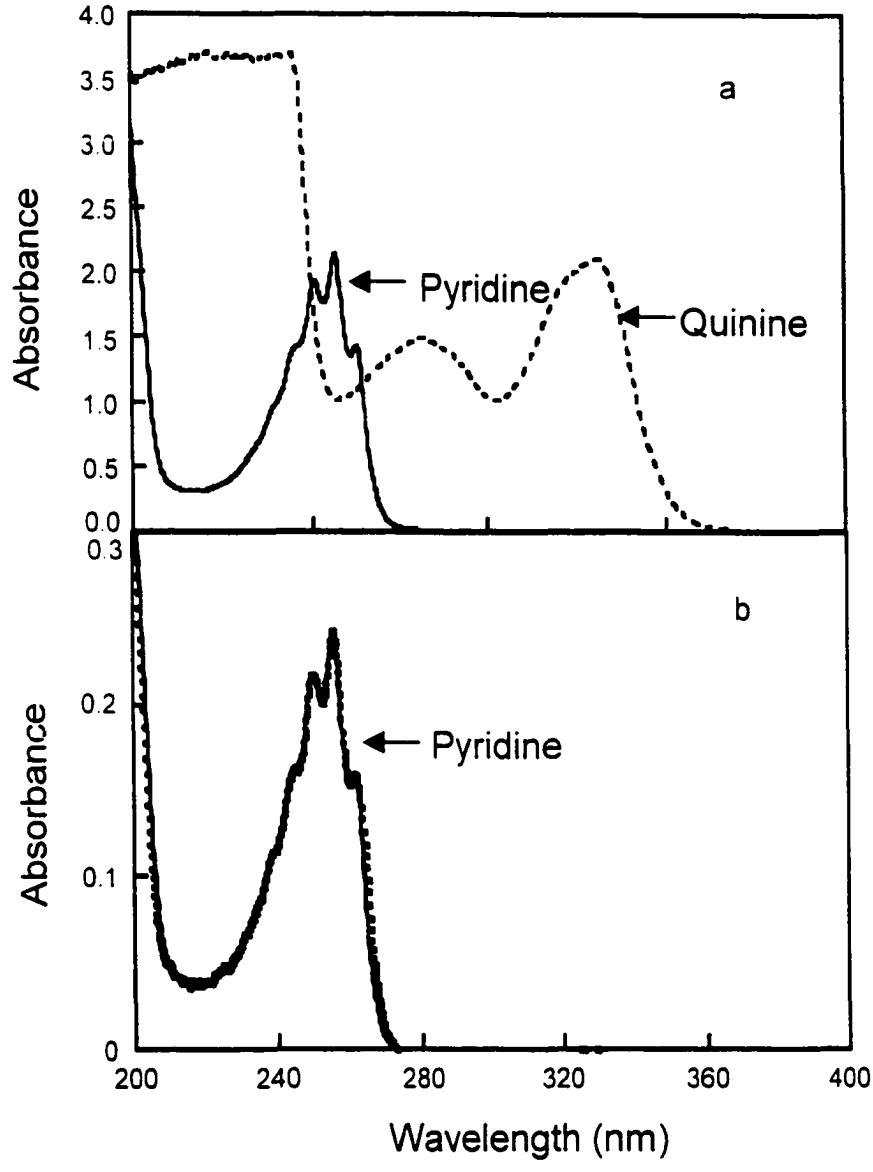

Figure 2.14 a) UV spectrum of pyridine and quinine
b) UV spectrum of the permeate after 72 hours

Table 2.2 Minimum Selectivity Coefficients

Small Molecule	Large Molecule	Minimum Selectivity Coefficient
Methyl viologen chloride	Ruthenium tris(2,2'-bipyridine)	1500
Pyridine	Quinine	15000

molecules in tubules when the size of the molecule approaches the diameter of the tubules. In the past it has not possible to fabricate tubules with precisely controlled diameters in the range that has been done here. Since the membranes described here were in same size range as the size of molecules, the diffusion coefficients were determined in membranes with different nanotubule diameters. All the experiments were conducted with both surface layers removed, to avoid the constrictions formed by both the surface layers.

The diffusion coefficients were determined as follows. At first, the flux of ninhydrin was determined in different membranes. Then, using Fick's first law of diffusion, the diffusion coefficients were calculated. Figure 2.15 shows the variation of the diffusion coefficient with the plating time. The diffusion coefficient dropped by two orders of magnitude from the bulk solution to the solution confined in the smallest nanotubules. Such a drop in the diffusion coefficient value has not been observed before. However, it must be noted that in the past it has been difficult to fabricate such small and uniform tubules, and studies were conducted by using large pores and large molecules like polymers or macromolecule.

CONCLUSIONS FOR CHAPTER 2

Gold nanotubular membranes were fabricated using a combination of an electroless deposition procedure and template method. The method was successfully adapted to form precisely tunable Au nanotubules. It was also shown that these membranes were capable of separating molecules based on their difference in sizes.

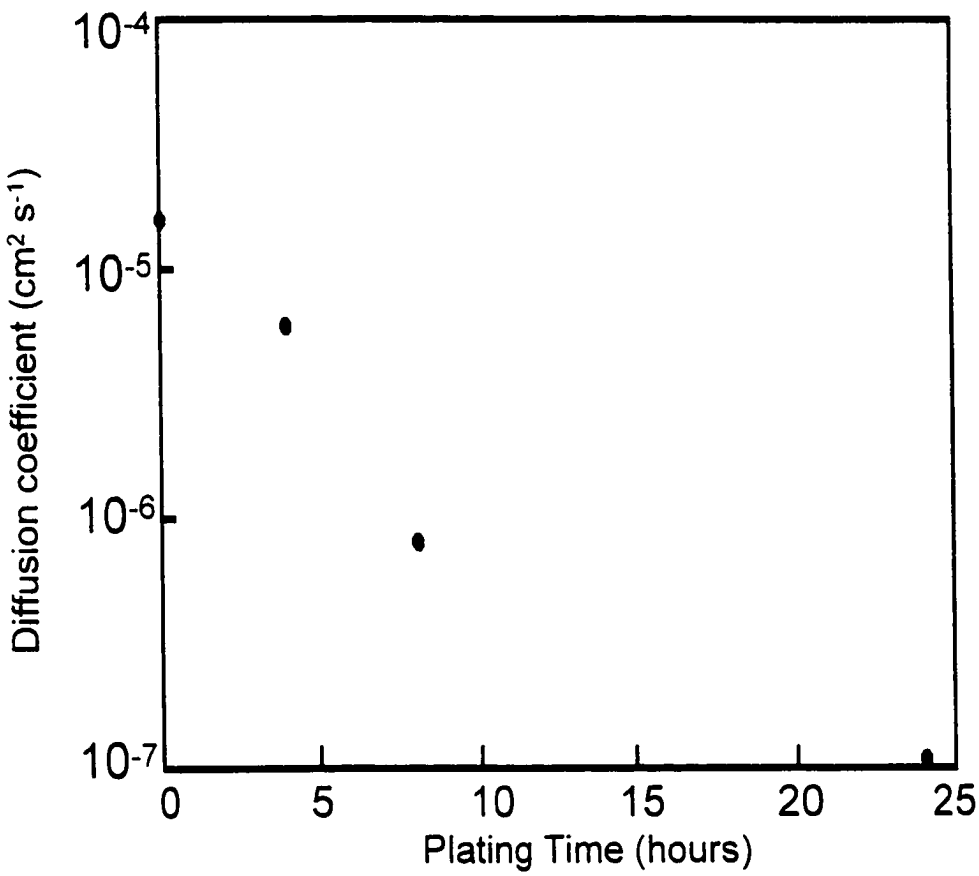

Figure 2.15 Variation of the diffusion coefficient of ninhydrin with plating time

In general, it was shown that for a given molecule, the flux decreased with decrease in nanotubule size. Also, for a given set of small and large molecules, the selectivity for the small molecule increased with decreasing nanotubule size. The membranes also showed a clean separation of the small molecule from the large molecule when present in a mixture. There was evidence that these nanotubules have constrictions on both the surfaces and acted as 'bottle-neck'. This is advantageous, because a higher flux can be achieved without compromising the selectivity.

Finally, the diffusion coefficients were determined in the nanotubules. The measured values were up to two orders of magnitude smaller than the bulk diffusion coefficient.

REFERENCES FOR CHAPTER 2

(1) Ho, W. S. W.; Sirkar, K. K. *Membrane Handbook*; Van Nostrand Reinhold: New York, **1992**.

(2) Nishizawa, M.; Menon, V. P.; Martin, C. R., Science **1995,** *268*, 700.

(3) Hwang, S.-T.; Kammermeyer, K. *Membranes in Separation*; Wiley: New York, **1975**.

(4) Porter, M. C. In *Synthetic Membranes: Science, Engineering and Applications*; Bungay, P. M., Lonsdale, H. K., de Pinho, M. N., Eds.; Reidel Publishing Company, 1986; Vol. 181, pp 225.

(5) Aptel, P.; Clifton, M. In *Synthetic Membranes: Science, Engineering and Applications*; Bungay, P. M., Lonsdale, H. K., de Pinho, M. N., Eds.; Reidel Publishing Company, 1986; Vol. 181, pp 249.

(6) Eutache, H.; Histi, G., J. Mem. Sci. **1981,** *8*, 105.

(7) Paul, D. R.; Yampol'skii, Y. P. *Polymeric Gas Separation Membranes*; CRC Press: Boca Raton, FA, **1994**.

(8) Breck, D. W. *Zeolite Molecular Sieves*; John Wiley: New York, USA, **1974**.

(9) Kusakabe, K.; Mutara, A.;; Kuroda, T.; Morooka, S., Chem. Eng. J. **1997,** *30*, 72.

(10) Kusakabe, K.; Yoneshige, S.; Murata, A.; Morooka, S., J. Mem. Sci. **1996,** *116*, 39.

(11) Yan, T. Y., Ind. Eng. Chem. Res. **1989,** *28*, 572.

(12) Jia, M.; Peinmann, K.; Behling, R., J. Mem. Sci. **1993,** *82*, 15.

(13) Huddersman, K.; Klimczyk, M., J. Chem. Soc. Farad. Trans. **1996,** *92*, 142.

(14) de Vos, R. M.; Verweij, H., Science **1997,** *279*, 1710.

(15) Hennis, J. M. S.; Tripodi, M. K., Science **1983,** *220*, 11.

(16) Abelson, P. H., Science **1989,** *224*, 1421.

(17) U.S. Department of Energy: Washington DC, 1990; Vol. Rep. DE90-01170.

(18) Liu, C. Dissertation, Texas A&M University, College Station, TX, **1991**.

(19) Spillman, R. W., Chem. Eng. Prog. **1989,** *85*, 41.

(20) Mulder, M. *Basic Principles in Membrane Technology*; Kluwer Academic: Dordrecht, Netherlands, **1990**.

(21) Funke, H. H.;; Argo, A. M.; Baertsch, C. D.; Falconer, J. L.; Noble, R. D., J. Chem. Soc. Farad. Trans. **1996,** *92*, 2499.

(22) Vroon, Z. A. E. P.; Keizer, K.; Gilde, M. J.; Verweij, H.; Burggraaf, A. J., J. Mem. Sci. **1996,** *113*, 293.

(23) Niwa, M.; Yamazaki, K.; Murakami, Y., Chem. Lett. **1989**, 441.

(24) Ozin, G. A.; Steele, M. R., Adv. Mat. **1994,** *6*, 300.

(25) Trocha, M.; Koros, W. J., J. Mem. Sci. **1994,** *95*, 259.

(26) Morooka, S.; Yan, S.; Yokoyama, S.; Kusakabe, K., Sep. Sci. Tech. **1995,** *30*, 2877.

(27) Raman, N. K.; Brinker, C. J., J. Mem. Sci. **1995,** *105*, 273.

(28) Nomura, M.; Yamaguchi, T.; Nakao, S., Ind. Eng. Chem. Res. **1997,** *36*, 4217.

(29) Deen, W. M., AIChE J. **1987,** *33*, 1409.

(30) Pappenheimer, J. R.; Renkin, E. M.; Borrero, L. M., Am. J. Physiol. **1951,** *167*, 13.

(31) Renkin, E. M., J. Gen. Physiol. **1954,** *38*, 225.

(32) Ferry, J. D., J. Gen. Physiol. **1936,** *20*, 95.

(33) Prieve, D. C.; Hoysan, P. M., J. Coll. Interf. Sci. **1978,** *64*, 201.

(34) Ruckenstein, E.; Tsai, M. C., AIChE J **1981,** *27*, 697.

(35) Kathawalla, I. A.; Anderson, J. L., Ind. Eng. Chem. Res. **1988,** *27*, 866.

(36) Guo, Y.; Langley, K. H.; Karasz, F. E., Macromolecules **1990,** *23*, 2022.

(37) Beck, R. E.; Schultz, J. S., Biochim. Biophys. Acta. **1972,** *255*, 273.

(38) Nitsche, J. M.; Balgi, G., Ind. Eng. Chem. Res. **1994,** *33*, 2242.

(39) Deen, W. M.; Bohrer, M. P.; Epstein, N. B., AIChE J. **1981,** *27*, 952.

(40) Menon, V. P.; Martin, C. R., Anal. Chem. **1995,** *67*, 1920.

(41) Kobayashi, Y.; Martin, C. R., J. Electroanal. Chem. **1997,** *431*, 29.

(42) Petzny, W. J.; Quinn, J. A., Science **1969,** *166*, 751.

CHAPTER 3

EFFECT OF THIOL CHEMISORPTION ON THE TRANSPORT PROPERTIES OF GOLD NANOTUBULAR MEMBRANES

INTRODUCTION

As discussed in Chapters 1 and 2, a general method called "template synthesis" has been used to fabricate micro- and nanostructures(1-4). A large number of techniques that include, electrodeposition(5), electroless plating(6), chemical and electrochemical polymerization(7), chemical vapor deposition(8), sol-gel synthesis(9), vacuum filtration(10) etc. have been used to achieve deposition of various kinds of materials. More recently, a large number of applications for these template-synthesized micro- and nanostructures have been developed. These include study of nanomaterials for Li-ion batteries(11), fabrication of composites(12), nanoelectrodes(6), carbon nanotubules for energy storage and production(13), synthesis of metallic and semi-conductor nanorod sols(14, 15) and various types of separations(16-19).

Since membrane based separations are potentially less energy intensive and more cost effective than competing separation methods, they constitute an emerging area of research and industrial technology; (20). Some of the novel

membrane based separation methods that use template based nano- and microstructures are based on popular principles such as facilitated transport(18), molecular-imprinting(21), electrochemical switchability(19) and molecular-sieving(16). Chapter 2 established that membranes with precisely tunable nanotubule membranes can be used to separate molecules based on their size. Previously, it has also been demonstrated that the charge on the membrane can be controlled electrochemically and this can be used to achieve ion-permselectivity(19).

This chapter discusses the use of SAMs to modify the nature of the surface of gold nanotubular membranes. It will be demonstrated that the chemical environment in the nanotubules can be controlled by changing the terminal group of the thiols used. Furthermore, this property of the membranes can be used to effectively separate molecules based on their hydrophobicity or hydrophilicity.

BACKGROUND

Self-Assembled Monolayers

Self-assembled monolayers (SAMs) are molecular assemblies that are formed spontaneously upon immersion of a substrate into a solution containing the active surfactant molecule(22). There are several types of SAMs. These include organosilicon on hydroxylated surfaces (silica on silicon, alumina on Al, glass)(23, 24), alkanethiols on gold(25), silver(26), copper(27), dialkyl sulfides on gold(28), dialkyl disulfides on gold(29), alcohols and amines on platinum(28) and carboxylic acids on alumina and silver(30). SAMs have been studied in great

detail and a large wealth of information is now available about their formation, properties and applications(22).

Molecules self-assemble in a SAM as follows. The self-assembling molecule can be divided into three parts (Figure 3.1). The first part is the head group, which chemisorbs to the substrate and is the most exothermic of the three processes. There is a strong interaction between the head group and the substrate, that result in the pinning down of the molecule on the surface by a chemical bond. The energy associated in this process is of the order of tens of kcal/mol. The second part of the molecule is the alkyl chain. The van der Waals interaction between the alkyl chains help stabilize the monolayers after they are formed. These interactions are also exothermic, but they have much smaller energies (less than 10 kcal/mol). The third part of the molecule is the terminal group. It is known that the terminal groups are disordered at room temperature, but the energy involved in the isomerization is very small (Trans-gauche isomerization is an endothermic process and ~0.7 kcal/mol). Thus, there is minimal contribution to the self-assembly process in terms of energy.

Thiols For Self-Assembly

Nuzzo and Allara first showed that dialkyldisulfides form oriented monolayers on gold surfaces(31). Since then the self-assembly of thiols on other surfaces such as Cu, Ag and Pt has been observed(26-28). However, a large amount of work has been done with Au, because Au does not have a stable oxide and it can be handled under ambient conditions.

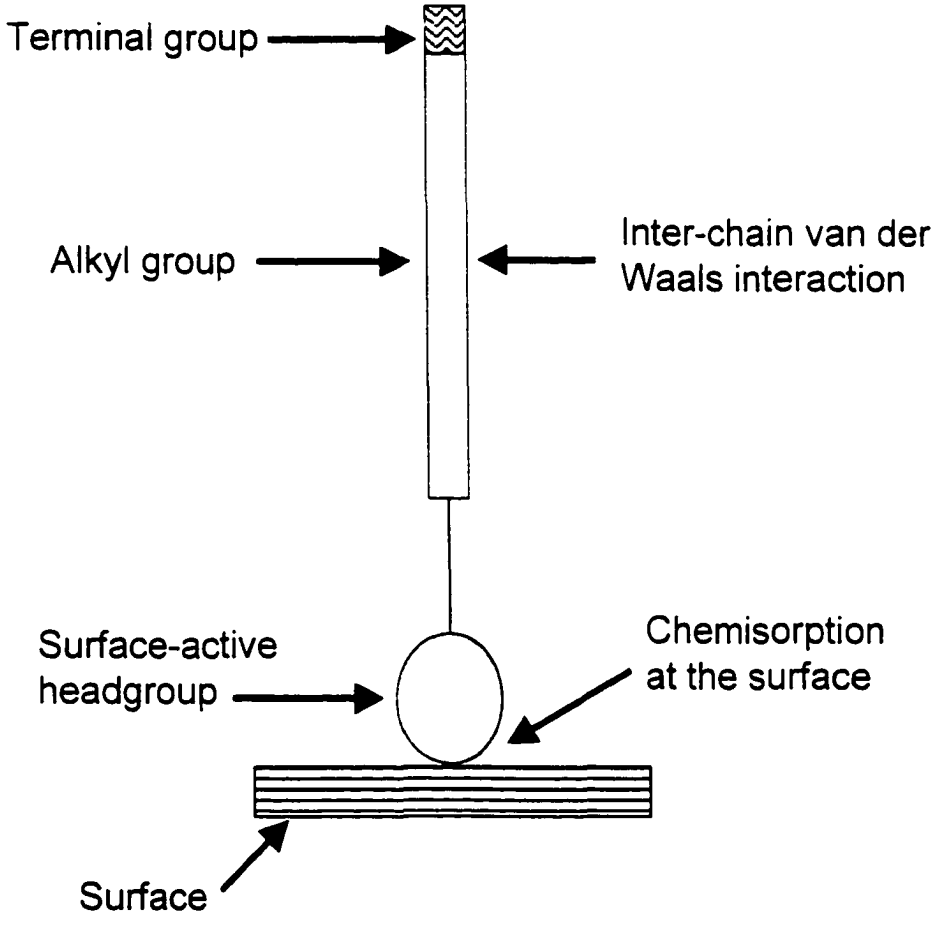

Figure 3.1 A schematic view of the surfactant molecule and the forces in a self-assembled monolayer

When a fresh clean hydrophilic surface of Au is immersed in a dilute solution (1 mM) of an organosulphur compound in an organic solvent a self-assembled monolayer of thiol is obtained. The immersion times vary from several minutes to hours for alkanethiols and days for sulfides and disulfides to obtain a close-packed, oriented monolayer can be obtained (Figure 3.2)

Studies on Au thiol monolayers indicate that the alkyl chain length determines the packing density, intermolecular environment and geometry of the packing. Porter et al. have shown that there is a perceptive difference in the structure of the short and long chain thiol monolayers(32). Optical ellipsometry, IR spectroscopy and electrochemistry was used to demonstrate that long chain thiols form a densely packed, crystalline-like assembly with fully extended alkyl chains tilted from the normal to the Au surface by 20-30°. With decreasing chain length, the structure became increasingly disordered with lower coverage and packing density.

Thiols For Surface Modification Via Self-Assembly

SAMs have been used in many instances to provide a protective coating and also to prevent corrosion(33, 34). In these cases, chemical modification of the surface by SAM of thiols, followed deposition of a silane. The silane is hydrolyzed with water followed by polymerization to form a protective coating. In the case of iron, the film shows an 88% protection against corrosion in NaCl, and 93% protection of copper against corrosion in 0.5 Na_2SO_4. Oxidation is prevented by decreasing the permeability to oxygen to the metal surface(33, 34).

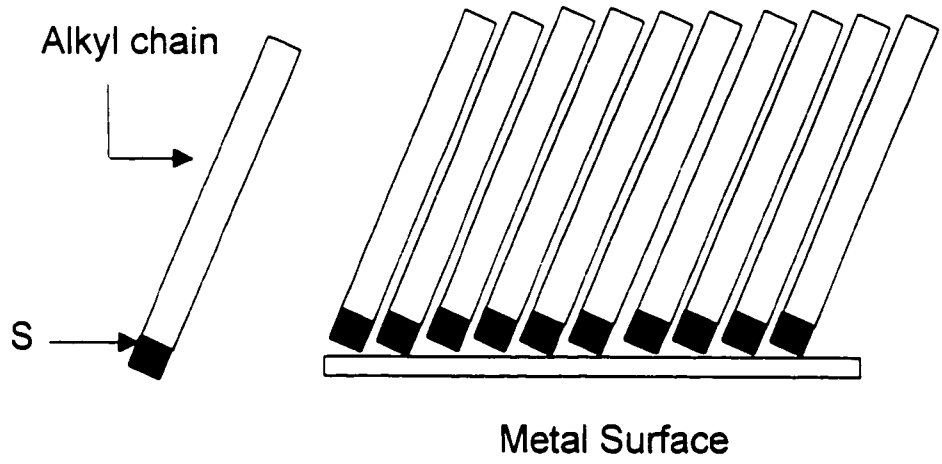

Figure 3.2 A self-assembled monolayer of alkanethiols on a gold surface

SAMs of thiols that have been used to modify surfaces of metals are well characterized. Studies conducted include varying the chain length of the thiol, the terminal groups, the solvent, the duration of immersions. Characterization of these SAMs was accomplished using a variety of techniques including contact angle measurements, Infrared spectroscopy, ellipsometry, X-ray photoelectron spectroscopy among others. Some of the observations and applications are summarized below.

Several authors have demonstrated that the hydrophobicity or hydrophilicity of a surface can be manipulated by changing the terminal group of the self-assembled monolayer(25). Bain et al. have studied contact angles of water on surface modified with a variety of thiols with different terminal groups ranging from hydrophilic groups (for example, -OH, -COOH) to highly hydrophobic groups such as $-CF_3$. They showed that, the hydrophobic thiols with terminal groups like $(C(CH_3)_3$ and CF_3 show large contact angles ($> 100^o$) for water (not easily wetted by water) and thiols with hydrophilic terminal groups are easily wetted by water.

Bain et al.(25) and Atre et al.(35) demonstrated a greater control over the wettability and chemical reactivity can be achieved by using thiol mixtures. The nature of the surface was studied by varying the composition of the thiols used in solution, thereby varying the composition of the monolayer. They observed that the wettability of mixed monolayer is not linear in composition to the surface. Thus for a surface composed of a polar and a non-polar component, the polar component was more hydrophilic when its concentration in the monolayer was

lower than when the concentration is high. The properties of the obtained surface can be controlled by changing the nature or the terminal group of the thiols to obtain the SAMs.

Surface Modification For Chemical Separations

Modification of electrodes or other substrates to improve selectivity, by rejection of undesired and interfering species has been a common practice in the area of biosensors. Some of the work by Wang and coworkers include the development of electrochemical detection methods, where the interferants are rejected based on size, charge and nature by using a thin film barrier (36-38). Wang and Lu have shown that stable coatings of phospholipid/cholesterol can be used to monitor different hydrophobic substances(36). A base-hydrolyzed cellulosic film on glassy carbon electrode was used to achieve a size-based separation of the compounds reaching the electrode(38). Another advantage of the film was the prevention of electrode fouling by protein adsorption. A glassy carbon electrode modified with poly(4-vinylpyridine) has been used in flow detectors(38). In this case, the large cationic polymer discriminated effectively against cationic interferants.

SAMs have also been used to modify surfaces to form thin films to achieve different types of separations. Wand and Lu report the use of n-alkane thiol monolayer to discriminate different hydrophobic compounds(39). In addition, Cheng and Brajter-Toth have shown that thioctic acid can be self-assembled on a gold surface to form a thin film that was permselective(40-42). They showed that the film is cation-selective at high pH, when the carboxyl group

was deprotonated. Thus, these films can be used as barriers in biosensors where it is necessary to prevent interfering ions like ascorbate from reaching the electrode(40). Furthermore, Sun and co-workers showed that SAMs of 4-aminothiophenol can be used for ion-binding. At low pH, the amino group was protonated and capable of electrostatically binding to negatively charged ions(43).

Another example of a separation involved a series of ω-mercapto carboxylic acids to obtain monolayers to study their suitability in the detection of neurotransmitters(44). The authors observed that long chain thiols were most suitable and this was due to a better organized film that was obtained(44). They used the monolayer to prevent interference from negatively charged species. Thus, thiol monolayers have been used to separate compounds based on the charge of the terminal group or to separate molecules based on their chemical nature.

In all the previously noted cases, the SAMs have been used as a thin film barrier. The research reported here involves chemically modifying the surface characteristics of gold nanotubular membranes by SAMs of thiols, to achieve separations based on the chemical nature of the compounds. The objective of the project was to modify gold nanotubular membranes with different thiols to render the membranes hydrophilic or hydrophobic (Figure 3.3). These membranes were then tested for their ability to separate hydrophilic and hydrophobic molecules. The structures of the thiols and the molecules used in this study are shown in Figure 3.4.

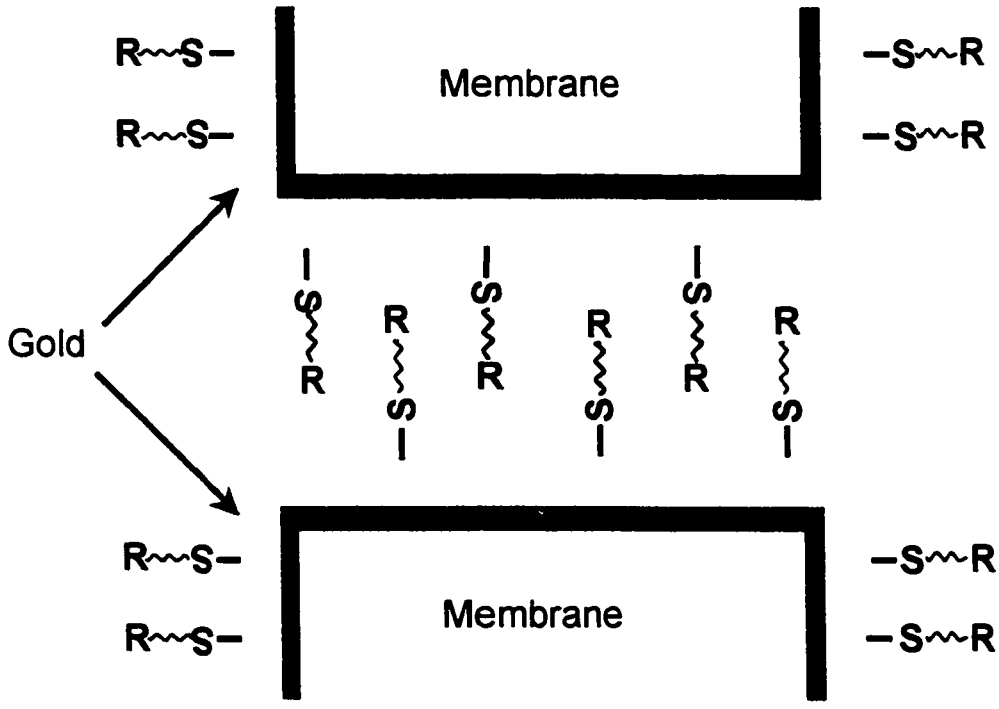

Figure 3.3 Functionalization of gold nanotubular membranes to control the environment in the nanotubules

Thiols used

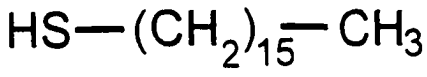

Hexadecylthiol
(Hydrophobic)

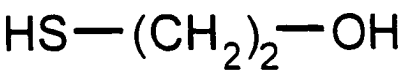

Mercaptoethanol
(Hydrophilic)

Molecules studied

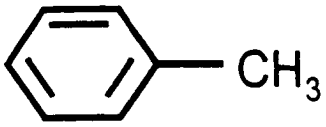

Toluene
(Hydrophobic)

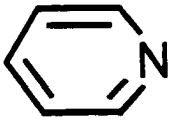

Pyridine
(Hydrophilic)

p-cresol

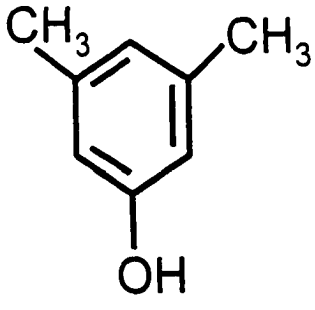

3,5 dimethylphenol

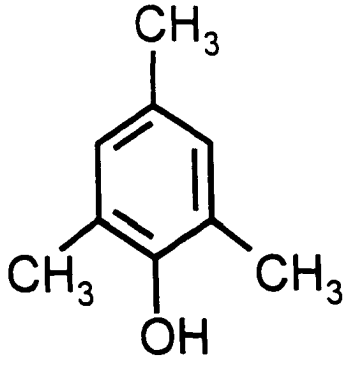

2,4,6 trimethylphenol

Figure 3.4 Structures of thiols and the molecules studied

EXPERIMENTAL

Materials

Polycarbonate "track-etched" membranes (6 μm thick, 30 nm diameter and $6x10^8$ pore cm^{-2}) were obtained from Corning Costar Corporation. Anhydrous $SnCl_2$, $AgNO_3$, $NaHCO_3$ (Aldrich), trifluoroacetic acid, Na_2SO_3, NH_4OH, H_2SO_4, formaldehyde, anhydrous methanol (Mallinckrodt) were used as received. Pyridine, toluene, p-cresol, 2,4 - dimethylphenol, 2,4,6 - trimethylphenol, $Ni(NO_3)_2$, propanethiol, decanethiol, hexadecanethiol and mercaptoethanol (Aldrich) were used as received. Commercial gold plating solution (Oromerse SO Part B) was obtained from Technic Inc. Milli Q 18Ω water was used to prepare all solutions and to rinse the membranes.

Electroless Gold Deposition

An electroless deposition procedure developed previously in the group was adapted to obtain more uniform deposition of gold(6). The template membrane was rinsed in methanol for five minutes and then immersed in a solution that was 0.025 M in $SnCl_2$ and 0.07 M in trifluoroacetic acid for 45 minutes. The membrane was rinsed in methanol two consecutive times for 2.5 minute each. The membrane with the sensitizer, (Sn^{2+}) anchored to the membrane was immersed in an aqueous solution of ammoniacal $AgNO_3$ for five minutes. The membrane was rinsed with methanol for five minutes to remove excess solution of silver nitrate.

Finally the membrane was placed in the gold plating bath which consisted of 0.5 mL of the commercial gold plating solution, 0.127 M Na_2SO_3, 0.625 M

formaldehyde and 0.025 M $NaHCO_3$. The pH of this solution was 12 and was adjusted to 10 by the dropwise addition of 0.5 M H_2SO_4 with constant stirring. The temperature of this plating bath was maintained at 5°C throughout the duration of the plating procedure. Gold nanotubular membranes with diameters 3.0 nm and 2.0 nm were obtained by immersing in the gold plating solution for four and five hours respectively.

Modification Of The Gold Nanotubular Membranes

The gold nanotubular membranes were placed in a 1 mM ethanolic solution of a thiol for 24 hours, in order to chemisorb the thiol. The membranes were then thoroughly rinsed in absolute ethanol for at least 15 minutes. Following rinsing, the membranes were dried and sandwiched between two pieces of Scotch tape (3M Scotch brand # 375) with a hole punched in them, to make the sample. The sample was placed in U-tube with water on both the sides for at least 12 hours before any permeation experiments were conducted.

Permeation Experiments

Permeation experiments were conducted in a U-tube. The membrane was placed between the two halves of the U-tube. Water was introduced on one side and on the other side (feed), a solution of the permeant molecule was introduced. The absorbance of the permeate was measured at regular intervals, then using Beer's law, the concentration of the species was determined. This was converted into number of moles, by multiplying the concentration by the volume of the permeate. The flux was obtained from the slope of a plot of the moles transported versus time.

The solutions on both the sides of the U-tube were stirred vigorously at all times to avoid concentration polarization. All experiments with pyridine were conducted with a 5 mM feed solution. The permeation experiments with toluene were conducted with 7 mM feed concentration and then normalized to a 5 mM feed concentration, to compare with the pyridine permeation experiments. In the case of toluene, special precautions were taken, to obtain a measurable flux of the molecule through the membrane. The solutions on both the sides were covered by screw caps to prevent evaporation of the analyte. Also, special O-rings were used to prevent the absorption of toluene by the O-ring or dissolution of species that were present in the O-rings which absorbed in the UV region and interfered with the UV spectrum of toluene. The absorbance at 256 nm for pyridine and 268 nm for toluene were monitored with a Hitachi U-3502 spectrophotometer to determine the concentration of the analyte molecule.

In a mixed molecule experiment with pyridine and toluene simultaneously present, the permeation experiments were performed with a mixture of 7 mM toluene and 50 mM pyridine in the feed. The flux of each molecule was normalized to a feed concentration of 5 mM. To determine the concentrations of the two molecules, the absorbance of the permeate was measured at two different wavelengths (256 nm and 268 nm). The concentration of the two molecules was determined, by solving two simultaneous equations obtained using Beer's law.

The permeation experiments with p-cresol, 2,6 dimethylphenol and 2,4,6 trimethylphenol were performed with 0.1 M, 0.01 M and 0.001 M feed

concentrations, respectively. The fluxes were then normalized for a feed concentration of 0.1 M. The UV absorbance was monitored at 277 nm, 270 nm and 270 nm respectively for p-cresol, 2,6 dimethylphenol and 2,4,6 trimethylphenol.

Permeation experiment with $Ni(NO_3)_2$ was carried out with a feed concentration of 0.5 M and the absorbance in the visible region (300 to 500 nm) was monitored over a period of time.

RESULTS AND DISCUSSION

In the first set of experiments, the flux of pyridine and toluene (single molecule permeation experiment) were determined in gold nanotubular membranes modified with two different thiols (separately) and unmodified membranes. The membranes used in these experiments were tested for their performance in a mixed molecule experiment (with pyridine and toluene present together in the feed).

Permeation Experiments With Pyridine (Single Molecule Experiment)

The flux of pyridine was determined in untreated and thiol treated gold nanotubular membranes. Figure 3.5 shows the flux of pyridine in gold nanotubular membranes of 3.0 nm diameter when treated with $-C_{16}$ and $-C_2H_4OH$ terminated thiols. An untreated membrane containing tubules with diameter 3.0 nm, showed a pyridine flux of $2.9\pm0.1 \times 10^{-9}$ moles cm^{-2} min^{-1}. The flux increases to $7.0\pm0.7 \times 10^{-9}$ moles cm^{-2} min^{-1} when modified with a $-C_2H_4OH$ terminated thiol. However, the flux decreases to $4.6\pm0.5 \times 10^{-10}$ moles cm^{-2} min^{-1}, in a membrane treated with $-C_{16}$ terminated thiol. The flux of pyridine was clearly

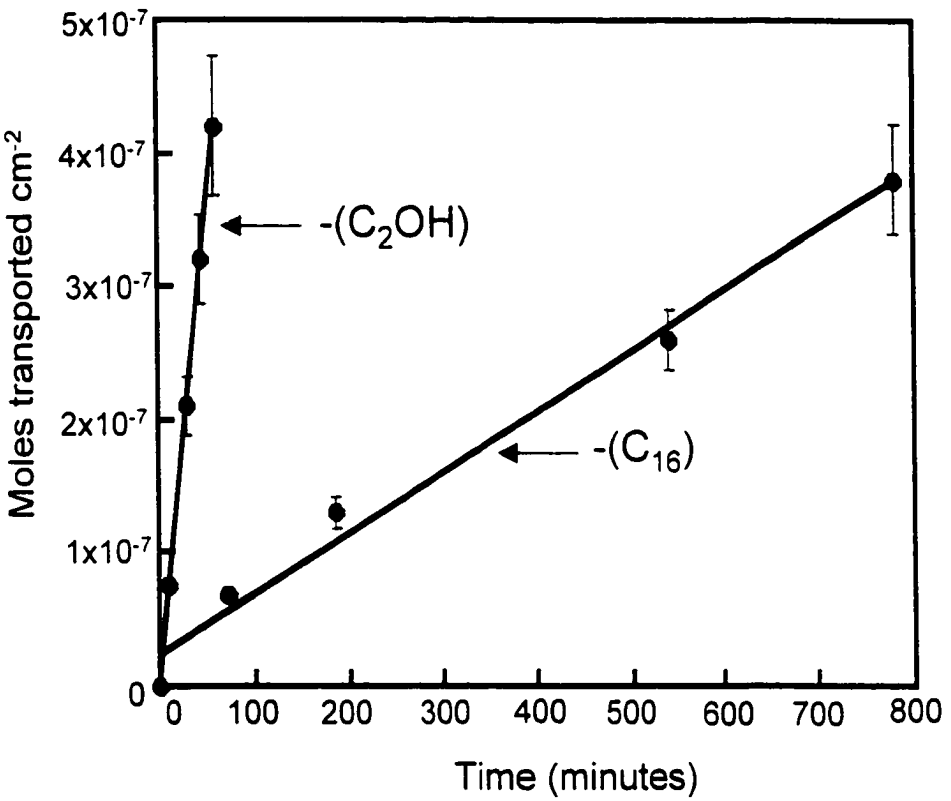

Figure 3.5 Moles of pyridine transported versus time in thiol modified gold nanotubular membranes (3.0 nm)

determined by the nature of the gold surface, whether it was untreated or treated with a thiol and the type of chemisorbed thiol. Thus, the membrane treated with -C_2H_4OH terminated thiol is more selective for pyridine compared to a membrane modified with a -C_{16} terminated thiol.

The effect of the nanotubule diameter on the selectivity of the terminal group for pyridine was also studied by determining the flux in smaller nanotubular membranes. Figure 3.6 shows the flux of pyridine in gold nanotubular membranes of 2.0 nm in diameter, when treated with the two thiols. The flux of pyridine in a membrane treated with -C_2H_4OH thiol was $5.6\pm0.4\times10^{-9}$ moles cm^{-2} min^{-1}, which was higher than in an untreated membrane, $1.3\pm0.2\times10^{-9}$ moles cm^{-2} min^{-1}. The flux in a membrane modified with -C_{16} thiol was $1.0\pm0.2\times10^{-10}$ moles cm^{-2} min^{-1}. This flux was dramatically lower than the flux in the membrane modified with -C_2H_4OH thiol.

These data can be interpreted as follows. First, it should be noted that both the 3.0 and 2.0 nm membranes modified with the -C_2H_4OH thiol, showed a higher flux for pyridine than the untreated membranes. Second, the selectivity (which is obtained by determining the ratio of fluxes in respective membranes) $\alpha_{-C2H4OH/-C16}$, is 15 for the membrane with gold nanotubules with diameter of 3.0 nm. This selectivity value increases to 60 for the membrane with smaller nanotubules, 2.0 nm in diameter. Thus, the selectivity, $\alpha_{-C2H4OH/-C16}$ increased with decreasing diameter of the Au tubules prepared.

The data in Figure 3.5 and 3.6 may also be argued as a case where the flux of the molecule decreased with the chemisorption of a long-chain thiol

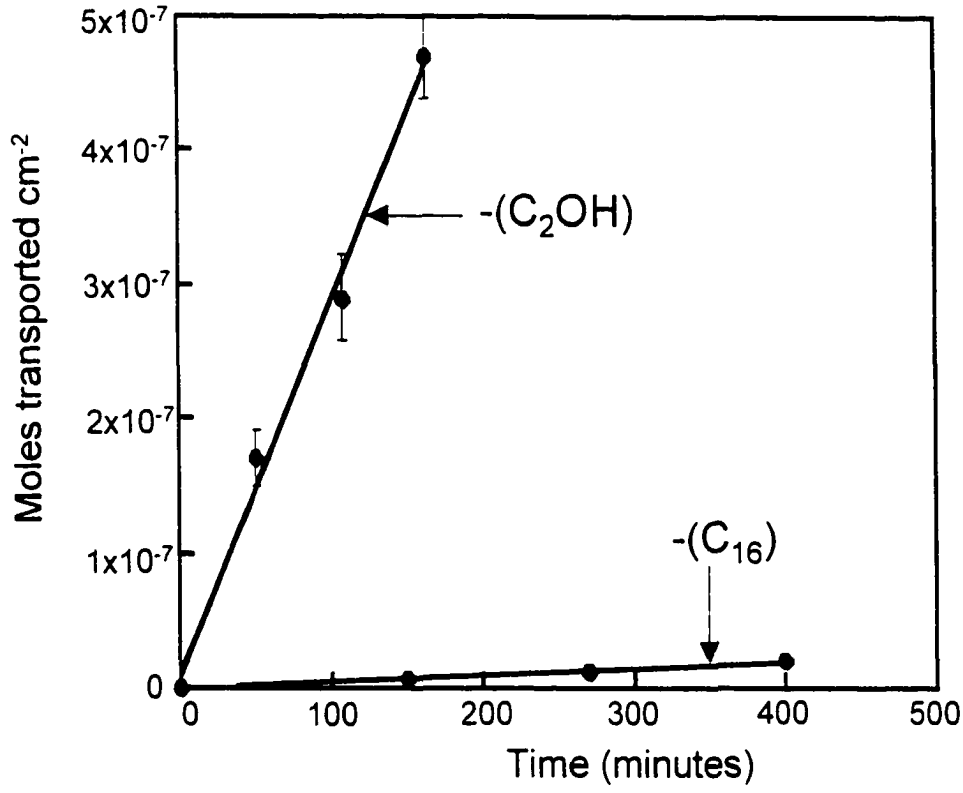

Figure 3.6 Moles of pyridine transported versus time in thiol modified gold nanotubular membranes (2.0 nm)

(sixteen carbon atoms) because of a decrease in the nanotubule diameter rather than a selectivity due to the chemistry of the surface. The membrane with the -C_{16} thiol chemisorbed indicated a lower gas flux, from which we can get an approximate value for the nanotubule diameter. For example a membrane with a nanotubule diameter, 3.0 nm, shows a H_2 gas flux value that indicates a nanotubule diameter of 2.0 nm after the chemisorption of the -C_{16} thiol. This gas flux data supports the idea that the nanotubule diameter did decrease to some extent upon chemisorption of the long chain thiol.

However, two observations support the hypothesis that, $\alpha_{\text{-C2H4OH/-C16}}$ was not entirely due to a decrease in the nanotubule diameter by chemisorption of the long chain thiol. First, the flux of pyridine in an untreated membranes of two different diameters, 3.0 nm and 2.0 nm were 2.9±0.1 x10^{-9} moles cm^{-2} min^{-1} and 1.3±0.5 x10^{-9} moles cm^{-2} min^{-1} respectively. These values differ only by a factor of two, which cannot explain the wide difference in the selectivity factors of 20 and 60 obtained for the 3.0 and 2.0 membranes, treated with the two thiols. In addition, an experimental result obtained from permeation experiments with toluene supports this hypothesis.

Permeation Experiments With Toluene (Single Molecule Experiment)

Permeation studies of toluene were conducted with the same membranes previously used in the case of the pyridine experiments. The flux of toluene in a 3.0 nm untreated gold nanotubular membrane was, 1.5±0.1 x10^{-8} moles cm^{-2} min^{-1}. In comparison, the flux of toluene in a membrane modified with the -

C_2H_4OH thiol, was 2.6±0.4 $x10^{-9}$ moles cm^{-2} min^{-1} and in a membrane treated with the $-C_{16}$ thiol was 2.8±0.2 $x10^{-8}$ moles cm^{-2} min^{-1} (Figure 3.7).

A comparison of the fluxes revealed that the flux of toluene in the untreated membrane was about six times higher than in the membrane treated with $-C_2H_4OH$ thiol. This trend is opposite to that observed in the case of pyridine. This suggests that gold nanotubular membranes naturally tend to be hydrophobic. Also, as expected, the flux of toluene was higher in a membrane treated with the $-C_{16}$ thiol, when compared to a membrane treated with $-C_2H_4OH$ thiol. This ratio was 10 in the 3.0 nm gold nanotubular membranes.

The permeation experiments were further extended to the smaller 2.0 nm gold nanotubular membranes. The flux values of toluene in a 2.0 nm gold nanotubular membranes were as follows, untreated: 2.0±0.1$x10^{-9}$ moles cm^{-2} min^{-1}, treated with $-C_{16}$ thiol: 2.0±0.1$x10^{-8}$ moles cm^{-2} min'1, and treated with $-C_2H_4OH$ thiol: 6.1±0.4 $x10^{-10}$ moles cm^{-2} min^{-1} (Figure 3.8). Again, it should be noted that the flux of toluene was at least three times higher in the untreated membrane than in the membrane treated with $-C_2H_4OH$ thiol. In addition, the selectivity factor(obtained by determining the ratio of the fluxes) $\alpha_{-C16/-C2H4OH}$, increases from 10 for 3.0 nm membranes to 30 for 2.0 nm nanotubule diameter membranes.

This increase in selectivity was due to the increase in the relative portion of the tubule area covered by the thiol molecule. Thus, as the tubule became smaller a larger portion of the tubule is covered by the thiol, this resulted in a

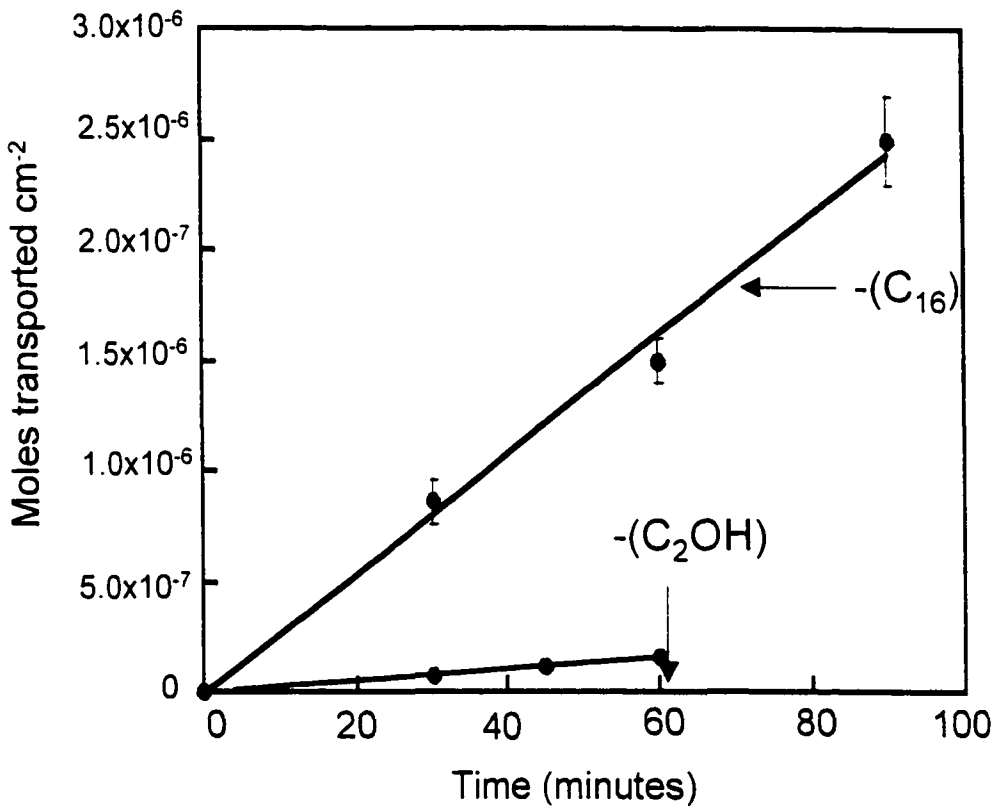

Figure 3.7 Moles of toluene transported versus time in thiol modified gold nanotubular membranes (3.0 nm)

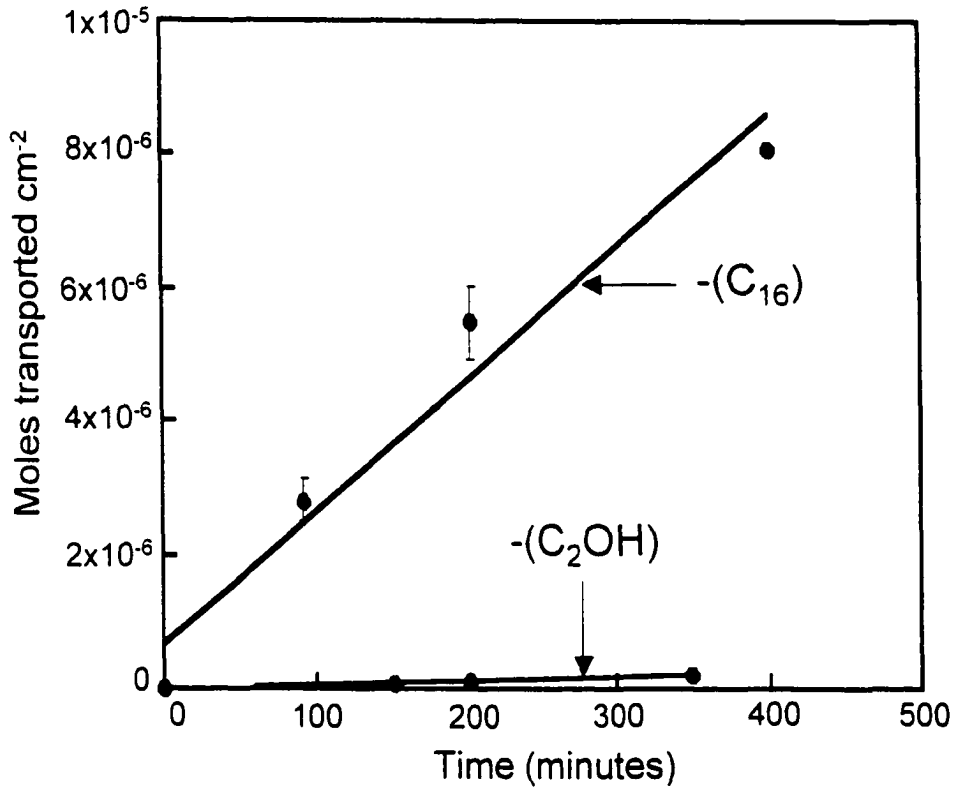

Figure 3.8 Moles of toluene transported versus time in thiol modified gold nanotubular membranes (2.0 nm)

greater partitioning of the molecule. Thus, larger selectivity values were obtained for the smaller tubules studied. Furthermore, the toluene permeation experiments with the thiols showed that the $\alpha_{-C2H4OH/-C16}$ selectivity values obtained for the pyridine experiments are not only due to decrease in nanotubule diameter by thiol chemisorption.

In general, the selectivity values obtained for pyridine were relatively higher than the values obtained for toluene. This suggests that there might also be a contribution to the selectivity, $\alpha_{-C2H4OH/-C16}$, by the decrease in nanotubule diameter. However, the selectivity was not entirely due to any decrease in diameter caused by the chemisorption of the thiol. It can be safely concluded from the above data, that the chemisorption of the thiol changed the chemical environment and affected the flux of the molecules through these membranes.

Permeation Experiments With Pyridine And Toluene (Mixed Molecule Experiment)

The experiments discussed in the first two sections of the results and discussions were performed by studying the permeation of only one molecule in membranes treated with two different thiols. The concept that the flux of the molecule was determined by the nature of the molecule, the nanotubule diameter and the thiol used to modify the gold surface was proven. In addition, another set of experiments was performed to study the effectiveness of the separation, if the two molecules were present together in the feed solution.

As previously determined, the flux of pyridine and toluene in a 3.0 nm gold nanotubular membrane modified with $-C_{16}$ thiol when each molecule was present

separately in the feed were, 4.6±0.5 $x10^{-10}$ and 2.7±0.2 $x10^{-8}$ moles cm^{-2} min^{-1} respectively. Thus, the $\alpha_{Toluene/Pyridine}$ was 60. A permeation experiment with both the molecules present in the solution gave flux values of, 7.1±0.5 $x10^{-10}$ and 2.7±0.2 $x10^{-8}$ moles cm^{-2} min^{-1} for pyridine and toluene. This results in a selectivity factor, $\alpha_{Toluene/Pyridine}$ of 40 which was close to the value obtained when the molecules were not present together in the feed solution.

The permeation experiments with the 2.0 nm nanotubule membrane yielded a $\alpha_{Toluene/Pyridine}$ value of 165 (Figure 3.9) when both the molecules were present together in solution compared to the value of 190 when these molecules were not mixed in the feed solution. Thus, the membranes were also capable of separating the molecules when they were present in a feed mixture without substantially compromising the selectivity values obtained when they were not present in a mixture.

Variation Of The Hydrophobicity Of The Molecule

The flux values of a series of molecules with varying hydrophobicity were determined with a membrane treated with $-C_{16}$ thiol in addition to a control membrane which was not treated with a thiol (Figure 3.10 a and b). The molecules studied were p-cresol, 2,6 dimethylphenol and 2,4,6 trimethylphenol. Using a membrane treated with $-C_{16}$ thiol, the flux increased with increasing hydrophobicity of the molecule. The $-C_{16}$ thiol, chemisorbed on the inner walls of the gold tubules aided the permeation of hydrophobic molecules. The fluxes were for p-cresol, 2,6 - dimethylphenol and 2,4,6 - trimethylphenol are $1.1x10^{-9}$, $4.4x10^{-9}$ and $1.4x10^{-8}$ moles cm^{-2} min^{-1}. The corresponding fluxes in a gold

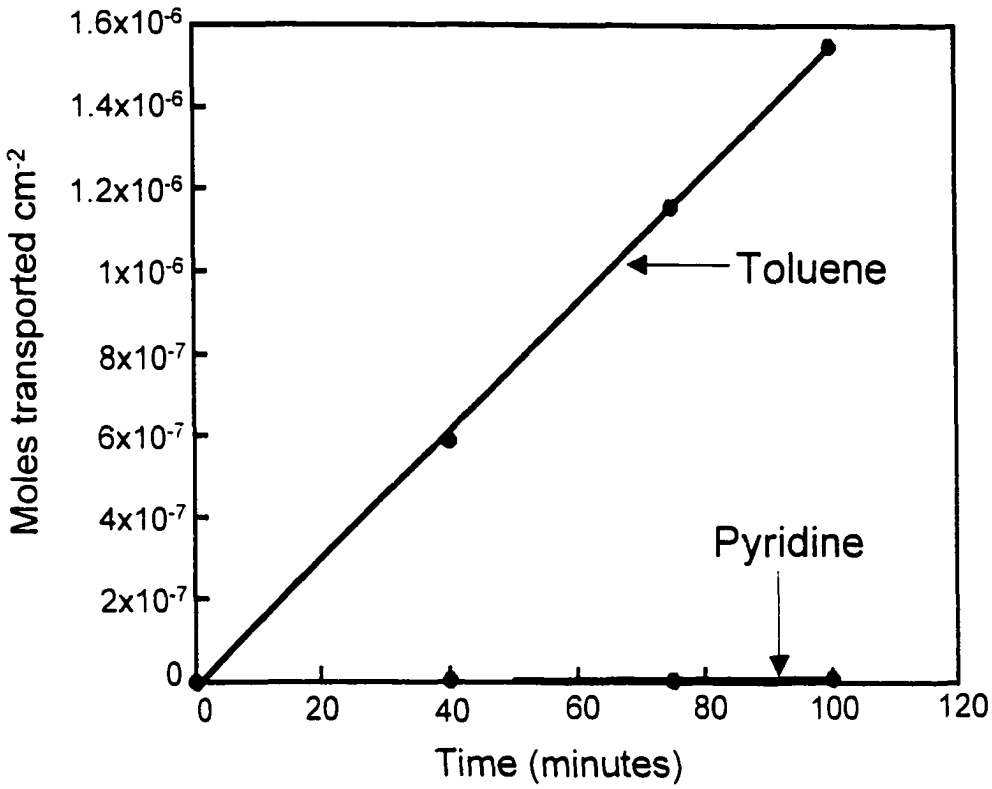

Figure 3.9 Moles of pyridine and toluene transported versus time when present in a mixture in -C_{16} thiol modified gold nanotubular membranes (2.0 nm)

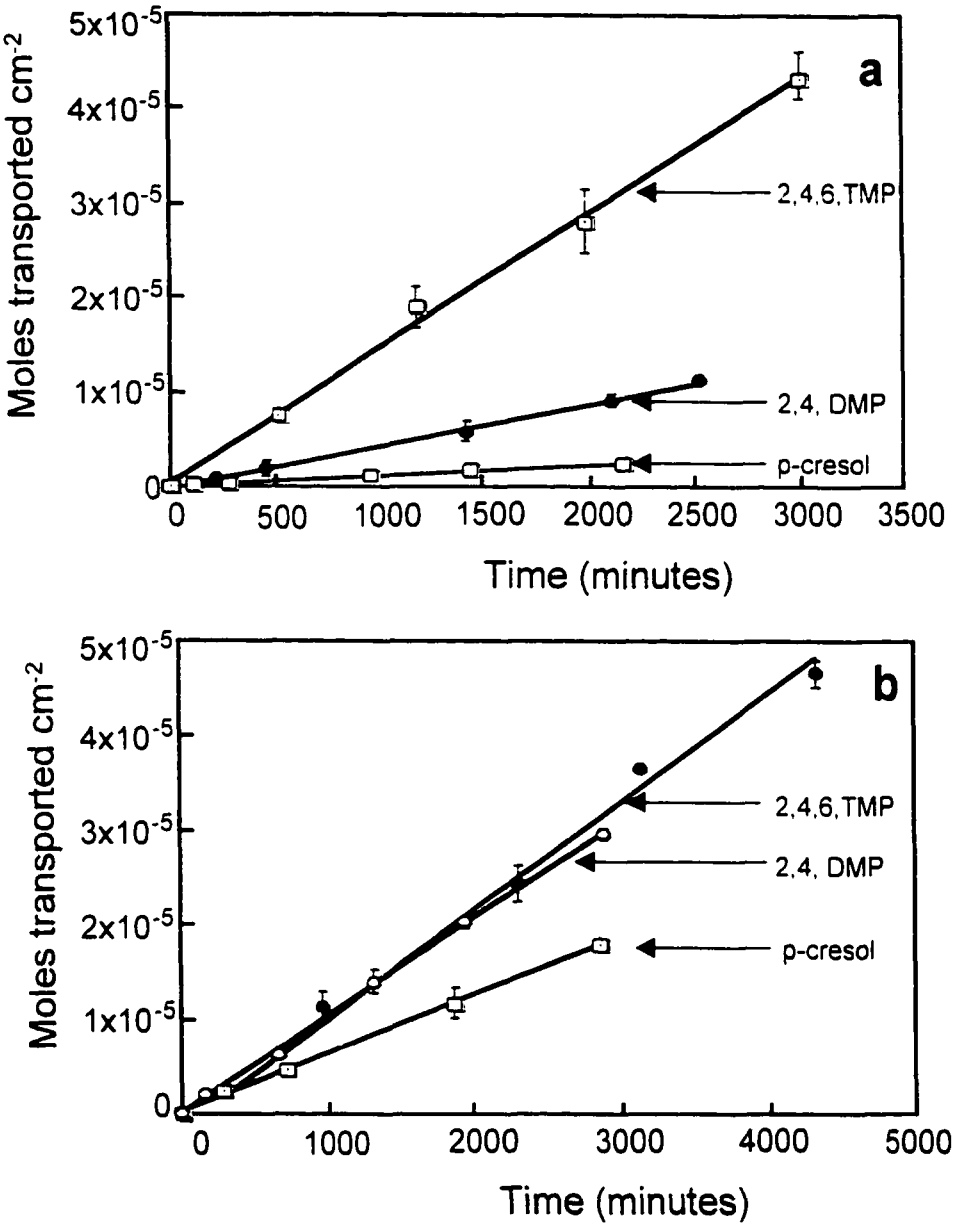

Figure 3.10 Moles of p-cresol, 2,4 dimethylphenol and 2,4,6 trimethylphenol transported versus time in a) -C_{16} thiol modified and b) bare gold nanotubular membranes

nanotubular membranes with no thiol chemisorbed were $1.8x10^{-9}$, $3.1x10^{-9}$ and $3.4x10^{-9}$ moles cm^{-2} min^{-1}.

Variation Of Chain Length Of The Thiol

The flux of toluene in gold nanotubular membranes with different chain lengths thiols was also studied. Gold nanotubular membranes with 2.0 nm diameter tubules and thiols with 3, 10, and 16 carbon atoms were employed. The flux of toluene was observed to increase with increasing number of carbon atoms in the thiol alkyl chain. Figure 3.11 shows the flux of toluene through membranes with different thiols chemisorbed on the surface of the gold tubules. The flux of toluene with a membrane modified with a $-C_3$ thiol was $1.6x10^{-9}$ moles cm^{-2} min^{-1}, this value was comparable to the flux in an unmodified Au membrane, $2.0x10^{-9}$ moles cm^{-2} min^{-1}. The flux increased to $3.8x10^{-9}$ moles cm^{-2} min^{-1} when a $-C_{10}$ thiol was used, the flux in a membrane modified with a $-C_{16}$ thiol was $2.0x10^{-8}$ moles cm^{-2} min^{-1}. This experiment showed that increasing the chain length of the alkyl thiol, led to a more hydrophobic environment in the Au nanotubule. This resulted in an increase of toluene partitioning in tubules and thus a higher flux was obtained.

Membranes Modified With $-C_{16}$ Thiol

It was also observed that the membranes treated with a $-C_{16}$ thiol were so hydrophobic that ions could not permeate through the membranes. Figure 3.12 shows the permeate after 48 hours with a membrane modified with a $-C_{16}$ thiol compared to a gold membrane without a C_{16} SAM after 4.5 hours. In both the cases the feed solution was 0.5 M $Ni(NO_3)_2$. The Ni salt was chosen so that the

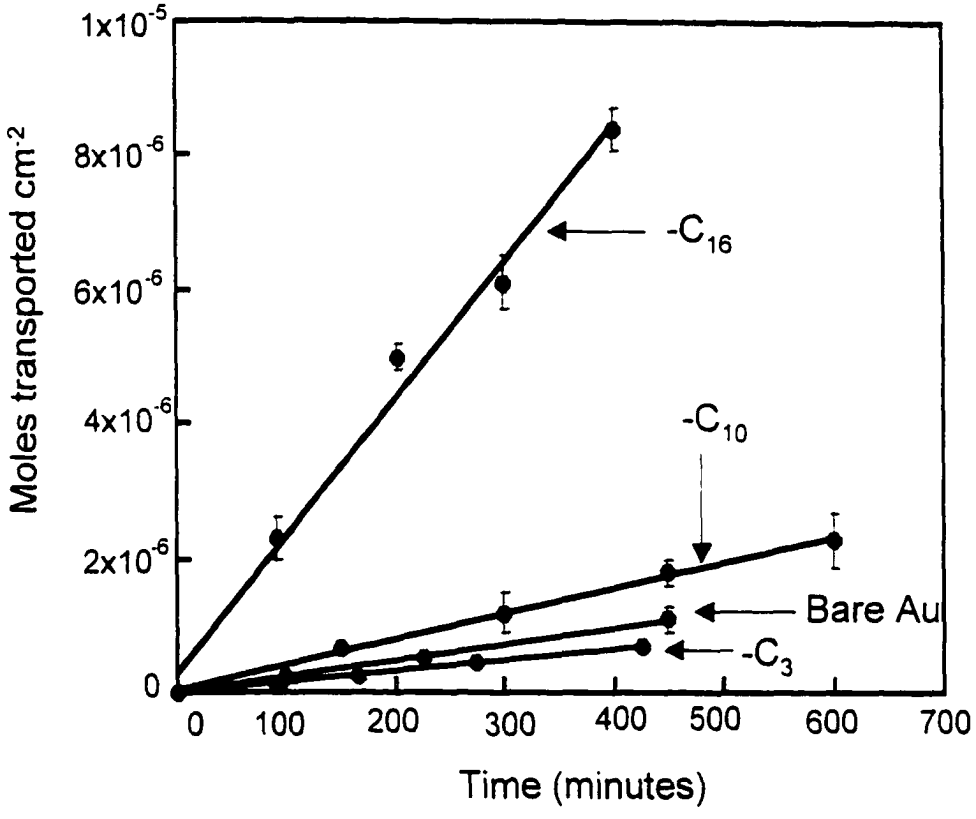

Figure 3.11 Moles of toluene transported in bare Au, $-C_3$, $-C_{10}$ and $-C_{16}$ thiol modified gold nanotubular membranes (2.0 nm)

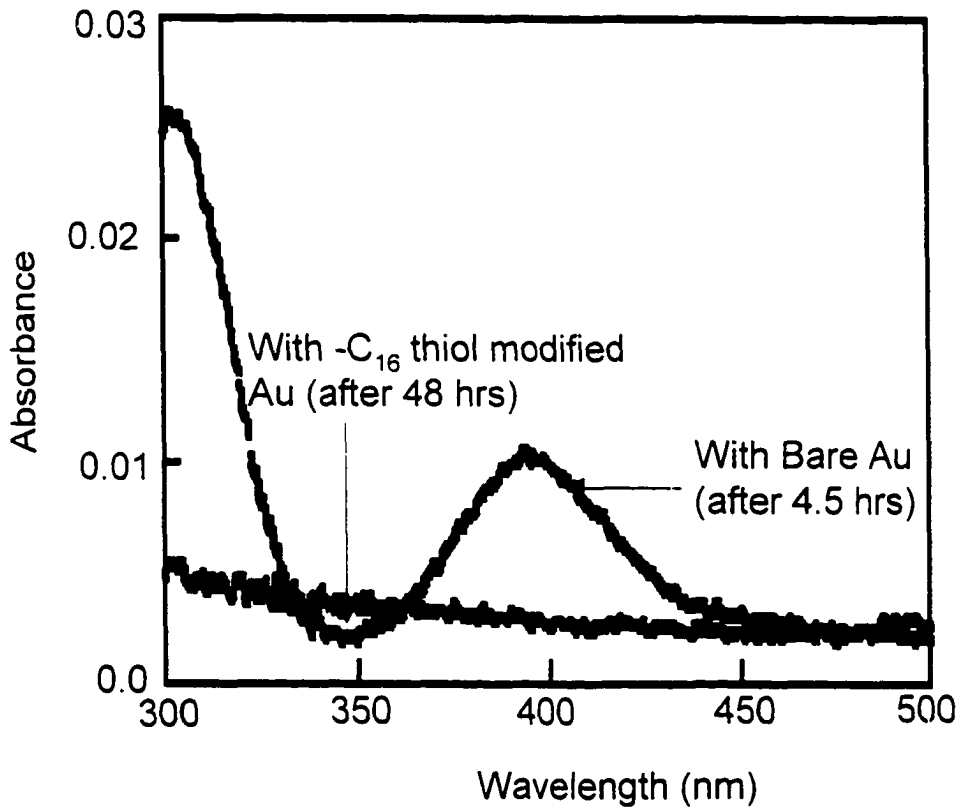

Figure 3.12 The visible spectrum of the permeate (Feed-0.5 M $Ni(NO_3)_2$) with gold nanotubular membranes

permeate could be analyzed for the presence of the salt by measuring the absorbance in the visible region. As seen in Figure 3.12, the membrane treated with the thiol did not allow ions to permeate because no peak was observed even after the permeate was analyzed after two days. In comparison, the bare gold (control membrane) showed ions permeating the membrane after 4.5 hours. Thus, the membranes are extremely hydrophobic after treatment with the $-C_{16}$ thiol.

CONCLUSIONS FOR CHAPTER 3

Gold nanotubular membranes were modified with two different thiols, one long chain hydrophobic thiol (C_{16}) and a hydroxyl terminated short chain thiol (C_2). It was shown that the hydrophobic thiol modified membrane had an enhanced flux for a hydrophobic molecule, like toluene while demonstrating a decreased the flux of a hydrophilic molecule like pyridine. The opposite effect was observed for a hydrophilic thiol modified membrane. In addition, a separation of pyridine and toluene in a mixture can be achieved with a membrane modified with the hydrophobic thiol. The selectivity achieved in this case was close to the value obtained when the molecules were present separately in solution.

Furthermore, a series of molecules with increasing hydrophobicity show a greater partitioning, and hence a higher flux in a membrane modified with a long chain hydrophobic thiol. It was also demonstrated that the flux of toluene increases with an increase in the chain length of the alkyl thiol used to modify the gold surface. Thus, the flux of the molecule in a gold nanotubular membrane

depends on a number of factors: the nature of the molecule, the nature of the surface, the nanotubule diameter. This chapter showed that effective separations can be achieved by modifying the surface of the gold tubules formed in a microporous template membrane.

REFERENCES FOR CHAPTER 3

(1) Martin, C. R., Science **1994,** *266*, 1961.

(2) Martin, C. R., Acc. Chem. Res. **1995,** *28*, 61.

(3) Martin, C. R., Chem. Mater. **1996,** *8*, 1739.

(4) Hulteen, J. C.; Martin, C. R., J. Mat. Chem **1997,** *7*, 1075.

(5) Brumlik, C. J.; Martin, C. R., J. Am. Chem. Soc. **1991,** *113*, 3174.

(6) Menon, V. P.; Martin, C. R., Anal. Chem. **1995,** *67*, 1920.

(7) Parthasarthy, R.; Martin, C. R., Nature **1994,** *369*, 298.

(8) Che, G.; Lakshmi, B. B.; Martin, C. R.; Fisher, E. R.; Ruoff, R. S., Chem. Mater. **1998,** *10*, 260.

(9) Lakshmi, B. B.; Dorhout, P. K.; Martin, C. R., Chem. Mater. **1997,** *9*, 857.

(10) Cepak, V. M.; Martin, C. R., Chem. Mater. **1999,** *accepted.*

(11) Che, G.; Jirage, K. B.; Fisher, E. R.; Martin, C. R., J. Electrochem. Soc. **1997,** *144*, 4296.

(12) Cepak, V. M.; Hulteen, J. C.; Che, G.; Jirage, K. B.; Lakshmi, B. B.; Fisher, E. R.; Martin, C. R., Chem. Mater. **1997,** *9*, 1065.

(13) Che, G.; Lakshmi, B. B.; Fisher, E. R.; Martin, C. R., Nature **1998,** *393*, 346.

(14) Cepak, V. M.; Martin, C. R., **1999,** *in preparation.*

(15) Cepak, V. M.; Martin, C. R., J. Phys. Chem. B **1998**, *102*, 9985.

(16) Jirage, K. B.; Hulteen, J. C.; Martin, C. R., Science **1997,** *278*, 655.

(17) Hulteen, J. C.; Jirage, K. B.; Martin, C. R., J. Am. Chem. Soc. **1998,** *120*, 6603.

(18) Lakshmi, B. B.; Martin, C. R., Nature **1997,** *388*, 1997.

(19) Nishizawa, M.; Menon, V. P.; Martin, C. R., Science **1995,** *268*, 700.

(20) U.S. Department of Energy: Washington DC, 1990; Rep. DE90-01170.

(21) Hong, J.; Anderson, P.; Qian, J.; Martin, C. R., Chem. Mater. **1998,** *10*, 1029.

(22) Ulman, A. *An Introduction to Ultrathin Organic Films*; Academic Press: Boston, **1991**.

(23) Sajiv, J., J. Am. Chem. Soc. **1980,** *102*, 92.

(24) Tillman, N.; Ulman, A.; Penner, T. L., Langmuir **1989,** *5*, 101.

(25) Bain, C. D.; Troughton, E. B.; Tao, Y.; Evall, J.; Whitesides, G. M.; Nuzzo, R. J., J. Am. Chem. Soc. **1989,** *111*, 321.

(26) Ulman, A., J. Mat. Ed. **1989,** *11*, 205.

(27) Stewart, K. R.; Whitesides, G. M.; Godfried, H. P.; Silvera, I. F., Surf. Sci. **1986,** *57*, 1381.

(28) Troughton, E. B.; Bain, C. D.; Whitesides, G. M.; Nuzzo, R. G.; Allara, D. L.; Porter, M. D., Langmuir **1988,** *4*, 365.

(29) Nuzzo, R. G.; Fusco, F. A.; Allara, D. L., J. Am. Chem. Soc. **1987,** *109*, 2358.

(30) Ulman, A., Chem. Rev. **1996,** *96*, 1533.

(31) Nuzzo, R. G.; Allara, D. L., J. Am. Chem. Soc. **1983,** *105*, 4481.

(32) Porter, M. D.; Bright, T. B.; Allara, D. L.; Chidsey, C. E. O., J. Am. Chem. Soc. **1987,** *109*, 3559.

(33) Laibinis, P. E.; Whitesides, G. M., J. Am. Chem. Soc. **1992,** *114*, 9022.

(34) Yamamoto, Y.; Nishihara, H.; Aramaki, K., J. Electrochem. Soc. **1993,** *140*, 436.

(35) Atre, S. V.; Liedberg, B.; Allara, D. L., Langmuir **1995,** *11*, 3882.

(36) Wang, J.; Lu, Z., Anal. Chem. **1990,** *62*, 826.

(37) Wang, J.; Hutchins, L. D., Anal. Chem. **1985,** *57*, 1536.

(38) Wang, J.; Golden, T.; Tuzhi, P., Anal. Chem. **1987,** *59*, 740.

(39) Wang, J.; Wu, H.; Angnes, L., Anal. Chem. **1993,** *65*, 1893.

(40) Cheng, Q.; Brajter-Toth, A., Anal. Chem. **1996,** *68*, 4180.

(41) Cheng, Q.; A., B.-T., Anal. Chem. **1992,** *64*, 1998.

(42) Cheng, Q.; A., B.-T., Anal. Chem. **1995,** *67*, 2767.

(43) Sun, L.; Johnson, B.; Travis, W.; Crooks, R. M., J. Phys. Chem. **1990,** *94*, 8869.

(44) Malem, F.; Mandler, D., Anal. Chem. **1993,** *65*, 37.

CHAPTER 4

FABRICATION OF CATION, ANION, AND "IDEAL" PERMSELECTIVE MEMBRANES

INTRODUCTION

In chapters 2 and 3, it was demonstrated that gold nanotubular membranes could be fabricated by electroless deposition and the "template method". Furthermore, the inside tubule diameters were varied and tubules as small as 1 nm were obtained. These membranes display "molecular sieving" and were capable of separating larger molecules when present in a mixture with small molecules. The chemical environment within the nanotubules was changed by the nature of the thiol chemisorbed and this was used to separate hydrophilic and hydrophobic molecules.

Previously, it has been shown that the charge on these membranes can be controlled by applying an electrical potential(1). The membrane can thus be made permselective to anions or cations by changing the nature of the applied potential. The membrane repelled ions of the same charge and was permeable to the ions of opposite charge.

This chapter discusses the modification of the charge on the gold nanotubules by changing the nature of the terminal groups of the thiols that were chemisorbed. For example, when a carboxylate (COO^-) terminated thiol was chemisorbed, the membrane was permselective to cations, and when protonated amino group (NH_3^+) terminated thiol was chemisorbed, was permselective to anions. Furthermore, it will be demonstrated that membranes with very small tubules in a concentration cell ideal permselectivity over a longer range of concentrations than observed previously(1). This was made possible by the use of large anions such as tetraphenylborate, which are excluded from the tubules due to their size.

BACKGROUND

Ion-Exchange Membranes

Ion-exchangers in general are defined as solid materials that carry exchangeable cations or anions(2). These ions can be exchanged stoichiometrically for equivalent ions of same charge when the ion exchanger is placed in contact with an electrolyte. Carriers of exchangeable cations are called cation exchangers and carriers of exchangeable anions are called anion exchangers.

Cation exchangers with different fixed ionic groups with varying degrees of acid strength are available. These include resins with groups such as sulfonic (SO_3H), carboxylic (COO^-), phosphonic (PO_3^{2-}), phosphinic (HPO^{2-}), arsonic (AsO_3^{2-}) acid groups(3). The various basic groups in anionic exchange resins

include different ammonium groups ($-NH^{3+}$, $-NH^{2+}$, $-N^{+}(CH_3)_3$), quartenary phosphonium and tertiary sulphonium groups(3).

Ion-exchange membranes consist of a framework carrying fixed ionic sites which are compensated by oppositely charged mobile counter-ions. In general, the ions in the electrolyte of the same charge as the framework fixed sites are called co-ions and the ions of the opposite charge are called counter-ions.

Two important properties of ion-exchange membranes are high electrical conductivity and permselectivity. The conductivity is determined by the concentration and the mobility of the counter-ions. The concentration of the counter-ions is in turn dependent on the concentration of the fixed ionic groups. The mobility of the counter-ion on factors such as extent of cross linking, the nature of the counter-ions and the temperature. The permselectivity is defined as the permeability difference of the membrane for the co-ions and the counter-ions.

Typically, ion-exchangers have high ionic concentrations, hence they have higher conductivities. The specific conductivity of typical ion-exchange resins with alkali metal or halide counter ions is of the order of 10^{-3} to 10^{-1} ohm^{-1} cm^{-1}. The permselectivity, on the other hand depends on the nature of the counter-ion, co-ion and the concentration of the electrolyte. Ideal permselectivity implies that the permeability of the co-ion is negligible compared to that of the counter-ion(4). Ion-exchangers are permselective to ions of one charge and reject ion of opposite charge due to "Donnan exclusion".

Donnan Exclusion

When an ion-exchange membrane is immersed in an electrolyte, the counter-ions can enter the membrane and replace the ions that were initially present. However, the entry of the co-ions into the membrane is prevented by the repulsive forces of the fixed ionic sites in the membrane. This is called Donnan exclusion in honor of the pioneering work by F. G. Donnan(5, 6).

The extent of exclusion of the co-ions by the fixed sites in the framework of the ion-exchange membrane determines its permselectivity which depends on the concentration of the fixed ionic sites. If the concentration of the co-ions in the electrolyte is greater than the concentration of the fixed ionic sites, the Donnan exclusion effect breaks down. Thus, the deviation from ideal permselectivity increases with increasing solution concentration, counter-ion valence, decreasing fixed-charge concentration and co-ion valence.

The permselectivity of a membrane can be determined by measuring the membrane potential (E_m) in a concentration cell(7-10). The membrane potential is defined as the electrical potential difference between two electrolyte solutions that separate the membrane. This can be determined by immersing appropriate electrodes in the two solutions(11).

If a cation-exchange membrane separates two solutions of the same electrolyte at different concentrations, ideally the membrane is permeable only to cations. The anions are repelled by the fixed charges. If the diffusion of the counter-ion continues, there is an electrical charge that builds up at the solution-membrane interfaces. In this case the dilute solution is more positive than the

concentrated solution. This electric potential that is developed is called membrane potential(12).

The membrane potential values can be used to calculate the transference numbers for cations and anion within the membrane using the equation 4.1.

$$E_m = 59\ (t_+ - t_-) \log a_h/a_l \quad mV \qquad (4.1)$$

where, a_h and a_l are the mean activities of the salt on the high and the low concentration sides of the membrane, t_+ and t_- are the transference numbers of the cation and the anion. Equation 4.1 indicates if a membrane is cation or anion permselective. If t_+ is greater than t_-, the membrane is cation permselective and if t_- is greater than t_+ the membrane is anion permselective. For an ideal cation permselective membrane $t_+ = 1$ and $t_- = 0$ and a plot of E_m versus log (a_h/a_l) will be a straight line with a slope of 59 mV based on equation 4.1.

Some of the most cation permselective membranes are the perfluorinated ionomer membranes. They were developed in the 60's for use in applications such as chlor-alkali cells. Some the properties and advantages of a perfluorinated membrane, nafion are discussed in the next section.

Perfluorinated Ionomer Membranes

The transport properties of these membranes have been studied in detail(13). Nafion is a perfluorosulfonated ionomer, consisting of tetrafluoroethylene with pendent side chains of perfluorinated vinyl ether which terminate in sulfonic acid groups. The chemical structure of nafion is shown in Figure 4.1.

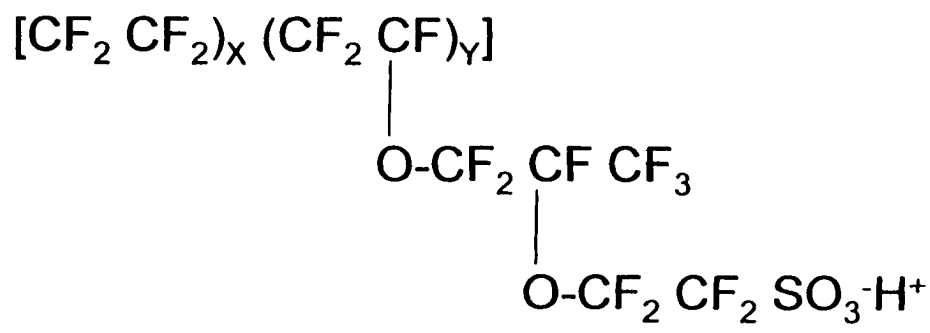

Figure 4.1 Chemical structure of Nafion

Nafion has several interesting and important properties that render it useful in several applications. Nafion is capable of absorbing large amounts of water and other solvents. Typically the polymer absorbs 10 to 50% of its dry weight depending on the equivalent weight, the counter ion form and the temperature. Nafion is stable in strong base, strong oxidizing and reducing acids, Cl_2, O_2, H_2, H_2O_2 at temperatures up to 125°C. Due to the large number of sulfonic acid groups, the membrane is highly permselective to cations(13).

Several studies have been conducted on the morphology, transport properties and the applications of Nafion. There are several models of the morphology that can explain the properties of nafion. One of these is based on a network of clusters suggested by Gierke in 1977(14). In the model nafion consists of two phases, a distinct water phase and a fluorocarbon phase. The water phase is in the form of 4 nm diameter spherical clusters connected by 1 nm channels, distributed in the fluorocarbon phase as shown in Figure 4.2(15, 16)

Another accepted model was proposed by Yeager et al.(17) which suggested that nafion consists of three distinct phases. Phase one is a fluorocarbon backbone while the second phase is an interfacial region consisting of pendant side chains, water and some sulfonate (SO_3^-) groups. The third phase consists of the majority of the SO_3^- groups, the counter-ions and most of sorbed water.

Applications Of Permselective Membranes

Permselective ionomer membranes were developed in the 1960s and the tremendous differences in the properties of the polymers were realized. For

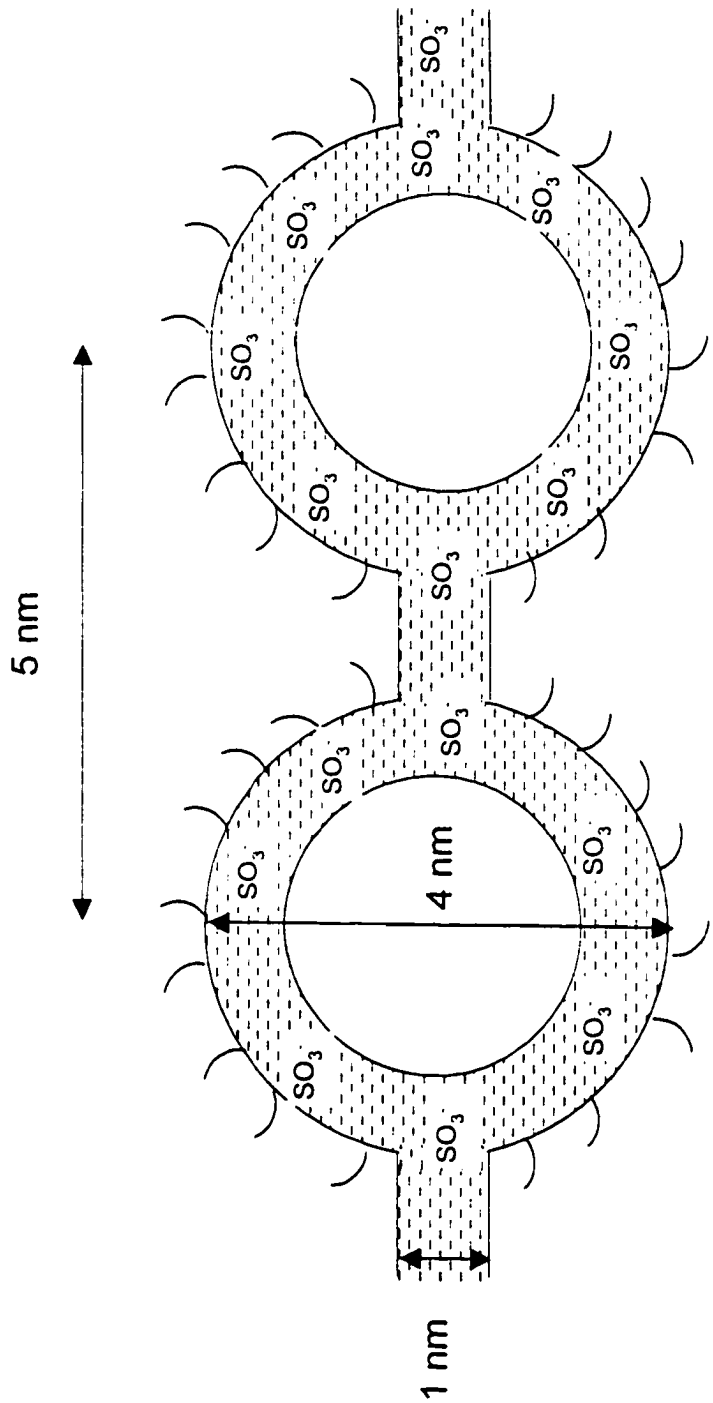

Figure 4.2 The cluster network model for Nafion (Adapted from Reference 15)

example, incorporation of ions into polymers caused the glass transition temperature to increase 500 fold(18), increase in modulus over three orders of magnitude(19), viscosity to increase by over four orders of magnitude(20). The incorporation of small amounts of ions (1 to 10 mol percent) in polymers yielded membranes with diffusion coefficients of water orders of magnitude higher than the non-ionic parent polymer. In addition, the membranes were permselective at the same time. One class of membranes that stood out was perflouroionomer membranes due their stability and excellent permselectivity.

The development of perfluoroionomer membranes revolutionized some of the electrochemical processes at that time. Chlor-alkali cells produce Cl_2 at the anode by the oxidation of Cl^- and, caustic(NaOH) and H_2 at the cathode by the reduction of water from brine (NaCl). The separator should allow the Na^+ to pass to the cathode excluding the Cl^- and prevent the OH^- from diffusing to the anode. Before the development of these highly stable and permselective membranes, the chlor-alkali cells for the synthesis of chlorine and caustic soda used mercury and diaphragm cells(21). These membranes allowed a new design which was less polluting with lower capital, energy and operating costs. These membranes were perfect as separators because they were stable under chlor-alkali cell conditions (high concentrations of NaOH) and were also permselective for the cations while preventing the anions (Cl^- and OH^-) from mixing(21).

Perfluoroionomer membranes such as nafion can also be used in hydrogen-oxygen fuel cells and electrolyzers(22). In the fuel cell the membrane acts as a solid polymer electrolyte. The reactions in the fuel cell are the

reduction of O_2 and oxidation of H_2 to produce water and protons and generate electrical power. The protons are transported from the anode to the cathode for reduction and are transported through the hydrated nafion membrane. The protons migrate by passing from one sulfonate group to another and since the groups are fixed the concentration of hydrated ions remains constant. In the case of the electrolyzers, the opposite reactions take place, namely the splitting of water to H^+ and OH^- to generate O_2 and H_2 gases. In this case, the purpose of the membrane is to separate the products by preventing the diffusion to the other half-cell.

Permselective membranes or thin films are also used in the area of sensors in electroanalytical chemistry. The purpose of the permselective film in this case is to prevent the interfering ions from reaching the electrode surface. For example, a common interferant in the detection of dopamine, a neurotransmitter is ascorbic acid. Ascorbic acid is electroactive and is present in large concentrations. Thus, it interferes with the signal due to dopamine.

Coatings of perfluorinated polymers such as nafion on electrodes have been used to repel negatively charged analytes in previous studies. There are some disadvantages with the use of nafion coatings. The diffusion coefficients of the analytes are very small ($D_{dopamine} = 2.3x10^{-9}$ cm^2 s^{-1})(23). This implies that very thin film have to be used to make fast measurements. Furthermore, the cations from the solution are attracted to the film and affect the electrochemical measurements. Even though the nafion coating are effective in preventing the

anions from reaching the electrode there are some disadvantages. Other methods were developed to overcome these drawbacks.

Malem and Mandler demonstrated that that self-assembled monolayers of ω-mercaptocarboxylic acids can be used to repel negatively charged species(24). They detected dopamine in the presence of large concentrations of ascorbic acid. The advantages of using the thiol monolayer were that the diffusion to the electrode is fast because the monolayer is thin compared to the film. There was minimal or no accumulation of ions near the electrode.

Overoxidized polypyrrole films have been used as cation permselective barriers to detect dopamine in the presence ascorbic acid(25, 26). Pinhole free films were electrodeposited on Pt and glassy carbon electrodes by repeated polymerization and overoxidation. Overoxidation of the film introduced carbonyl groups in the polymer backbone. The anions were repelled by neutral carbonyl groups due to the high electron density. This was advantageous over nafion coatings because the electrostatic binding of cations does not occur and saturate the carbonyl binding sites.

Permselective thiol monolayers of thioctic acid have also been used in amperometric sensing(27). It was demonstrated that the thiol monolayer was permselective to anions when the pH of the system was 7.4. No voltammetric signal was observed for $[Fe(CN)_6]^{3-}$ but a well-defined signal was observed for $Ru(NH_3)_6^{3+}$. It was also shown that the thiol monolayers of thioctic acid can be used for amperometric pH sensing for the determination of the pK_a of COOH group of the thiol.

Sol-gel films prepared from organosilanes containing acidic and basic groups show permselectivity towards anions or cations depending on the groups and the charge(28). For example films obtained from silanes with amine functionalities were selective to $[Fe(CN)_6]^{3-}$ while $Ru(NH_3)_6^{3+}$ was not detected. In comparison, when the film was obtained from carboxylic acid derivatized silanes containing the opposite trend was observed.

Another sensor application of a cation permselective barrier is the use of poly(ester sulfonic acid), as a thin film on a glassy carbon electrode(29). This film was permselective to anions, had anti-fouling properties and also performed as an ion-exchange. These properties made it ideal for use in electroanalytical applications.

Liu and coworkers reported a pH-switchable ultrathin film prepared from multilayer polymer composites(30). The composite consisted of amine terminated dendrimers and poly(maleic anhydride)-c-(methyl vinyl ether). When a thin film was grafted to an electrode, it exhibited fully reversible pH-switchable permselectivity for both anionic and cationic probes. When the pH is low, the amine groups are protonated and the film is anion permselective. At high pH the carboxyl group is deprotonated thus resulting in an anion permselective film.

Anion permselective films have also been developed to prevent interfering cations in sensors. Protonated poly(4-vinylpyridine) coated on glassy carbon electrode by Wang et al.(31). The electrode was developed as an amperometric sensor for detection of anionic solutes such as uric acid, catechol, and ascorbic acid among others. The permeability of cationic solutes was observed to

decrease at least two orders of magnitude due to the presence of the cationic polymer coating.

This chapter describes the application of gold nanotubular membranes as permselective membranes. This was achieved by chemisorbing thiols with different terminal groups. It will be demonstrated that membranes modified with carboxylate terminated thiol are cation permselective and membranes modified with protonated amino group terminated thiol are anion permselective. Furthermore, Donnan exclusion failure was not observed with membranes containing small tubules for large ions even at very high concentrations of the electrolyte. Donnan exclusion at such high concentrations has not been observed previously. The ions are excluded due to their large size and the "rnolecular sieving" property of the membrane.

EXPERIMENTAL

Materials

The materials for electroless gold deposition were used as received and are described elsewhere (Chapters 2 and 3). Polycarbonate "track-etched" membranes ($6x10^8$ pores cm^{-2}, 50 nm diameter and 6 μm thickness) were obtained from Poretics. Thioctic acid, NaCl, sodium tertaphenylborate and 2-aminoethanethiol hydrochloride were purchased from Aldrich and used as received. Milli-Q water was used for rinsing and to prepare solutions unless specified. The membranes were equilibrated with commercial buffers 4 and 10 were used to ensure that the terminal groups on the thiols were charged.

Fabrication and Modification Of Gold Nanotubular Membranes

The gold deposition procedure described in chapters 2 and 3 was used to fabricate the membranes. The deposition temperature was 15°C and plating times were two hours and three hours for two sets of membranes. All membranes were cleaned electrochemically before use by applying a constant potential at -0.5 V vs. Ag/AgCl for 15 minutes in 50 mM KF. This was done to remove any ions that may be adsorbed to the membrane. KF was the electrolyte of choice because F^- does not adsorb to gold(32).

The gold nanotubular membranes were modified with the thiol by immersing the membrane in 1 mM solution in absolute ethanol for 24 hours. The membranes were then rinsed in absolute ethanol for 15 minutes and dried in air for less than a minute. The membrane was placed in a U-tube with the appropriate buffer solution overnight before the concentration cell experiments were conducted. Please refer to chapter 2 for a description of the U-tube apparatus.

Concentration Cell Experiments

The membrane potential (E_m) across the Au nanotubular membranes was measured using a concentration cell (Figure 4.3). The membrane was sandwiched between two pieces of scotch tape with a hole in it (1/8 th inch) and was clamped between the two halves of U-tube. The two halves of the cell contained a solution of the same electrolyte but at different concentration. The concentration in one half cell was maintained at 0.1 mM and the concentration in the other half cell was varied between 1 mM to 1000 mM.

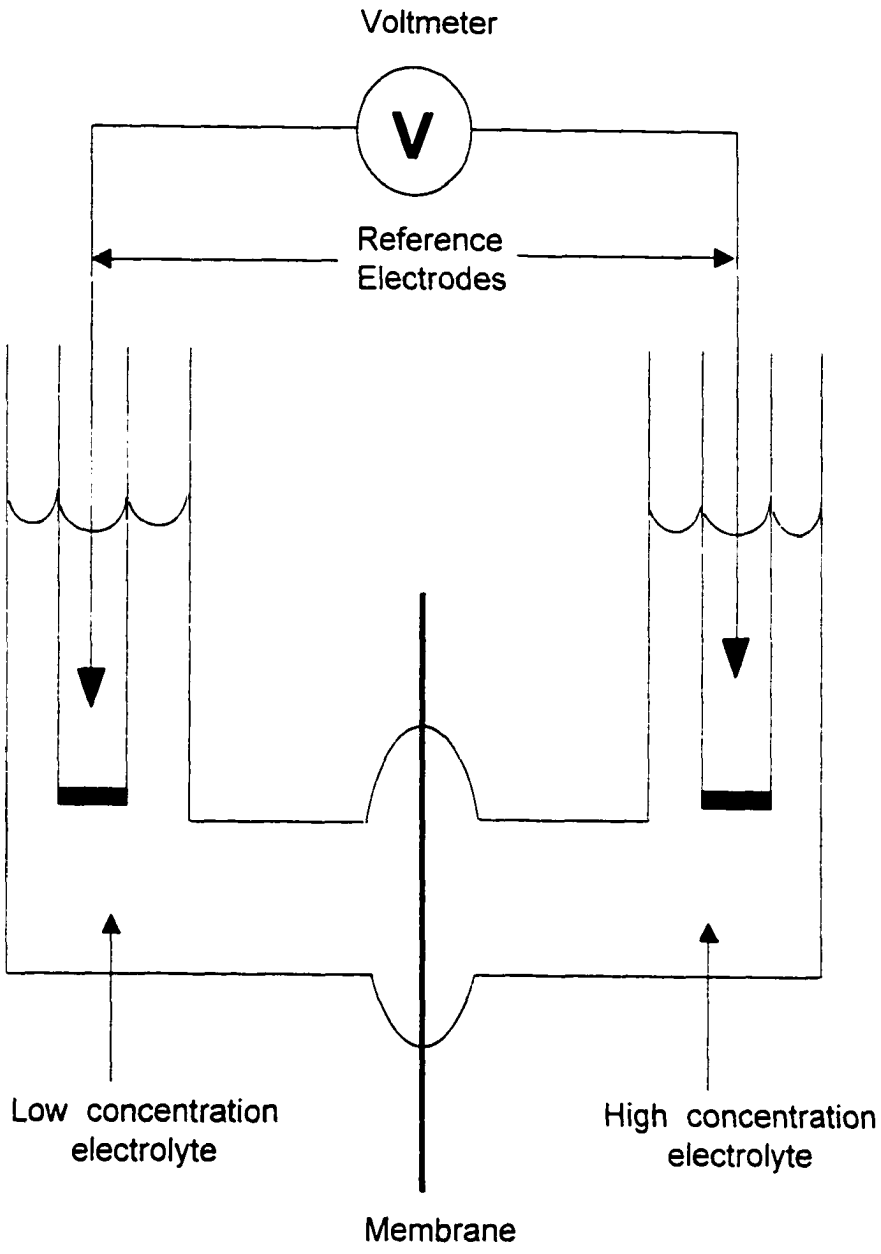

Figure 4.3 Schematic of the concentration cell used for membrane potential measurements

Two Ag/AgCl reference electrodes(33) with agar gel salt bridges were placed in each half-cell. A multimeter was used to measure the potential difference between the two reference electrodes to give the E_m. The membrane potential was allowed to stabilize for at least 6 minutes before it was recorded.

RESULTS AND DISCUSSION

Permselectivity In Gold Nanotubular Membranes

For an ideal permselective membrane, E_m developed in a concentration cell with solutions differing in concentration by 10 times is 59 mV (Refer to equation 4.1). In a previous study, the variation of E_m with the applied potential was measured with gold nanotubular membrane separating two solutions of each KF, KCl, KBr and KI. The applied potential was varied between - 0.5 V to + 0.5 V vs. Ag/AgCl reference electrode(1).

When using KF as the electrolyte, a sigmoidal shape was obtained for the response of E_m to the applied potential. This implied that the membrane was reversibly ion-permselective. That is to say, when a positive potential is applied the membrane is ideally anion permselective. Applying a negative potential to the membrane resulted in an ideal cation permselective response. At the potential of zero charge (pzc) the membrane is non-permselective(1).

In the case of KCl, KBr and KI, a different trend was observed. These ions chemisorb to the gold surface, thus surface is negatively charged. Application of a potential does not change the charge on the surface. Therefore, the membrane is cation permselective irrespective of the applied potential(1).

In comparison, the E_m can be measured in a concentration cell set-up with KCl, KBr or KI. The variation of the E_m with the $\log(a_h/a_l)$ was predicted to be a straight line with a slope equal to 59 mV. Figure 4.4 shows this plot for C_l = 0.1 mM and C_h = 1 mM to 1000 mM for a gold nanotubular membrane with diameter 1.2 nm. The data fits with theoretical line at lower concentrations and deviates at higher concentration. This is due to Donnan exclusion failure expected at higher concentrations (explained below)

Thus, the membrane is cation permselective due to the repulsion caused by the anions adsorbed on the gold surface. In theory, if the charge on the membrane can be changed the nature of permselectivity can be changed also. This was tested by changing the charge on the surface by chemisorption of thiols with different terminal groups.

Variation Of E_m With Nature Of Thiol And Diameter

Gold nanotubular membranes with two different diameters were modified with COO^- and NH_3^+ terminated thiols. The variation of E_m with $\log(a_h/a_l)$ for the four membranes was determined.

Figure 4.5 shows the variation of E_m with $\log(a_h/a_l)$ for two membranes with diameters 3.0 nm and 1.0 nm, modified with a $-COO^-$ terminated thiol. The solid line represents the ideal value for Em expected according to equation 4.1. This figure indicates two results. First, that the extent of cation-permselectivity observed depends on the size of the tubules. Second, that it also depends on the concentration of the electrolyte.

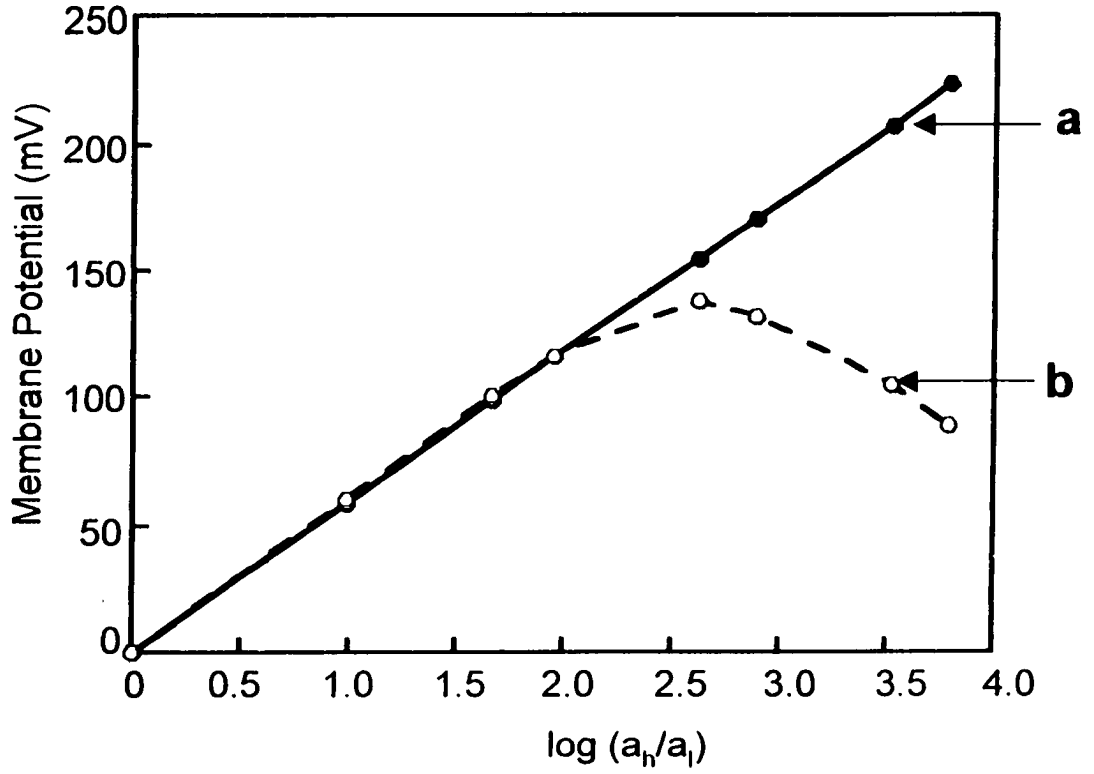

Figure 4.4 Plot of E_m versus $\log(a_h/a_l)$ a) Theoretical b) Au nanotubular membrane with diameter 3 nm (C_l = 0.1 mM KCl)

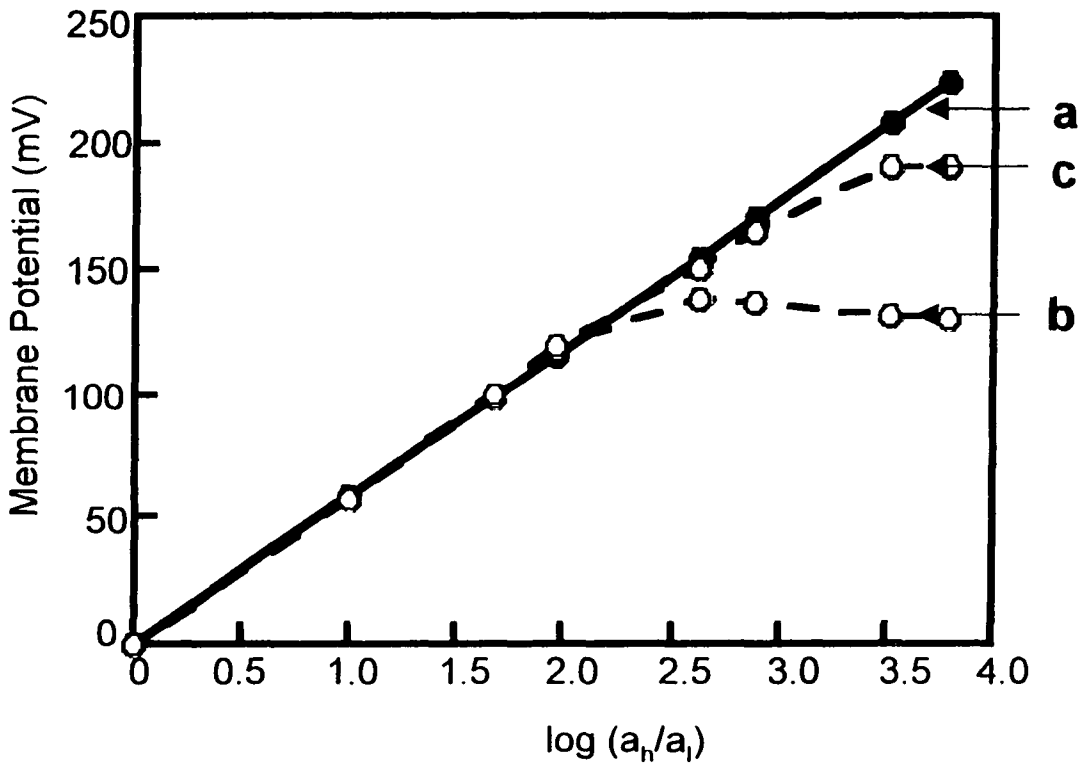

Figure 4.5 Plot of E_m versus $\log(a_h/a_l)$ a) Theoretical and for membranes modified with COO- terminated thiol with diameters b) 3 nm c) 1 nm

The deviation of the E_m at lower concentrations for the smaller tubules is due to the variation of the double layer thickness with the concentration. Guoy-Chapman theory predicts that the thickness of the double layer varies from 30 nm (at the lowest concentration) to 0.3 nm (for the highest concentration)(34). Thus, at lower concentrations, the radius of the tubule is relatively small compare to the thickness of the double layer and ideal ion-permselectivity is observed. However, at higher concentrations, the radius is large compared to the double layer thickness and both anions and cations can enter the tubules resulting in a loss of permselectivity.

Figure 4.6 shows the variation of E_m with $\log(a_h/a_l)$ for membranes with two different diameter nanotubules (3.0 and 1.0 nm) modified with $-NH_3^+$ terminated thiol. The results were similar to that obtained in the case of $-COO^-$ terminated thiol, except in this case the membranes were permselective to anions instead of cations as one would expect.

In summary, gold nanotubular membranes can be made anion or cation permselective by changing the charge on the terminal group of the chemisorbed thiol. The membranes modified with COO^- were found to be cation permselective and those modified with NH_3^+ were found to be anion permselective. However, in both the cases the E_m values obtained at large concentrations deviated from the theoretical value. The permselectivity of the unmodified gold nanotubular membranes were tested with large anions and the results are explained below.

Concentration Cell With Sodium Tetraphenyl Borate

Membranes with gold nanotubules less than 1 nm were used in this study.

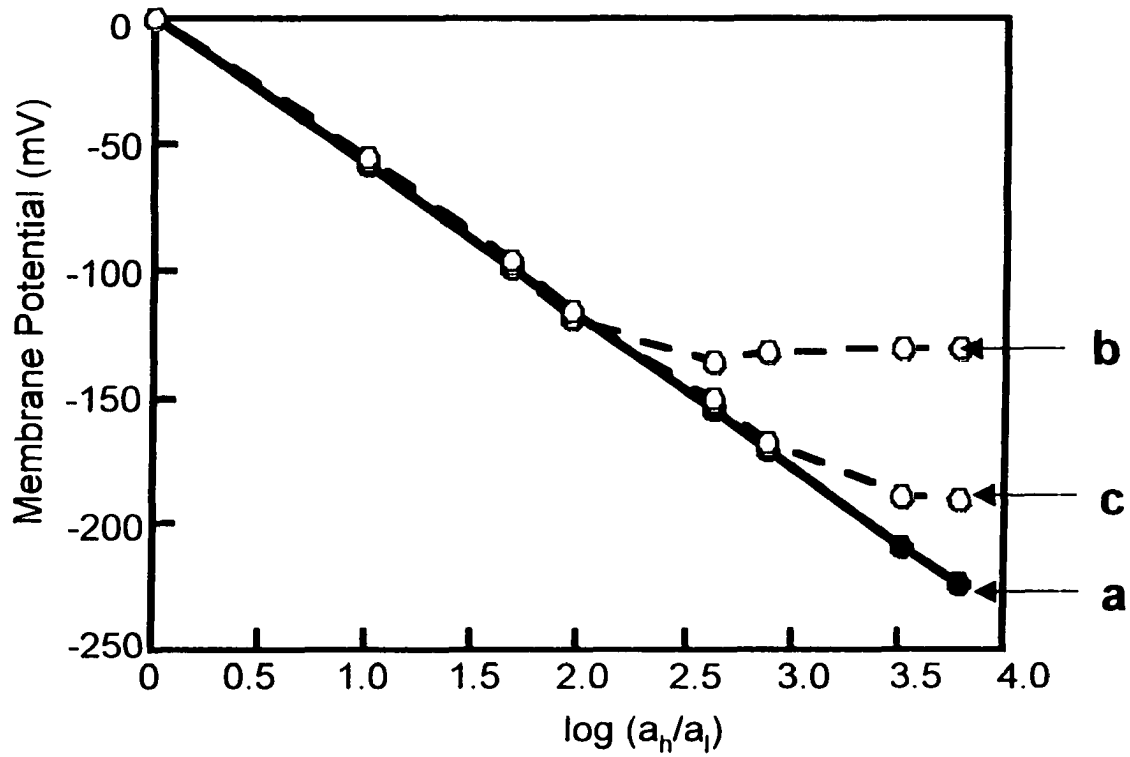

Figure 4.6 Plot of E_m versus $\log(a_h/a_l)$ a) Theoretical and for membranes modified with NH_3^+ terminated thiol with diameters b) 3 nm c) 1 nm

A concentration cell was set up in the same way as described in the previous section. The electrolyte used was sodium tetraphenyl borate. As demonstrated previously, even for the smallest nanotubules the E_m value deviates from the theoretical value. This is because at very high concentrations the charge on membrane is not large enough to exclude the ions or the radius is small enough in comparison to the thickness of the double layer.

However, in the case of the concentration cell setup with sodium tetraphenyl borate, the anion is excluded from the nanotubules due to its large size(Chapter 2). Thus, it is expected that the E_m for the membrane in this cell is not expected to deviate from the theoretical value even at very high concentrations. Figure 4.7 shows the variation of E_m with $\log(a_h/a_l)$ for C_h = 1000 mM. The observed E_m value is in good agreement with the theoretical value expected from the Nernst equation. Such as a good fit of the observed Em with the theoretical value has not been demonstrated before in such a high concentration range. Thus, by fabricating gold nanotubular membranes with very small tubules, advantage was taken of the "molecular sieving" in these membranes to fabricate, "ideal" permselective membranes.

CONCLUSIONS FOR CHAPTER 4

Membrane potentials across gold nanotubular membranes were determined in a concentration cell under different conditions. Membranes with different diameters and modified with different thiols were tested. The nature of ion permselectivity can be changed by changing the terminal group. When a negatively charged terminal group is used, the membrane was permselective to

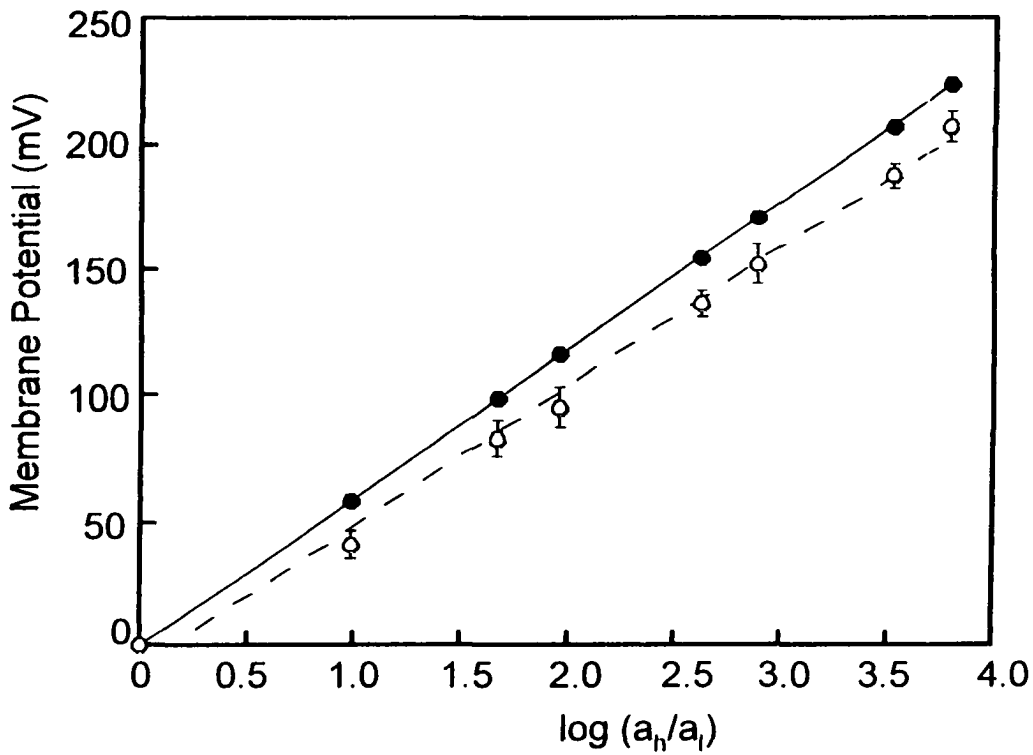

Figure 4.7 Plot of E_m versus $\log(a_h/a_l)$ a) Theoretical and b) Au nanotubular membrane (Electrolyte = Na^+TPB^-)

cations. However, when a positively charged terminal group thiol was used, the membrane was observed to be permselective to anions.

The ion-permselectivity was close to the ideal value for smaller nanotubules and at lower concentrations. This is due to the decrease in the double layer thickness with the concentration. Furthermore, "ideal" permselectivity was demonstrated for the first time in a large range of concentrations. Membranes with very small nanotubules and large anion, tetraphenylborate were used in the study. The anions were excluded due to their large size. Hence, these nanotubular membranes allow one to measure expected E_m values even at very high concentrations of the electrolyte.

REFERENCES FOR CHAPTER 4

(1) Nishizawa, M.; Menon, V. P.; Martin, C. R. *Science* **1995,** *268*, 700.

(2) Helfferich, F. *Ion-Exchange*; McGraw-Hill Book Company: New York, 1962, Chapter 1.

(3) Helfferich, F. *Ion-Exchange*; McGraw-Hill Book Company: New York, 1962, 14.

(4) Helfferich, F. *Ion-Exchange*; McGraw-Hill Book Company: New York, 1962, 324.

(5) Donnan, F. *Z. Electrochem.* **1911,** *17*, 572.

(6) Donnan, F. *Z. Electrochem.* **1911,** *17*, 576.

(7) Lakshminarayanaiah, N. *J. Phys. Chem.* **1969,** 73, 1.

(8) Rosenberg, N. W.; George, J. H. B.; Potter, W. D. *J. ELectrochem. Soc.* **1957,** *104*, 111.

(9) Ellison, T. M.; Spencer, H. G. *J. Poly. Sci.* **1963,** *B1*, 707.

(10) Hale, D. K.; McCauley, D. J. *Trans. Faraday Soc.* **1961,** *57*, 135.

(11) Helfferich, F. *Ion-Exchange*; McGraw-Hill Book Company: New York, 1962, 368.

(12) Helfferich, F. *Ion-Exchange*; McGraw-Hill Book Company: New York, 1962, 374.

(13) Eisenberg, A.; Yeager, H. L. *Perfluorinated Ionomer Membranes*; American Chemical Society: Washington D. C., 1982, 1.

(14) Gierke, T. D. *J. Electrochem. Soc.* **1977,** *77*, 119.

(15) Hus, W. Y.; Gierke, T. D. *J. Mem. Sci.* **1983,** *13*, 307.

(16) Yeo, W. Y.; Eisenberg, A. *Polym. Prepr., Am. Chem. Soc.* **1975,** *16*, 104.

(17) Yeager, H. L.; Steck, A. *J. Electrochem. Soc.* **1981,** *128*, 1880.

(18) Eisenberg, A.; King, M. *Ion Containing Polymers*; Academic Press: New York, 1977, 57.

(19) Eisenberg, A.; King, M. *Ion Containing Polymers*; Academic Press: New York, 1977, 149.

(20) Eisenberg, A.; Ovans, K.; Yoon, H. N. *Ions in Polymers*; American Chemical Society: Washington D. C., 1980, Chapter 17.

(21) Dotson, R. L.; Woodward, K. E. In *Perfluorinated Ionomer Membranes*; Eisenberg, A., Yeager, H. L., Eds.; American Chemical Society: Washington D. C., 1982; Vol. 180.

(22) Yeo, R. S. In *Perfluorinated Ionomer Membranes*; Eisenberg, A., Yeager, H. L., Eds.; American Chemical Society: Washington D. C., 1982; Vol. 180.

(23) Kristensen, E. W.; Kuhr, W. G.; Wightman, R. M. *Anal. Chem.* **1987,** *59*, 1752.

(24) Malem, F.; Mandler, D. *Anal. Chem.* **1993,** *65*, 37.

(25) Hsueh, C.; Brajter-Toth, A. *Anal. Chem.* **1994,** *66*, 2458.

(26) Witkowski, A.; Brajter-Toth, A. *Anal. Chem.* **1992,** *64*, 635.

(27) Cheng, Q.; A., B.-T. *Anal. Chem.* **1995,** *67*, 2767.

(28) Hsueh, C.; Collinson, M. M. *J. Electroanal. Chem.* **1997,** *420*, 243.

(29) Wang, J.; Golden, T. *Anal. Chem.* **1989,** *61*, 1397.

(30) Liu, Y.; Zhao, M.; Bergbreiter, D. E.; Crooks, R. M. *J. Am. Chem. Soc.* **1997,** *119*, 8720.

(31) Wang, J.; Golden, T.; Tuzhi, P. *Anal. Chem.* **1987,** *59*, 740.

(32) Rath, D. L.; Nansen, W. N. *Surf. Sci.* **1984,** *136*, 195.

(33) Sawyer, D. *Electrochemistry For Chemists*; Wiley Interscience: New York, 1995.

(34) Bard, A. J.; Faulkner, L. R. *Electrochemical Methods: Fundamentals And Applications*; John Wiley & Sons: New York, 1980, Chapter 12.

CHAPTER 5

FABRICATION OF Au-POLYACRYLIC ACID COMPOSITE AND ITS APPLICATION AS AN ELECTROCHEMICALLY CONTROLLED VALVE

INTRODUCTION

There is interest in polymeric hydrogels that have polymeric chains that extend and contract in response to external stimuli such as pH(1, 2), solvent composition(3), electric field(4) and temperature(5-7). These materials have potential applications in drug release, biotechnology and in environmental problems(8, 9).

One of the common studies conducted on pH sensitive polymers involved grafting the polymer on track-etched membranes(10-12). It was observed that these grafts contract and expand with a change in the pH of the environment that they are placed in. Permeation experiments conducted with polyacrylic acid (PAA) grafted onto polycarbonate have shown that grafted polymer shrinks in acidic solutions and expands in basic solutions. Atomic force microscopy (AFM) also confirmed this observation(13, 14).

Thus chapter discusses the fabrication of Au-PAA composite using polyester track-etched membrane as a template. It will be demonstrated that the

composite can function as an electrochemically controlled valve. The PAA layer shrunk and expanded when H^+ and OH^- are generated at the Au electrode by passing an oxidizing and reducing current respectively.

BACKGROUND

Micro-Composites And Their Applications

A large number of micro-composites have been developed for a variety of applications(15-18). These range from micro/nano-composites resistant to high temperature oxidation(15) to the preparation of silica-cadmium sulfide nanocomposites for potential applications in non-linear optics(19).

Rledel and coworkers synthesized a silicon nitride/silicon carbide (Si_3N_4/SiC) composite by heating amorphous silicon carbonitride (general formula - $Si_{3+x}N_4C_{x+y}$) to 1000°C under Ar(20). At this temperature a composite of α-Si_3N_4 and α-SiC nanocrystals was obtained. The composite formed was resistant to oxidation in oxidizing environments up to 1600°C.

There is a great deal of interest in the development of crystalline magnetic materials encapsulated in graphitic cages and tubules(21-24). Encapsulation of magnetic materials serves two purposes: to protect the air-sensitive particles against degradation and reducing the coupling between individual particle. These composites could have potential applications as ultra-high-density recording media. Cobalt nanocyrstals have been encapsulated in graphite-like carbon cages for these applications, by co-depositing cobalt and carbon by ion-beam sputtering with subsequent annealing(25).

Partial oxidation by air or nitric acid has been used to open the tips of carbon nanotubes in order to deposit materials inside them(24). Vanadium pentaoxide (V_2O_5) was deposited in carbon nanotubes which were produced by the arc-discharge method. The template carbon nanotubes can be removed by oxidizing carbon below the melting point of V_2O_5. These composites have potential applications in the development of new kinds of nanostructured materials.

Chang et al. developed a novel method to fabricate colloidal silica-cadmium sulfide (SiO_2-CdS) nanocomposites(19). A water-in-oil microemulsion was used to produce silica colloid by controlled hydrolysis of tetraethyl orthosilicate (TEOS) in the water droplets of the emulsions. However, if CdS was co-precipitated in the water droplet, nanocomposites of SiO_2-CdS were obtained. The morphology and the size of the composites can be changed by controlling the co-precipitation of CdS. These composites were developed for use as catalytic support materials.

Membrane Based Composite Materials

Polycarbonate track-etched membranes have been used to fabricate both concentric-tubular and multi-layer composite materials(26-32). Cepak et al. demonstrated that the polymeric membranes can be used as a template for the sequential deposition of materials as a general route to synthesize tubular composites(26, 27). A large number of techniques including electrochemical and electroless deposition of metals, chemical vapor deposition, sol-gel were used to synthesis a large number of composites.

A conductor/insulator/conductor composite consisting of Au/insulating polymer/polypyrrole was synthesized using electroless and electrochemical deposition of the metal and polymers respectively(26, 27). A similar composite consisting of graphitic carbon/polyacrylonitrile/Au was also fabricated by sequential deposition of the layers. Chemical polymerization of acrylonitrile yielded PAN which was thermally graphitized to carbon, followed by deposition of another PAN layer, the insulating layer. The third layer of Au was obtained by electrochemical deposition.

Che and co-workers have shown that Au-TiS_2 composite fabricated by this method can be used as electrodes in Li-based batteries(33). These electrodes provide higher discharge capacities than conventional electrodes prepared by the same material.

In addition to the concentric-tubular composites, "track-etched" filter membranes have also been used to fabricate several multilayers for different applications. Wang and coworkers deposited Ni-Cu multilayers electrochemically to achieve a nanowire composite(30). Such composites have potential applications due to enhanced magnetic properties(31, 32, 34).

Phase Transition In Polymeric Gels Induced By External Stimuli

Many polymeric hydrogels undergo abrupt changes in volume in response to external stimuli such as changes in pH(2, 10, 35, 36), solvent composition(3), electric field(4) and temperature(5-7) (Figure 5.1). These hydrogels have potential applications in drug release, as "smart actuators" in medicine biotechnology and industry. Hence, there is increasing interest in new

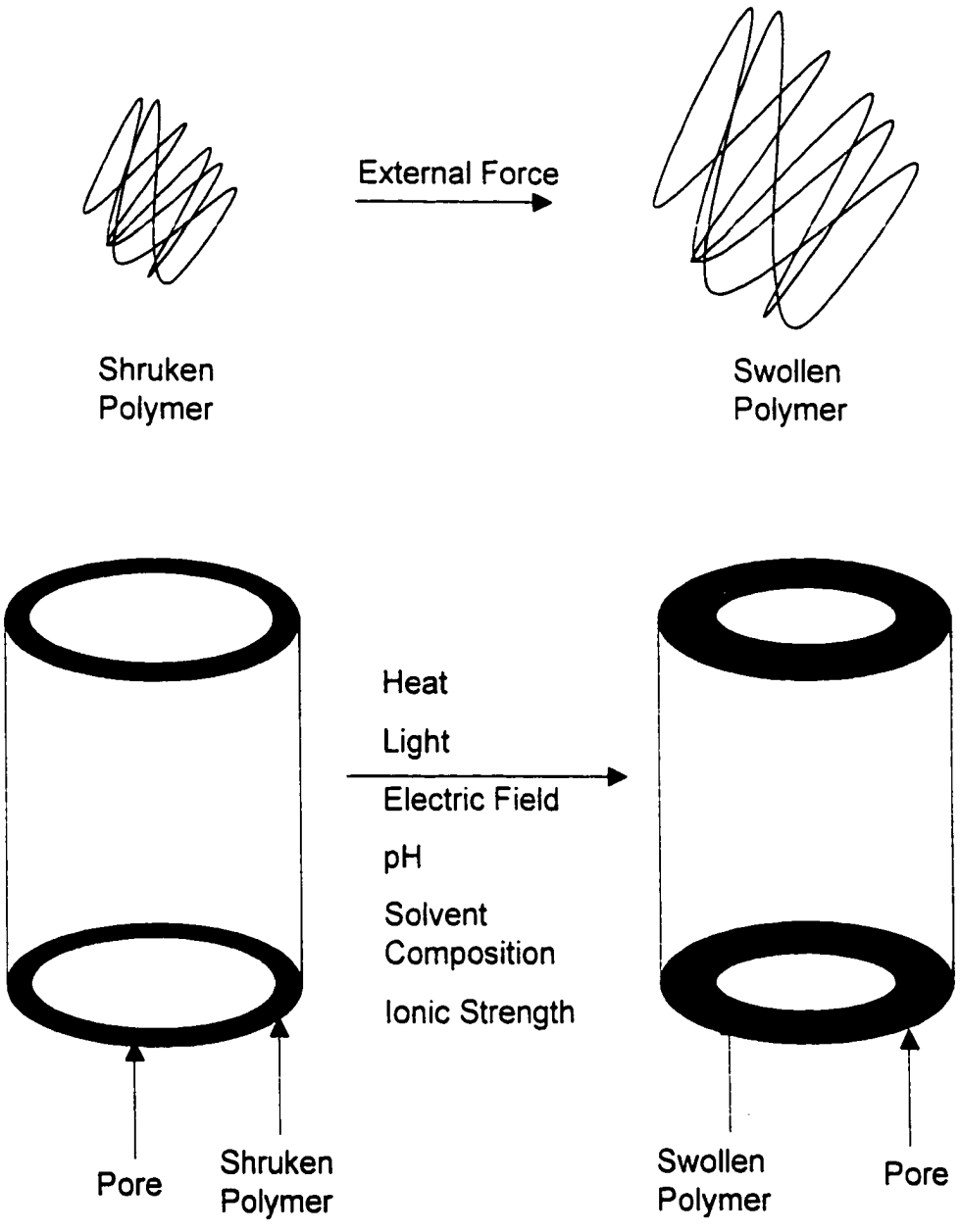

Figure 5.1 Volume change in polymeric hydrogel in response to external stimuli

designs and to increase the response times of swelling and de-swelling(37, 38).

Temperature and Light Induced Volume Change

Poly(*N*-isopropylacrylamide) (PIPAAm) is soluble in water at temperatures below 32°C, its critical solution temperature (CST). Above this temperature, the polymer underwent a discontinuous phase transition precipitating reversibly over a short temperature range. Yoshida and co-workers developed a new type of PIPAAm, which has a comb structure and the chains have one free mobile end. The new gel is unlike the conventional gel where both the ends of the chains are crosslinked. This hydrogel developed by the authors shows a rapid response (20 minutes) to temperature compared to the conventional gels which can take up to a month(5). This is due to hydrophobic pockets that are developed in the gel that aid in the expulsion of water from the network during collapse.

Another thermo-responsive polymer acryloyl-L-proline methyl ester (A-proOMe) was grafted on a polymeric membrane(7). This polymer has CST of 14°C. It swelled below this temperature by absorbing water and shrunk above this temperature, releasing water. The volume of the swollen polymer was about 400 times that of the shrunken polymer. The flux of p-nitrophenol was three orders of magnitude different in the closed and open states, when A-proOMe was grafted on a "track-etched" polymeric membrane (above and below the CST).

Chen and Hoffman synthesized copolymer of monomers that were pH-sensitive acrylic acid and temperature-sensitive *N*-isopropyl acrylamide(38). The copolymer was simultaneously sensitive to both pH and temperature. Gels containing *N*-isopropyl acrylamide and a light sensitive chromophore were

copolymerized to obtain a polymer sensitive to light. By introducing the light sensitive chromophore, the gel can be forced to shrink and expand by changing the intensity of light that was shone on the polymer.

Electric Field Induced Volume Change

Another polyacrylamide gel prepared by free radical polymerization, showed a phase transition in an electric field(4). The electric field caused the charged sites of the network of the gel to produce a stress gradient along the electric field lines in the gel. Above a certain stress level, the gel was swollen and below the level the gel was in a collapsed state.

Electrochemical Control For Change Of Flux And Chemical Release

Electrochemical control on water permeation, ion flux, release of chemicals in polymeric hydrogels has also been examined(39-43). Ito et al. demonstrated that an oxidoreduction-sensitive polymer can be grafted to a porous membrane. The water permeation can be controlled by changing the oxidation state of the polymer or the ionic strength of the solution(43).

Ehrenbeck and Juttner demonstrated that the ion conductivity and permselectivity in a polypyrrole film formed on polycarbonate membrane changes depending on whether the film was in the oxidized or reduced state(42). It was shown that the polymer exhibits appreciable ion conductivity with pronounced anion permselectivity in the oxidized state. However, when the film was modified by incorporating long chain anions, it showed a distinct cation permselectivity in the reduced states.

Polypyrrole has also been studied as a material that can release

chemicals upon application of a current or potential pulse(41). This is made possible because polypyrrole is conducting and can incorporate anions in the polymer backbone as counter-ions. Zinger et al. demonstrated that polypyrrole films can be doped with ferrocyanide or glutamate(39, 41). These anions can be released by the application of an electric or potential pulse. Miller and Zhou developed another conducting polymer that was a cation binder. This polymer could incorporate dopamine, which could be released by an electrochemical switch.

pH Induced Volume Change

Permeation behavior of pH sensitive polymer has been examined in many different forms. Large ultrathin nylon capsule membranes were grafted with various kinds of polymers having dissociative side chains(44). The capsules were loaded with NaCl and large dyes and their permeation was studied by varying the pH. The pH affected the side chains and thus changed the permeation characteristics of the salt and the dyes. Both acidic and basic groups were part of different side chains studied. The side chains were capable of acting as permeation valve with change in pH.

Polypeptide membranes consisting of hydrophobic leucine and hydrophilic *N*-(β-(aminoethyl)-L-glutamine) residues were synthesized(45, 46). These membranes show pH induced conformational changes which cause swelling and shrinking, thereby changing the permeation characteristics of solutes.

Higuchi and co-workers synthesized poly(butylmethacrylate)-polypeptide graft copolymer in which the permeability could be regulated by changing the pH

which caused a change in the conformation of the polypeptide(45). The flux of sodium ions and styrene glycol was examined with variation in pH. It was observed that both the fluxes were higher when the pH was 11 compared to pH 3. This was due to the structural change of the polypeptide chain between the ordered and the disordered conformation. A dissociation of the carboxyl groups resulted in a change in the hydrophilicity and the mobility of the polypeptide domain caused this change in the flux.

In another study Chung et al. studied the pH-induced regulation of permeability of sugars by a polyvinyl-polypeptide graft membrane(47). The permeability of sugars and styrene glycol in poly(butyl methacrylate)-poly(L-glutamic acid) or -poly(L-aspartic acid) was measured. The results were same as that obtained by Higuchi and co-workers. Studies with poly(L-glutamic acid) and poly(L-aspartic acid) in other systems yielded similar results(36, 48, 49). The permeability in all these systems was dependent on the pH which caused a change in the hydrophobicity of the membrane.

A large number of investigations of polyacrylic acid (PAA) grafted on to polycarbonate membranes have demonstrated that the flux can be controlled by varying the pH(1, 11-13, 50) (Figure 5.2). The pores were imaged using AFM and clearly showed the closing and the opening of the pores with change in pH(13, 14). Polyacrylic acid is known to swell in basic solution and shrink in acidic solution. Thus, larger fluxes were observed at low pH and lower fluxes were observed at higher pHs.

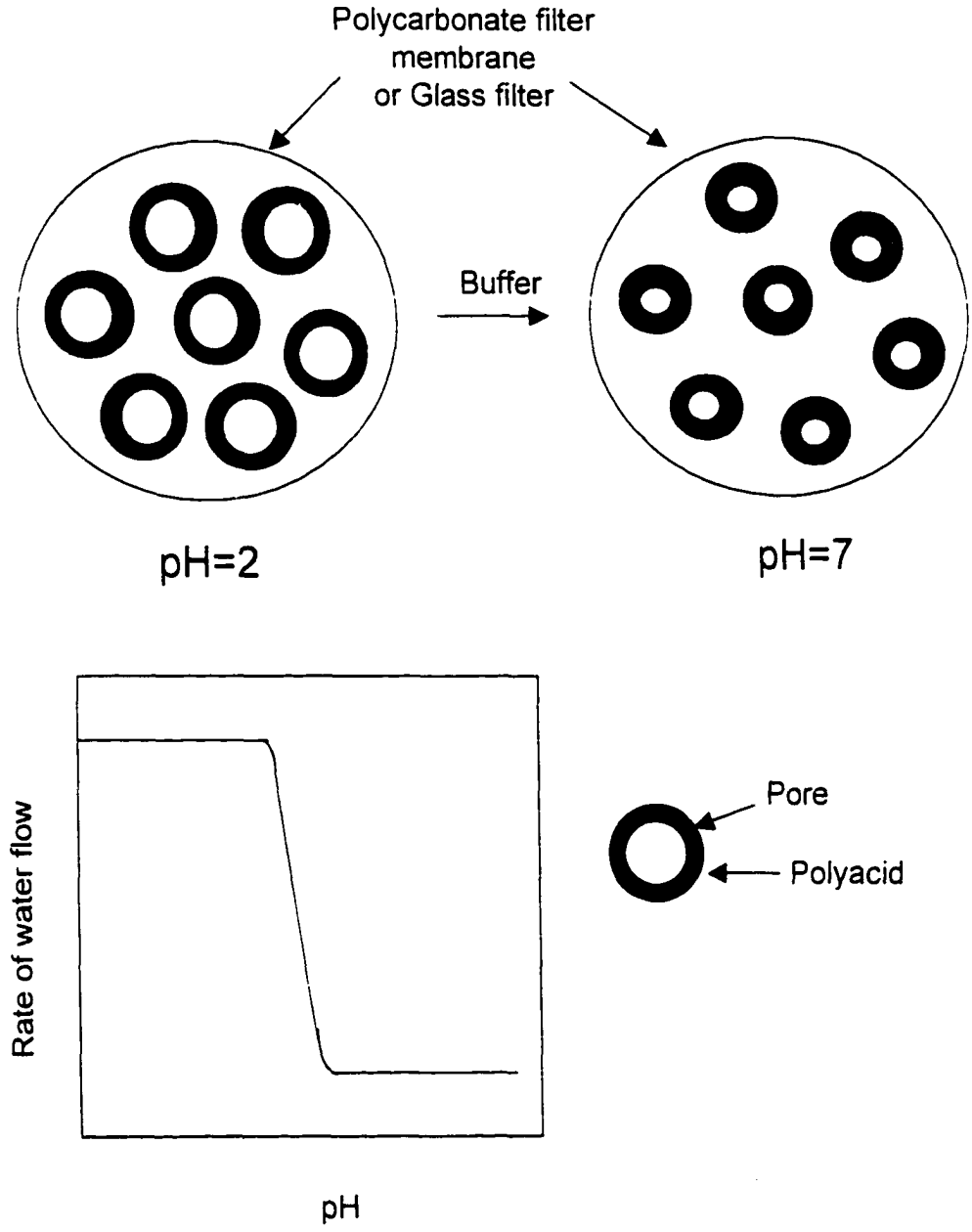

Figure 5.2 Typical response of Polyacid grafted on to polycarbonate track-etched membranes

EXPERIMENTAL

Materials

Polyester track-etched membranes (10 μm thick, 3 μm diameter and $2x10^8$ pore cm^{-2}) were obtained from Poretics. Reagents for the electroless gold deposition, were used as received and are described in chapters 2 and 3. Polyacrylic acid (PAA) (MW=450000), benzoic acid (Aldrich), phosphoric acid (Mallinckrodt) and pH 7 commercial buffer were used as received. Milli-Q water was used for rinsing and for all aqueous solutions.

Fabrication Of Au-Polyacrylic Acid (PAA) Composite

The Au-PAA composite was fabricated by the sequential deposition of gold and polyacrylic acid. The gold was deposited in polyester membranes used as a template by an electroless deposition procedure described elsewhere (see chapters 2 and 3 for details). The Au plated membrane was rinsed in water and one of the surface layers was removed by wiping the surface with laboratory tissue dampened with methanol.

To complete the fabrication of the Au-PAA composite, PAA was deposited inside the Au microtubules by a vacuum-assisted deposition(51) (Figure 5.3). A hole was punched in Aluminum tape with adhesive and the Au plated membrane was placed on it. Whatman filter paper was pasted on the bottom to cover the adhesive. A 5% aqueous solution was placed on top of the membrane and vacuum was applied to draw the solution through the pores. It has been shown that this method can be used to deposit a large number of polymers including

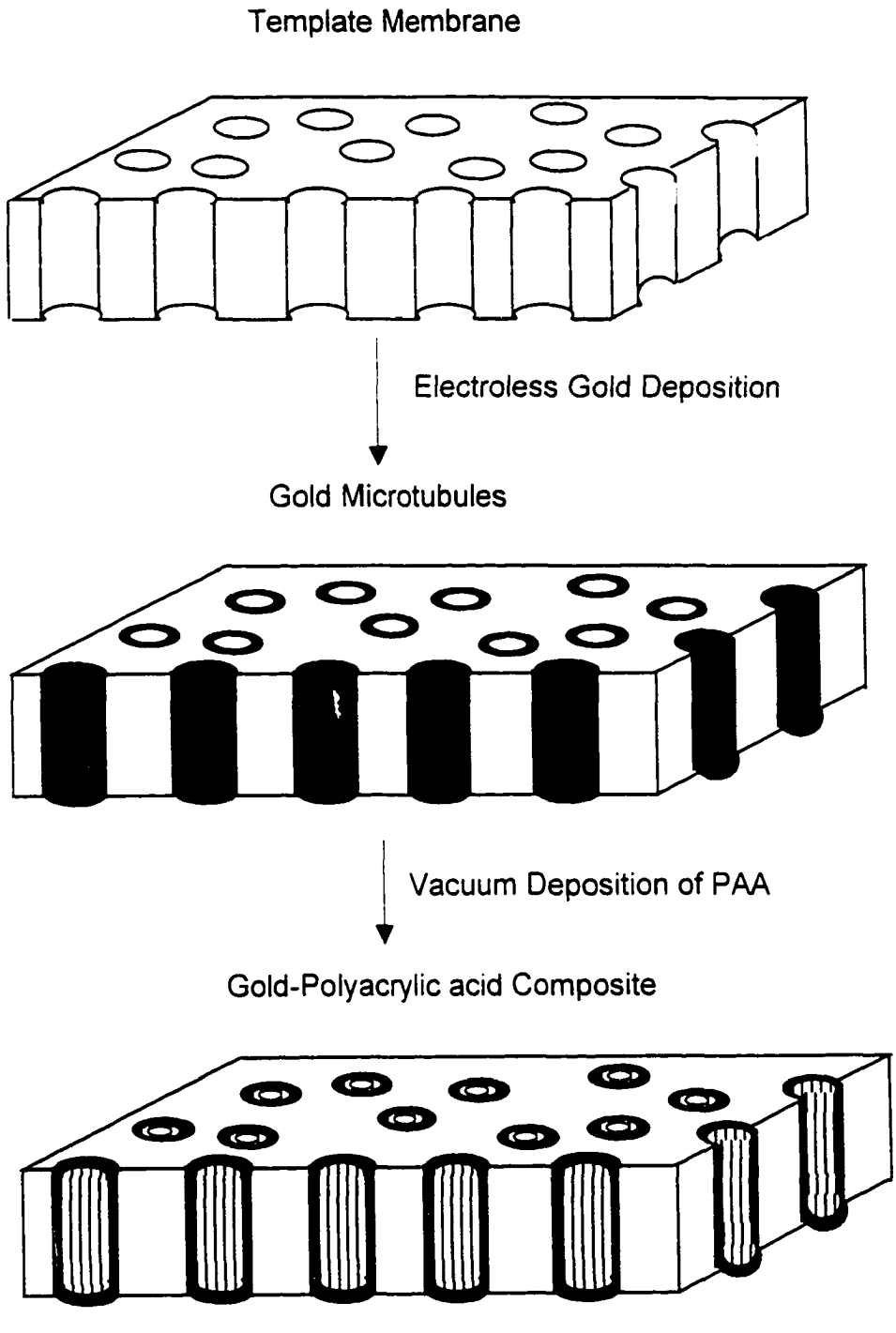

Figure 5.3 Schematic of the fabrication process of Au-PAA composite

polylactic acid, polystyrene, poly(methylmethacrylate) and poly(vinyledene) fluoride from solution(51).

Permeation Experiments

Permeation experiments were performed with a two compartment U-tube setup as described in chapters 2 and 3 for demonstration as a chemical valve using buffer solution. Permeation experiments for the electrochemical control of the valve were accomplished using a 3 compartment set up as shown in Figure 5.4. The glass frit was necessary prevent the ions generated at the counter electrode from reaching the middle compartment. All experiments were done with 10 mM feed solution of benzoic acid and all the solutions were stirred during the experiments.

Demonstration As A Chemical Valve Using Buffer Solution

The Au-PAA composite was placed in a U-tube setup overnight in the buffer before the permeation experiment was conducted. A commercial buffer and 0.1 M phosphoric acid were used to maintain the pH at 7 and 3 respectively. In each of the experiment at different pH, the feed benzoic acid solution was prepared in the solution used to maintain the pH.

Electrochemical Control Of The Valve

The Au surface was used to make contact with the individual Au-PAA microtubules. The pH at the electrode was changed by passing current using a PAR 273 potentiostat. The current was maintained at 10 μA for 10 minutes to generate protons and the permeation experiment was performed. The current was changed to -50 μm to generate hydroxyl ions in situ for 10 minutes before

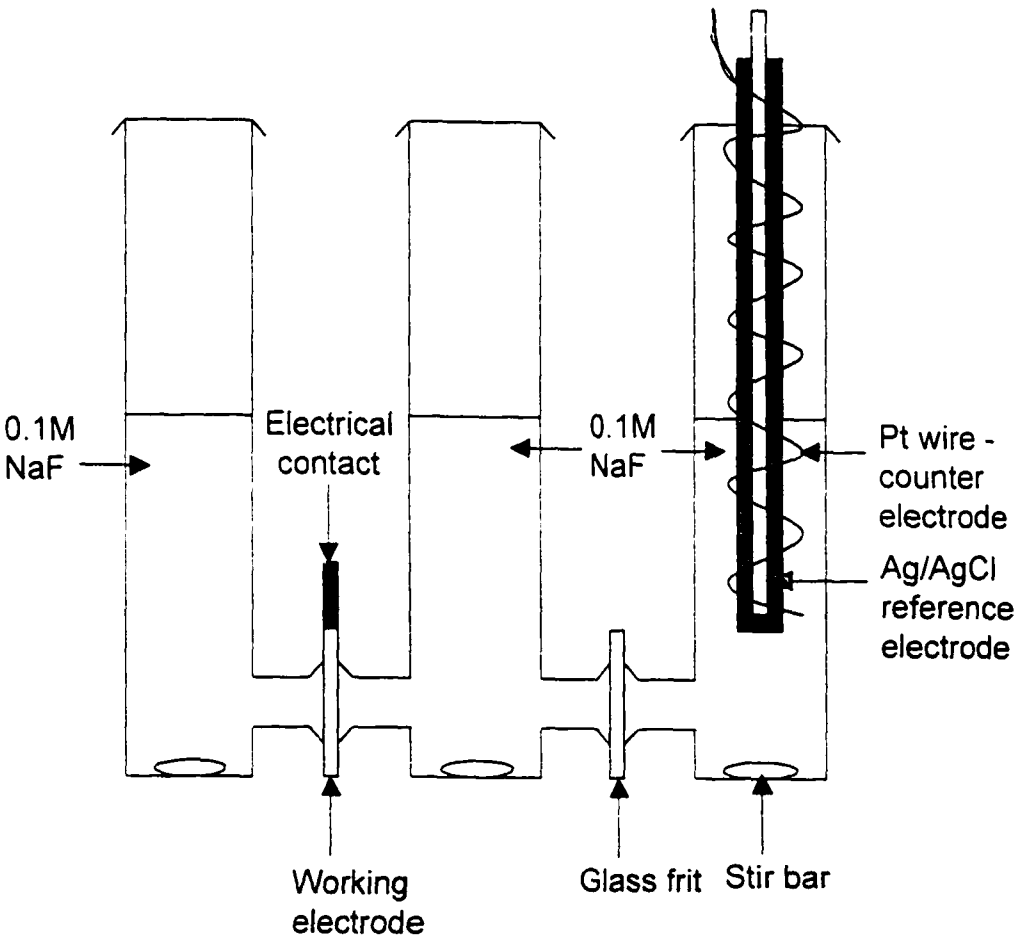

Figure 5.4 Experimental set up for the electrochemical experiments

performing the permeation experiment. This cycle was repeated to determine if the process was reversible.

RESULTS AND DISCUSSION

Fabrication Of The Au And Polyacrylic Acid Microtubules

Gold microtubules were fabricated using track-etched polyester membranes as template and electroless deposition. The deposition was performed at room temperature for 3 hours. Figure 5.5 shows a SEM of the membrane with gold tubules with the membrane intact and after the removal of the membrane. Polyacrylic acid was deposited using vacuum assisted deposition method. Figure 5.6 shows the microtubules obtained by this method.

Fabrication Of Au-Polyacrylic Acid Composite

The Au-PAA composite was obtained by the consecutive deposition of gold and PAA by using the methods described in the previous two sections. There was no discernible difference between the SEMs obtained before and after the deposition of PAA. However, the experiments discussed in the next two sections will support the formation of an Au-PAA composite.

Demonstration Of Au-PAA Composite As A Chemical Valve Using Buffer

It is well known that polyacrylic acid shrinks in an acidic solution and swells in a basic solution. It has also been previously shown that grafting polyacrylic acid on polycarbonate 'track-etched' membrane can be used to design a chemical valve(11). This was done by measuring the flux of water through the membrane in basic and acidic buffers. Before demonstrating that the Au-PAA composite can function as an electrochemically controlled valve, tests

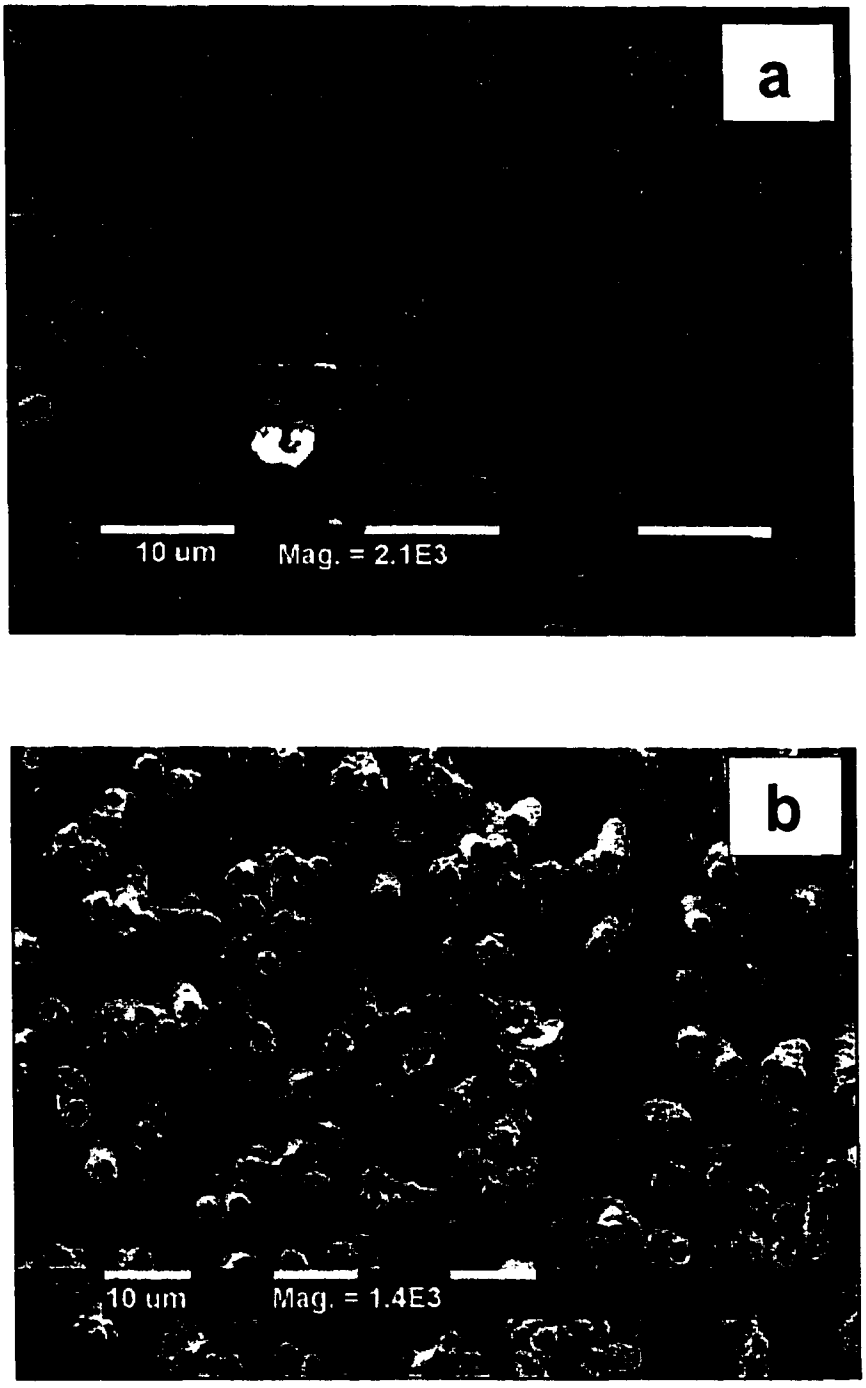

Figure 5.5 Scanning electron micrograph of a) Au in polyester membrane b) Au microtubules with the template membrane removed

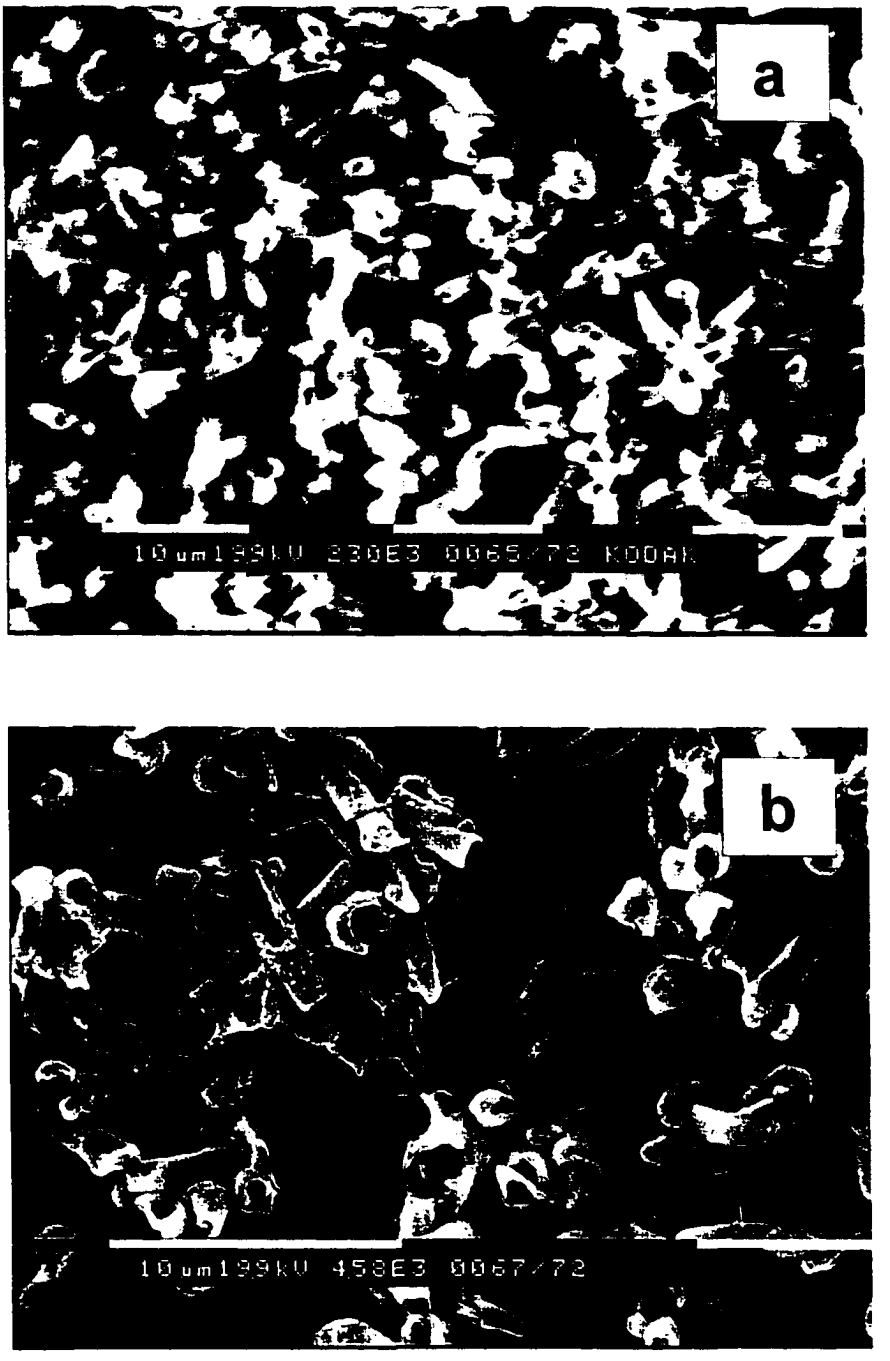

Figure 5.6 Polyacrylic acid microtubules deposited in polyester template membrane

were performed using buffers to change the pH of the system. The flux of benzoic acid was measured at pH 7 and 3, to determine if the PAA layer was swollen and shrunk respectively.

Figure 5.7 shows the flux of benzoic acid at pH 7 and 3. The flux of benzoic acid is $1.0x10^{-8}$ moles cm^{-2} min^{-1} at pH 7 while it increases to $8.0x10^{-8}$ moles cm^{-2} min^{-1} when the pH of the solution is decreased to 3. This demonstrated that the polyacrylic acid inner tubules shrunk at pH 3 and swelled up at pH 7 and that the process was reversible. When the pH was increased to 7, the flux of benzoic acid decreased to $9x10^{-9}$ moles cm^{-2} min^{-1}. These results are in agreement with previous observations (11, 13).

In order to confirm that the change in the flux of benzoic acid is due to the swelling and shrinkage of PAA in the Au-PAA composite, similar experiments were carried out with a control membrane. This consisted of only gold microtubules. Figure 5.8 shows the results obtained. The flux of benzoic acid is the same whether the pH is 7 or 3. This confirmed that the change in flux of benzoic acid in the Au-PAA composite was due to the change in the morphology of PAA with pH.

Electrochemical Control Of The Valve

In the previous section it was established that the Au-PAA composite can function as a chemical valve. The opening and closing of pores was controlled by changing the pH of the solution. It would be advantageous if the pH at the Au surface could be changed to cause the PAA to shrink and expand rather than changing the pH of the whole system.

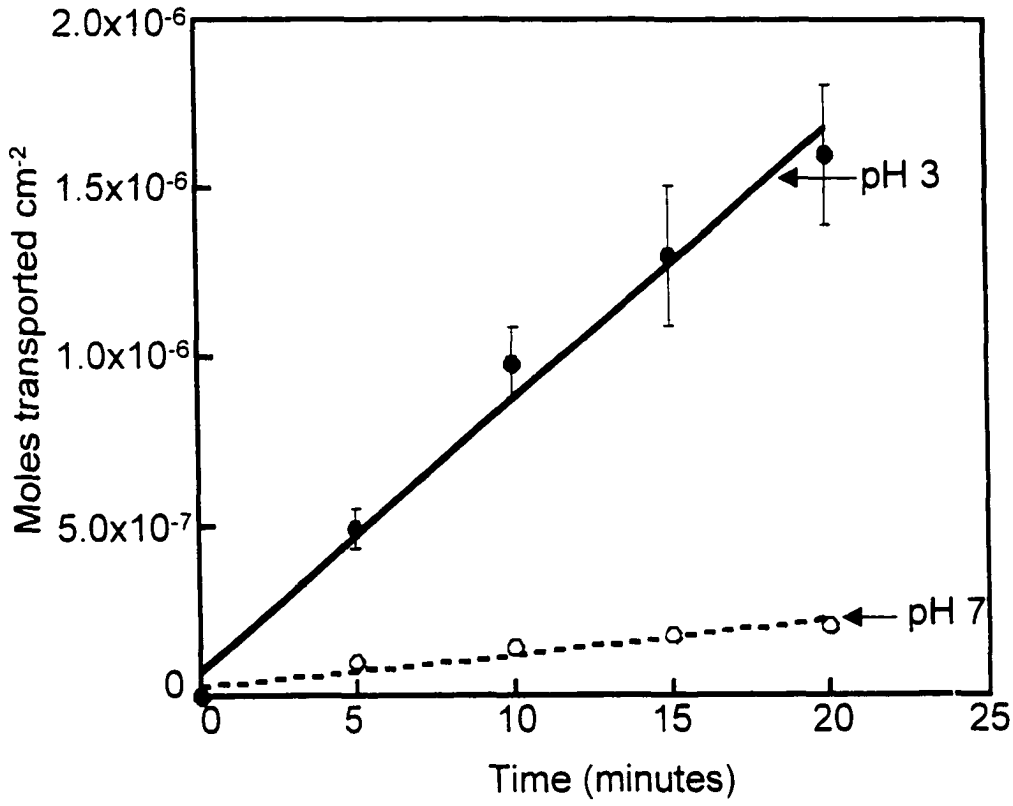

Figure 5.7 Moles of benzoic acid transported versus time in Au-PAA composite membrane at pH 3 and 7

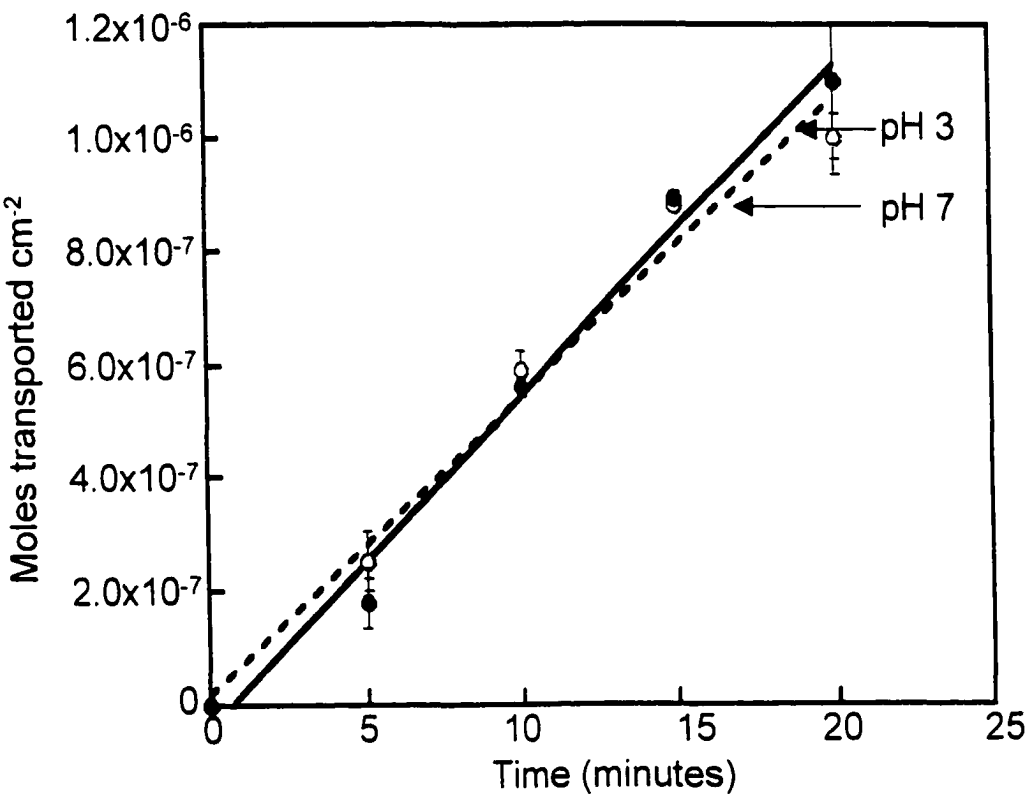

Figure 5.8 Moles of benzoic acid transported versus time in Au microtubular membrane at pH 3 and 7

An Au-PAA composite with one surface layer of Au intact was fabricated as described in the previous section. The gold layer was used as an electrical contact to pass current in order to carry out the necessary reactions at the Au surface. One of the following reactions was carried out to generate either H^+ or OH^- ions at the electrode surface.

$$O_2 + 2H_2O + 4\bar{e} = 4\,OH^- \quad (5.1)$$

$$2H_2O = O_2 + 4H^+ + 4\bar{e} \quad (5.2)$$

The reduction of oxygen will generate protons (equation 5.1) and the oxidation of water will generate hydroxyl ions (equation 5.2). This concept was first tested by using a pH indicator. When phenolphthalein was added to the solution and oxygen was reduced at the electrode, the color at the surface of the electrode turned pink. This indicated generation of hydroxyl ions. When water was oxidized by passing a negative current, the pink color disappears indicating generation of protons at the surface.

This ability to generate protons and hydroxyl ions at the surface of the electrode was used as a stimulus to change the diameter of the inner PAA tubules in the Au-PAA composite. First, a reducing current was passed for 10 minutes and the flux of benzoic acid was measured. Second, an oxidizing current was passed for 10 minutes and the flux of benzoic acid was measured. Figure 5.9 shows the results obtained from this experiment.

Initially, the flux of benzoic acid was 3.7×10^{-7} moles cm^{-2} min^{-1}. After the passage of the oxidizing current the flux decreased to 4.8×10^{-8} moles cm^{-2} min^{-1}. Reversibility was demonstrated by applying a reducing current again and

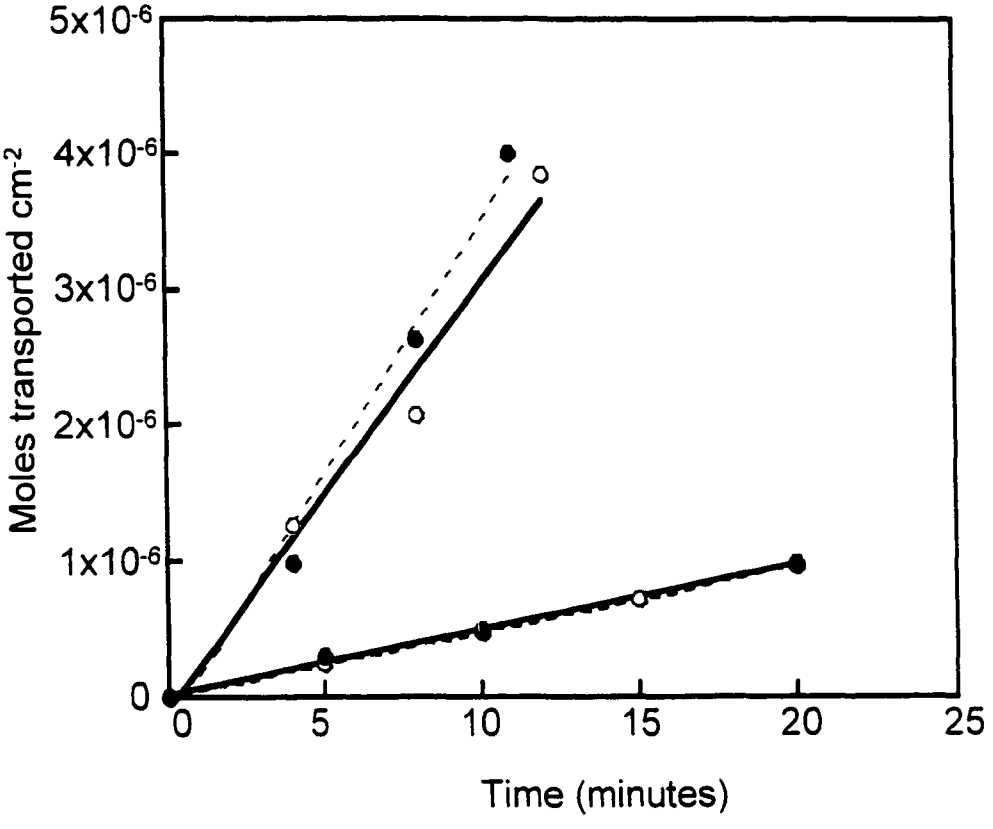

Figure 5.9 Moles of benzoic acid transported versus time in Au-PAA composite membrane by generating protons and hydroxyl ions at constant current

determining the flux of benzoic acid. The flux decreased to 3.1×10^{-7} moles cm^{-2} min^{-1}. Thus, the Au-PAA composite can function as an electrochemically controlled valve and the process is reversible.

CONCLUSIONS FOR CHAPTER 5

An Au-PAA composite was fabricated by successive deposition of gold and PAA in a template polyester membrane. First, the Au was deposited using an electroless deposition procedure. After the fabrication of Au microtubules, PAA microtubules were prepared by vacuum assisted deposition from solution. It was demonstrated that the Au-PAA composite could function as a chemical valve by changing the pH of the solution it was placed in. In addition, the Au-PAA composite could also perform as an electrochemically activated valve by generating protons and hydroxyl ions electrochemically at the surface of the gold.

REFERENCES FOR CHAPTER 5

(1) Ito, Y.; Kotera, S.; Inaba, M.; Kono, K.; Imanishi, Y., Polymer **1990,** *31*, 2157.

(2) Ito, Y.; Inaba, M.; Chung, D.; Imanashi, Y., Macromolecules **1992,** *25*, 7313.

(3) Webber, R. M.; Anderson, J. L.; Jhon, M. S., Macromolecules **1990,** *23*, 1026.

(4) Tanaka, T.; Nishio, I.; Sun, S. T.; Nishio, S. U., Science **1982,** *218*, 467.

(5) Yoshida, R.; Uchida, K.; Kaneko, Y.; Sakai, K.; Kikuchi, A.; Sakurai, Y.; Okano, T., Nature **1995,** *374*, 240.

(6) Yoshida, M.; Asano, M.; Safranj, A.; Omichi, H.; Spohr, R.; Vetter, J.; Kataki, R., Macromolecules **1996,** *29*, 8987.

(7) Yoshida, M.; Asano, M.; Suwa, T.; Reber, N.; Spohr, R.; Kataki, R., Adv. Mater. **1997,** *9*, 757.

(8) Dong, L. C.; Hoffman, A. S., J. Contrl. Rel. **1990,** *13*, 21.

(9) Suzuki, M. *Polymer Gels*; Plenum: New York, **1991**.

(10) Israles, R.; Gersappe, D.; Fasolka, M.; Roberts, V. A.; Balazs, A. C., Macromolecules **1994,** *27*, 6679.

(11) Ito, Y.; Inaba, M.; Chung, D.; Imanishi, Y., Macromolecules **1992,** *25*, 7313.

(12) Park, Y. S.; Ito, Y.; Imanishi, Y., Chem. Mater. **1997,** *9*, 2755.

(13) Ito, Y.; Park, Y. S.; Imanishi, Y., Macromol. Rapid. Commun. **1997,** *18*, 221.

(14) Ito, Y.; Park, Y. S.; Imanishi, Y., J. Am. Chem. Soc. **1997,** *119*, 2739.

(15) Yang, P.; Lieber, C. M., Science **1996,** *273*, 1836.

(16) Douglas, T.; Dickson, D. M.; Betteridge, S.; Charncock, J.; Garner, D.; Mann, S., Science **1995,** *269*, 54.

(17) Golden, J. H.; DiSalvo, F. J.; Frechet, J. M.; Silcox, J.; Thomas, M.; Elman, J., Science **1996,** *273*, 782.

(18) Marinakos, S. M.; Brousseau, L. C.; Jones, A.; Feldheim, D. L., Chem. Mat. **1998,** *10*, 1214.

(19) Chang, S.; Liu, L.; Asher, S. A., J. Am. Chem. Soc. **1994,** *116*, 6739.

(20) Riedel, R.; Kleebe, H.-J.; Schonfelder, H.; Aldinger, F., Nature **1995,** *374*, 526.

(21) Saito, Y., J. Appl. Phys. **1994,** *75*, 134.

(22) Yoshida, Y.; Shida, S.; Ohsuna, T.; Shiraga, N., J. App. Phys. **1994,** *78*, 4533.

(23) Ajayan, P. M.; Iijima, S., Nature **1993,** *361*, 333.

(24) Ajayan, P. M.; Stephan, O.; Redlich, P.; Colliex, C., Nature **1995,** *375*, 564.

(25) Hayashi, T.; Hirono, S.; Tomita, M.; Umemura, S., Nature **1996,** *381*, 772.

(26) Cepak, V. M.; Hulteen, J. C.; Che, G.; Jirage, K. B.; Lakshmi, B. B.; Fisher, E. R.; Martin, C. R., Chem. Mater. **1997,** *9*, 1065.

(27) Cepak, V. M.; Hulteen, J. C.; Che, G.; Jirage, K. B.; Lakshmi, B. B.; Fisher, E. R.; Martin, C. R., J. Mater. Res. **1998,** *13*, 3070.

(28) Chakravarti, S. K.; Vetter, J., J. Micromech. Microeng. **1993,** *3*, 57.

(29) Hoyer, P.; Baba, N.; Masuda, H., Appl. Phys. Lett. **1995,** *66*, 2700.

(30) Wang, L.; Zhang, K.; Metrot, A.; Bonhomme, P.; Troyon, M., Thin Solid Films **1996,** *288*, 86.

(31) Blondel, A.; Meier, J. P.; Doudin, B.; Ansermet, J. P., App. Phys. Lett. **1994,** *65*, 3019.

(32) Piraux, L.; George, J. M.; Despres, F.; Leroy, C.; Ferain, E.; Legras, R.; Ounadjela, K.; Fert, A., App. Phys. Lett. **1994,** *65*, 2484.

(33) Che, G.; Jirage, K. B.; Fisher, E. R.; Martin, C. R., J. Electrochem. Soc. **1997,** *144*, 4296.

(34) Dubois, S.; Marchal, C.; Beuken, J. M.; Piraux, L.; Duvail, J. L.; Fert, A.; George, J. M.; Maurice, J. L.. App. Phys. Lett. **1997,** *70*, 396.

(35) Park, Y. S.; Ito, Y.; Imanishi, Y., Chem. Mat. **1997,** *9*, 2755.

(36) Maeda, M.; Kimura, M.; Hareyama, Y.; Inoue, S., J. Am. Chem. Soc. **1984,** *106*, 250.

(37) Ito, Y. In *Synthesis of Biocomposite Materials: Chemical and Biological Modification of Natural Polymers*; Imanishi, Y., Ed.; CRC Press Inc.: Boca Raton, FL, 1992.

(38) Chen, G.; Hoffman, A. S., Nature **1995,** *373*, 49.

(39) Miller, L. L.; Zhou, Q. X., Macromolecules **1987,** *20*, 1594.

(40) Burgmayer, P.; Murray, R. W., J. Am. Chem. Soc. **1982,** *104*, 6139.

(41) Zinger, B.; Miller, L. L., J. Am. Chem. Soc. **1984,** *106*, 6861.

(42) Ehrenbeck, C.; Juttner, K., Electrochim. Acta **1996,** *41*, 511.

(43) Ito, Y.; Nishi, S.; Park, Y. S.; Imanishi, Y., Macromolecules **1997,** *30*, 5856.

(44) Okahata, Y.; Noguchi, H.; Seki, T., Macromolecules **1987,** *20*, 15.

(45) Higuchi, S.; Mozawa, T.; Maeda, M.; Inoue, S., Macromolecules **1986,** *19*, 2263.

(46) Kinoshita, T.; Kakiuchi, T.; Takizawa, A.; Tsujita, Y.; Oya, M.; Iizuka, Y.; Iwatsuki, M., Macromolecules **1994,** *27*, 1389.

(47) Chung, D.; Higuchi, S.; Maeda, M.; Inoue, S., J. Am. Chem. Soc. **1986,** *108*, 5823.

(48) Speck, E. J.; Gong, Y.; Kallenbach, N. R., J. Am. Chem. Soc. **1995,** *117*, 10773.

(49) Minoura, N.; Aiba, S.; Fujiwara, Y., J. Am. Chem. Soc. **1993,** *115*, 5902.

(50) Ito, Y.; Ochiai, Y.; Park, Y. S.; Imanishi, Y., J. Am. Chem. Soc. **1997,** *119*, 1619.

(51) Cepak, V. M.; Martin, C. R., Chem. Mater. **1999,** *accepted*.

CHAPTER 6

CONCLUSIONS

Nanomaterials are important because of their potential applications as well as interesting fundamental properties. For example, the optical, magnetic and electronic property of a material changes from bulk material to a nanoparticle of the same material. Several applications of nanomaterials and their properties have been explored.

Membrane-based template synthesis has proved to be a very simple and reproducible method to fabricate nanomaterials. Several techniques such as electrochemical and chemical polymerization, sol-gel chemistry, electroless deposition of metals, chemical vapor deposition have been adapted to deposit a variety of materials in various templates. Materials that have been deposited include metals, semiconductors, conducting and insulating polymers. Nanomaterials corresponding to dimensions of the pores or cavities in the template are obtained. Thus, the size of the final material can be controlled by changing the initial template used.

Several fundamental studies as well as applications have been developed

for template based nanomaterials. One of them is the use of gold nanotubular membranes for separation of molecules, based on the size, charge and chemical nature.

Part 1. Gold Nanotubular Membranes For Various Separations

Gold was deposited electrolessly in a template polycarbonate membrane. Gold nanotubules with tunable diameters were fabricated using this method. The initial pore diameter in the template membrane was 30 nm, this was decreased to less than 1 nm by the deposition of gold. The diameters of nanotubules obtained were comparable to the size of molecules. These membranes exhibited "sieving" and were selective to molecules based on their difference in size. Furthermore, these membranes were capable of separating molecules differing in size by 0.5 nm. Complete separation was demonstrated for two sets of molecules.

It was also observed that the nanotubules have constrictions on the ends. This was advantageous because higher fluxes are obtained without compromising the selectivity. The diffusion coefficients of ninhydrin, a relatively large molecule were determined in nanotubules of different diameters. The values indicated that there was considerable decrease compared to the bulk value. The diffusion coefficient value decreased by of two orders of magnitude, such a decrease has not been observed previously.

In Chapter 3, the chemical environment of the gold nanotubules was varied by chemisorbing different thiols. It was demonstrated that the nanotubules are hydrophobic when long chain, $-C_{16}$ terminated thiols were chemisorbed and these membranes are selective to hydrphobic molecules such as, toluene.

Furthermore, the membranes were rendered hydrophilic when modified with short chain hydroxyl group terminated thiols and these membranes were selective for hydrophilic molecules such as, pyridine. It was also demonstrated that the thiol modified membranes were capable of effectively separating the molecules when present in a mixture.

Furthermore, the extent of hydrophobicity of the tubules can be controlled by changing the chain length of the thiol used to modify the tubules. This was demonstrated by measuring the flux of toluene in membranes modified with different chain length thiols, $-C_3$, $-C_{10}$ and $-C_{16}$. The flux increased with an increase in the chain length of the alkyl group. Thus, the chemical environment in the nanotubules can be controlled to a large extent and can be used to achieve separations of various molecules based on their chemical nature.

Thiols terminated with terminal groups of different charges were chemisorbed in the gold nanotubules. In chapter 4, it was demonstrated that the membranes can be rendered cation or anion permselective depending on the charge of the terminal group. For example, the membrane was cation permselective when COO^- terminated thiol was chemisorbed and anion permselective when NH_3^+ terminated thiol was chemisorbed.

The membranes were permselective only at low concentration. This loss of permselectivity has been observed previously and is due to Donnan exclusion failure. However, exclusion of ions at very concentrations (higher than observed previously) was demonstrated by the use of very small nanotubules and large

anions. The anions were excluded due to their large size but as a result, the membrane was permselective even at high concentrations.

Part 2. Fabrication Of Au-PAA Composite And Application As A Chemical Valve

Au-PAA composite was fabricated by the sequential deposition of gold and polyacrylic acid in a template polyester membrane. Au was deposited by an electroless deposition procedure and the PAA by vacuum assisted deposition. It has been demonstrated previously that polyacrylic acid swells and shrinks depending on the pH of the surrounding solution. This property was used to fabricate a chemical valve that opens and closes as the pH of the solution is changed.

It was demonstrated that the Au-PAA composite also behaves in the same fashion with the change in the pH of the solution, it was placed. The flux of benzoic acid was measured as an indicator of the extent to which the PAA is shrunken or swollen. The flux of benzoic acid is an order of magnitude higher when it as placed in a solution of pH 4, compared to a solution of pH 7.

Furthermore, the composite also functioned as a chemical valve when the H^+ and OH^- were generated electrochemically. It was demonstrated that when the pH at the surface of the Au electrode was decreased by generating H^+ by the oxidation of water, the flux of benzoic acid was high. The flux decreased by an order of magnitude when the pH at the electrode surface was increased by the generation of OH^-, by the reduction of O_2. Thus, the Au-PAA composite functioned as an electrochemical controlled valve.

APPENDIX

SELECTIVITY ANOMALY

In general, it was observed that the selectivity, $\alpha_{MV2+/RB2+}$ increases with decrease in the nanotubule diameter. However, at a certain nanotubule diameter, this selectivity drops. For example, a selectivity of 200 was obtained for a membrane with nanotubules, 3.0 nm. This decreased to 50 in a membrane with nanotubules, 2.0 nm in diameter. It was proposed that this may be due to the diameter of the nanotubule being comparable to the thickness of the double layer. Furthermore, the molecules studied were charged (bi-positive).

Some experiments were conducted to study this anomaly. In the first set of experiments, the same molecules were studied but, the adsorption of Cl^- ions on the gold surface was prevented by chemisorption of propanethiol. The flux of both MV^{2+} and RB^{2+} was determined in the membranes with the nanotubule diameters, in which the anomaly was observed, but with the propanethiol chemisorbed on the surface. The selectivity observed in membrane with nanotubule diameter of 3.0 nm, is 100 and is 120 in a 2.0 nm membrane. The flux values and the selectivity values are different than those obtained without the chemisorption of the thiol. However, they indicate that the drop in the selectivity

may be caused by the double layer effect and this is more prominent only when the nanotubule diameter is very small.

The second set of experiments involved using a neutral "small molecule/large molecule" pair. The molecules chosen were pyridine and ninhydrin. The selectivity in this case, goes up from 200 (in 3.0 nm) to 700 (2.0 nm). This indicates that the anomaly observed is related to the molecules being charged. It is also possible that the fluxes of molecules, are affected when the nanotubule diameter is small in comparison to the double layer thickness, when they are charged. Although, the anomaly is not completely understood, there are indications about its origin. However, this did not affect the main objective of this project, that is to fabricate membranes that completely cut the flux of the larger molecule. Thus, with membranes with the smallest possible nanotubules (< 0.6 nm) no RB^{2+} flux observed